COORDINATION CHEMISTRY OF VANADIUM(IV/V) WITH HYDRAZINE BASED LIGANDS

A Thesis
Submitted for the Degree of
Doctor of Philosophy

By
ANINDITA SARKAR

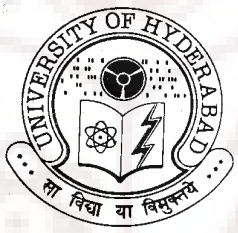

School of Chemistry
University of Hyderabad
Hyderabad 500 046
India

April 2009

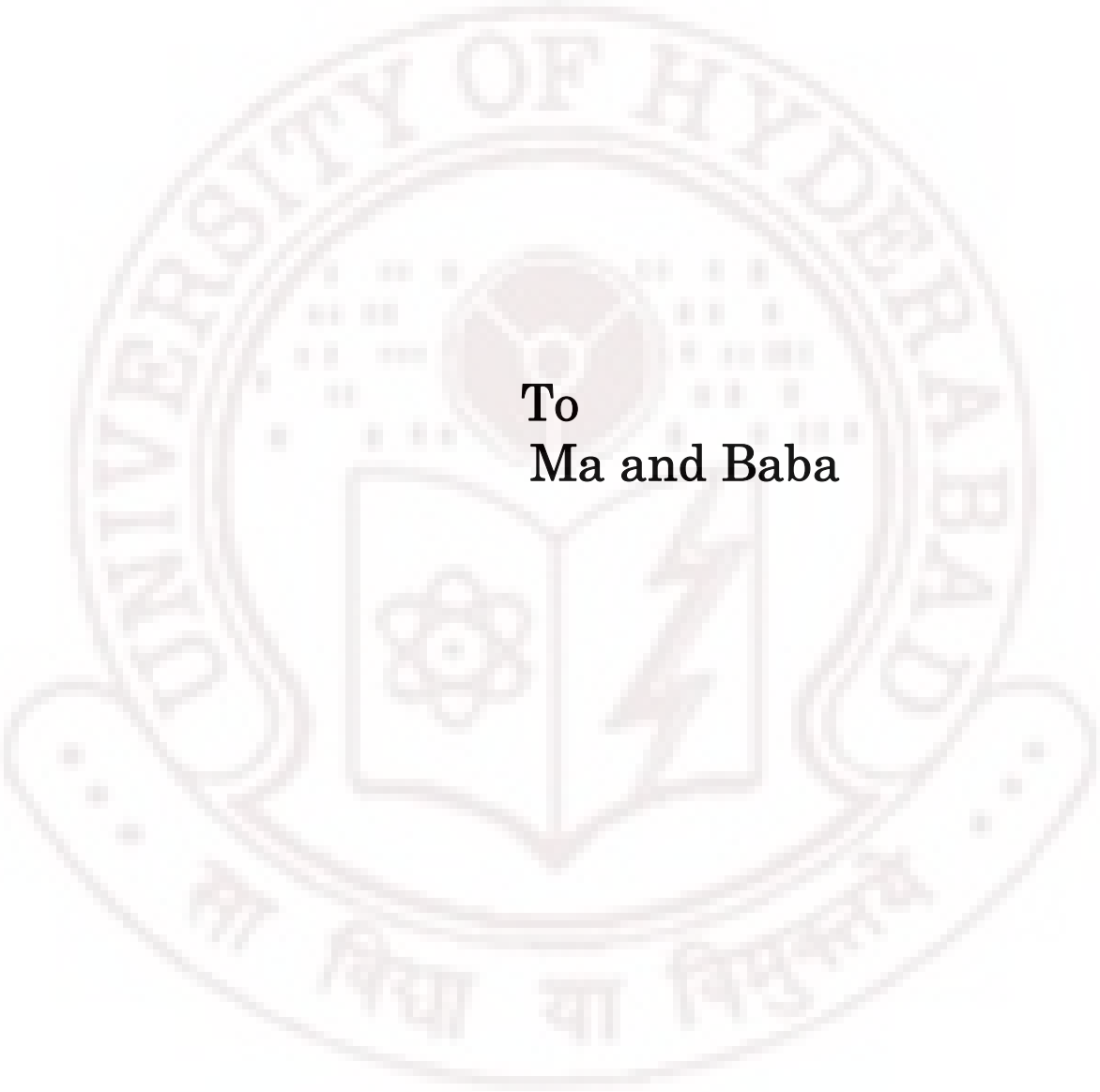

To
Ma and Baba

CONTENTS

STATEMENT

I hereby declare that the matter embodied in this thesis entitled "***Coordination Chemistry of Vanadium(IV/V) Complexes with Hydrazine based Ligands"*** is the result of the investigations carried out by me in the School of Chemistry, University of Hyderabad, under the supervision of **Prof. Samudranil Pal**.

In keeping the general practice of reporting scientific observations, due acknowledgement has been made wherever the work is described is based on findings of other investigators. Any omission, which might have occurred by oversight or error, is regretted.

April 2009 **Anindita Sarkar**

PROF. SAMUDRANIL PAL
SCHOOL OF CHEMISTRY
UNIVERSITY OF HYDERABAD
HYDERABAD-500 046, INDIA

Phone: +91-40-23134756
(office)
Fax: +91-40-23012460
Email: spsc@uohyd.ernet.in

27th April, 2009

CERTIFICATE

Certified that the work embodied in the thesis entitled "***Coordination Chemistry of Vanadium(IV/V) Complexes with Hydrazine based ligands"*** has been carried out by **Ms. Anindita Sarkar** under my supervision and the same has not been submitted elsewhere for any degree.

Prof. Samudranil Pal
(Thesis supervisor)

Dean
School of Chemistry
University of Hyderabad

Acknowledgement

I express my deep sense of gratitude and profound respect to my research supervisor Prof. Samudranil Pal for his invaluable guidance, support and constant encouragement. I have learned a great deal from him and consider my association with him to be a rewarding experience. Any discussion with him has been always very enriching. He has allowed me to grow as a chemist by letting me work on my own ideas and having me learn from my own mistakes.

I would like to thank the former and present Dean, School of Chemistry, for their kind co-operation and providing available facilities and infrastructure. I am extremely thankful individually to all the faculty members of the school for their help, cooperation and encouragement at various stages of my stay in the school.

I thank all the non-teaching staff of the school for their cooperation; Dr. Raghavaiah for his efforts for mounting the tiny crystals, Mr. Suresh and Mr. Satyanarayana for collecting EPR and NMR spectra respectively, Mr. B. Rao for LCMS and Ms. Asia for IR spectra.

Financial assistance from CSIR, New Delhi is gratefully acknowledged.

I am deeply indebted to Prof. Pinaki Bandopadhyay, Department of Chemistry, North Bengal University for his encouragement.

Each of the members of our group has helped me to enrich my experience in their own way. I thank all my seniors in the lab: Drs. S.S. Gupta, Vamsee, S. Das, A. Mukhopadhyay and R. Raveendran, with whom I am associated at various stages of my stay in the lab. I thank my juniors Nagaraju, Samy and Tulika for their support and in maintaining a lively atmosphere in the lab.

I am grateful to Tamalda, Binoyda, Dinuda, Rahulda, Archanda, Manabda, Subashda, Jethuda, Shatabdidi and Abhijitda. I have learnt a lot from them in various stages of my research life. I wish to thank Bhargavi, Sarita, Manasi, Biju, Arumugam, Anwar, Shakti, Mausumi and Monima for cooperation and encouragement at various stages of my stay in the campus. I also thank my juniors Tapto, Tanmoy, Ghanta, Pati, Arindam, Sandip, Sanjeev, Rishi, Ranjit, Naba, Susruta, Dinesh, Mehboob, Tamay Jr., Sudhangshu, Sandip Jr., Pramiti, Supratim and other Bengali newcomers. I wish to thank my Ph.D batchmates Ghana, Pradip, Suparna and Bipul. I will miss many people of this campus with whom I have shared the last five years of my life. My stay on this campus has been pleasant with the association of all the scholars at the School of Chemistry.

I gratefully acknowledge Joya, Vasudhara, Bhaswati (Sr. and Jr.), Rumpa, Sharmistha, Onion, Sanghamitra, Meghna, Sriparnadi, Geetasri for creating a cherish atmosphere in hostel. I really enjoyed the time spent with them while cooking or watching movies in hostel.

I would like to thank my friends Arnab, Maitreyee, Subir, Chaiti, Amit and many more for their constant encouragement and support.

I am at a loss of words to express gratitude to my parents. The tireless support and encouragement of my parents needs a special mention. I owe everything to them. I am grateful to my sweet brother who has been a strong support to me. My special thanks are due to Niloy Kaku and Sumita Kakima for their unwavering support. I am grateful to all my relatives for their encouragement.

I convey my profound regards to all my teachers who taught me throughout my student life. I end by thanking each and everyone who helped me to reach here.

Anindita Sarkar

Introduction

1.1. Abstract

In this chapter, the importance of vanadium chemistry has been briefly discussed. The aim of the present investigation in the background of known vanadium chemistry has been stated.

1.2. Overview

1.2.1. Importance of vanadium chemistry

The continuing interest in the coordination chemistry of vanadium is primarily due to its vital roles in a variety of biochemical processes such as nitrogen fixation, haloperoxidation, phosphorylation and insulin mimicking and the potential/proven use of oxovanadium species as catalysts in various organic reactions.[1-19]

1.2.2. Role of vanadium in biology

While vanadium can exist in at least six oxidation states, only the three highest, i.e. +3, +4, and +5 are important in biological systems. Vanadium-nitrogenases and vanadium dependent haloperoxidases are the two classes of vanadium enzymes,[1] found in nature. V-nitrogenase is comprised of a Fe protein containing ferredoxin type Fe-sufur cluster as an integral part of the structure (Fig. 1.1). Vanadium nitrogenase protonates dinitrogen which is converted to ammonia and can be accessible by plants.

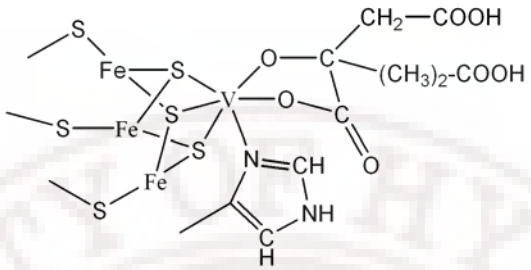

Fig. 1.1. Proposed vanadium environment in vanadium-nitrogenase, based on XAS findings and analogy to molybdenum-nitrogenases.

Vanadate-dependent haloperoxidases contain V^V in their active site and they have been found in marine brown and red algae, in a lichen and a mould.[10,11] Schematic structures of the vanadium sites are shown in Fig.1.2.

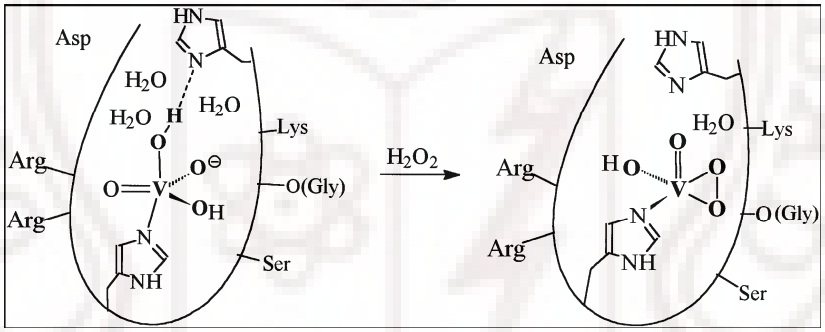

Fig. 1.2. Active site structures of chloroperoxidase from the fungus *C. inaequal*.

Peroxovanadium complexes most probably are intermediates in halide oxidation by vanadate-dependent peroxidases. Vanadium peroxo complexes continue to be studied and are going to be important models for the haloperoxidase enzymes. Vanadium(V) forms many stable peroxo complexes both with and without auxiliary heteroatom ligands. One of the simplest and most interesting vanadium-containing natural products is Amavadin.[12] It has been

known for some time that the common mushroom *Amanita muscaria* or fly agaric, concentrates vanadium to a considerable extent. However, it was not until 1972 that Bayer and Kniefel isolated the vanadium-containing compound and gave it the name Amavadin.

1.2.3. Vanadium in catalysis

Vanadium has found many synthetic applications in homogeneous catalytic oxidations than Mo(VI) and W(VI) and even Ti(IV) because vanadium(V) centres are usually strong Lewis acids, as a consequence of their low radius/charge ratio, which makes them suitable for activation of peroxidic reagents.[13] Another reason is that peroxovanadium complexes form stable alkoxo-derivatives with substrates containing the OH group. This is the reason why the epoxidation of allylic alcohols by peroxocomplexes under catalytic conditions are very fast and highly selective.[14] Bis(acetylacetonato)oxovanadium(IV), $[VO(acac)_2]$, an inexpensive and easy to prepare complex has been studied extensively as catalyst for many organic oxidation reactions such as the epoxidation of allylic alcohols.[15,16] Several vanadium complexes are known to catalyse the oxidation of unfunctionalised olefins. Simple vanadium(V) peroxide complexes also are efficient and selective catalysts in the oxidation of prochiral dialkyl, arylalkyl or diaryl sulfides to the corresponding sulfoxides. The hydroxylation of aromatic hydrocarbons to the corresponding phenolic compounds forms another type of reaction that peroxovanadium(V) complexes are able to catalyse. Vanadium complexes with Schiff-base ligands were found to be active catalysts for bromination of substrates. Coordination complexes of oxovanadium(V) (VO^{3+}) and dioxovanadium(V) (VO_2^{+}) have been also found to be very useful as catalysts in oxidation reactions of various substrates in presence of peroxides.[17-19]

1.2.4. Coordination chemistry of vanadium:

1.2.4.1. Complexes with bidentate ligands

1.2.4.1.1. Complexes with O,O- and O,N-donor ligands

In general, $[V^{IV}OL_2]$ type complexes are formed when bidentate ligands react with $[VO(acac)_2]$ in inert condition, but on exposure to air it slowly oxidizes to dioxovanadium(V) species. If KOH is added $K[VO_2L_2].2H_2O$ complexes are formed.[20]

1.2.4.1.2. Complexes with O,S- and S,S-donor ligands

In presence of salts such as $[Ph_4P]Cl$ or $[Me_4N]Cl$ (BCl), sodium salt of these type of bidentate ligands react with $[VO(acac)_2]$ to give $Na(B)[VOL_2]$. However, in the absence of any salt $[Na_4(acac)_2][VOL_2]$ species are obtained.[21-23]

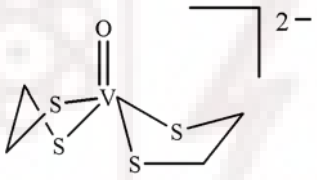

Fig. 1.3. Oxovanadium complex with SS^-donor ligands.

1.4.1.2. Complexes with tridentate ligands

1.2.4.2.1. Complexes with O,N,S-donor ligands

In general, the coordination chemistry of oxovanadium(IV/V) with sulfur donor ligands has received much less attention compared to that with O/N donor ligands. Also for oxovanadium(IV/V) species it is generally anticipated that the hard metal centre should prefer hard O/N donor ligands rather than soft sulfur

donor ligands. As a result very few structurally characterized complexes of oxovanadium(V) moieties (VO^{3+}, VO_2^{+} and $V_2O_3^{4+/3+}$) with sulfur coordinating ligands are known.[17,18,24-30]

[VO(OMe)L] type of complexes are generally formed by these type of ligands and the complexes are square pyramidal with O, N and S atoms of the ligand and O atom of the methoxide at the basal plane while oxo group at the apical position.[25]

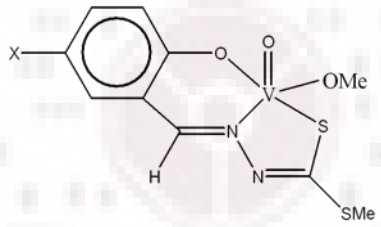

Fig. 1.4. Oxomethoxo vanadium(V) complex with ONS donor ligand.

1.2.4.2.2. Complexes with O,N,O-donor ligands

In methanolic media, the O,N,O-donor ligands provide complexes containing the $\{VO(OMe)\}^{2+}$ motif.[31] On the other hand, complexes containing the $\{OV(\mu\text{-}O)VO\}^{4+}$ core with the same ligand system have been isolated from non-protic acetonitrile media.[32] Examples of some other O,N,O-donor compounds which provide such complexes are shown in Fig. 1.5.

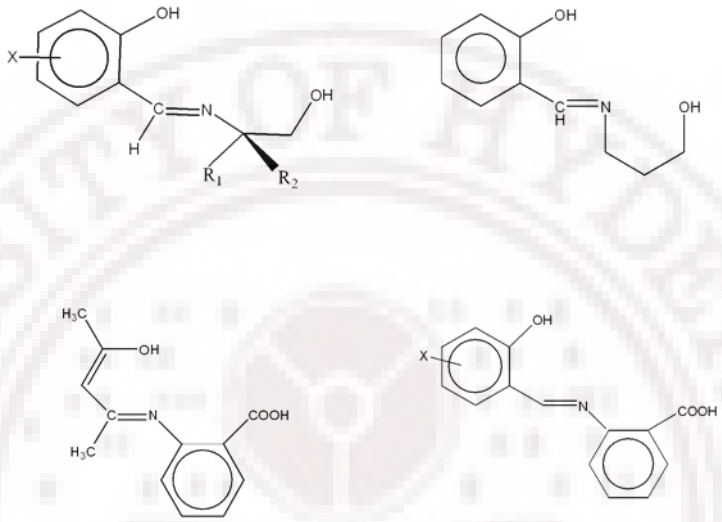

Fig. 1.5. Examples of O,N,O-donor compounds.

1.2.4.2.3. **Complexes with N,N,O- and N,N,S-donor ligands**

The N,N,O-donor ligand such as monoanionic deprotonated 4-R-benzoic acid pyridin-2-ylmethylene-hydrazides are found to be very efficient in stabilizing the VO_2^+ unit. In this case, either a dimeric species (two edge-shared octahedra) formed by a square-pyramidal complex of VO_2^+ or mononuclear trigonal bipyramidal complexes of VO_2^+ have been isolated.[33-35]

Reaction between equimolar amounts of [$VO(acac)_2$] and O,N,N-donor ligands such as (Hacpy-inh) in dry, refluxing methanol yielded oxovanadium(IV) complexes [VO(acac)(acpy-inh)]. These complexes slowly oxidize in methanol to give the corresponding dioxovanadium(V) complexes. A few drops of water facilitate this oxidation. Fig. 1.6 represents the synthetic procedure.[36]

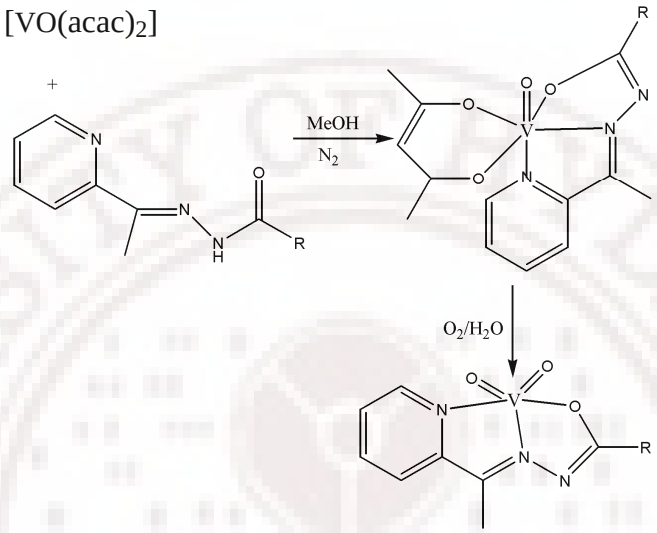

Fig. 1.6. Reaction scheme for the synthesis of VO_2^+ complexes.

With N,N,S-donor ligands such as Schiff bases derived from acetylpyridine and S-metyldithiocarbazate (smdt)[37] or S-benzyldithiocarbazate (sbdt),[38] dioxovanadium(V) complexes $[VO_2L]$ are formed by reacting the Schiff bases with $[VO(acac)_2]$ in presence of air. A ternary $\{VO\}^{3+}$ complex with such a ligand and a malonate has been also reported (Fig. 1.7).

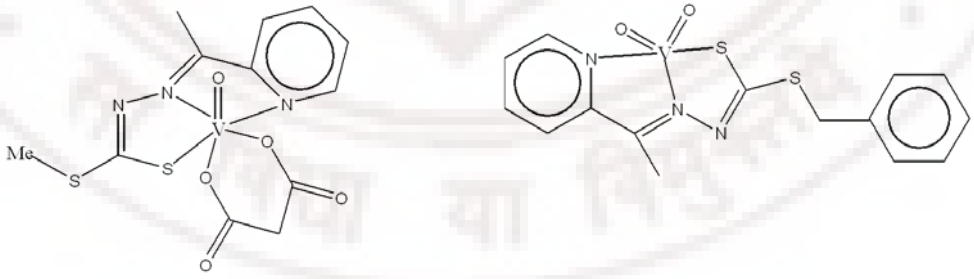

Fig. 1.7. Vanadium(V) complexes with N,N,S-donor ligands.

1.2.4.2.4. [VOL(OO)] type complexes

It has been observed that one molecule of acetylacetonate of $[VO(acac)_2]$ undergoes ligand exchange reaction while the other remains intact with vanadium when monobasic tridentate O,N,N- or N,N,N-donor ligands react with $[VO(acac)_2]$ (Fig. 1.8).

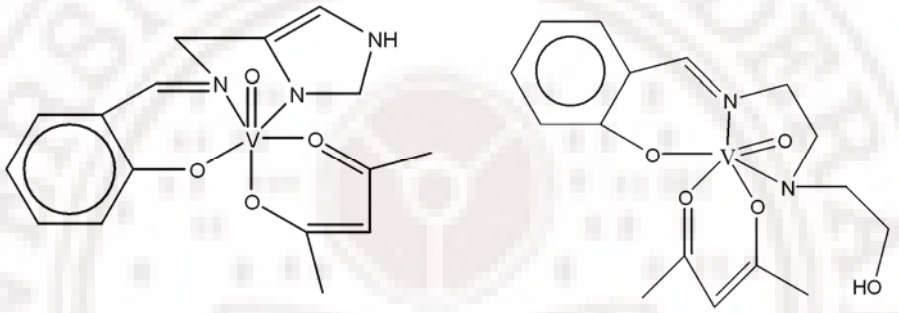

Fig. 1.8. Examples of [VOL(OO)] complexes.

1.2.4.2.5. Mixed-valent complexes

Dinuclear oxovanadium(IV,V) species containing $\{V_2O_3\}^{3+}$ core represent the largest class among the various types of mixed–oxidation compounds. As described by Dutta et. al[39] it can be prepared from the constituent $\{V^{IV}O\}^{2+}$ and $\{V^{V}O_2\}^{+}$ ions. The first reported complex of $\{VO(\mu\text{-}O)VO\}^{3+}$ was reported by Nishizawa et. al[40] (Fig. 1.9). Mixed valent complexes can also be prepared by reducing divanadium(V) complexes coulometrically at a constant potential as described by Chakravorty et. al.[41]

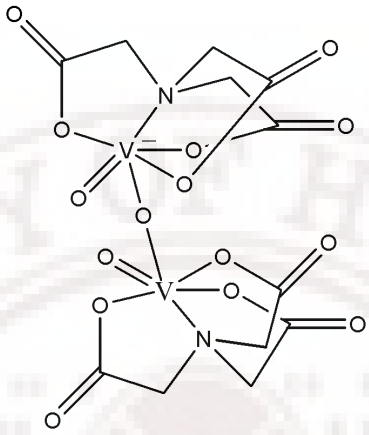

Fig. 1.9. The first example of a complex of $\{OV(\mu\text{-}O)VO\}^{3+}$ core.

1.3. About the present investigation

In the present investigation, we have used some hydrazine based compounds (Fig. 1.10) to explore the vanadium(IV/V) chemistry. We have been able to synthesize some ternary oxovanadium(IV), dioxovanadium(V),

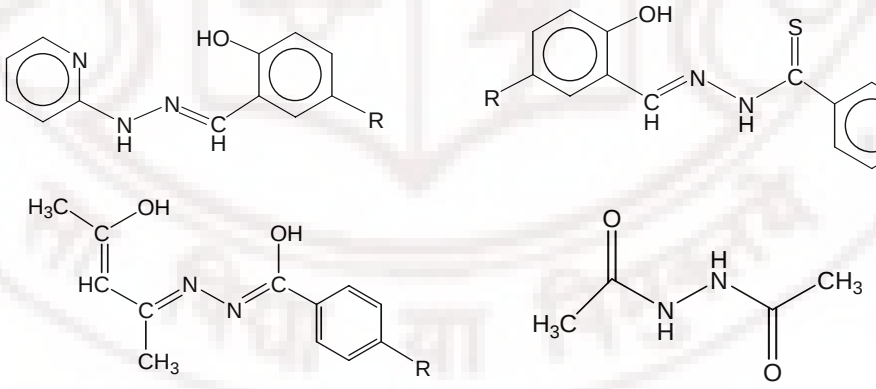

Fig. 1.10. Hydrazine based compounds.

oxomethoxovanadium(V), symmetrical $\{V_2O_3\}^{4+}$, unsymmetrical $\{V_2O_3\}^{3+}$ and tetravanadium(IV,V,V,IV) complexes. The complexes have been characterized with the help of elemental analysis, various spectroscopic and electrochemical measurements. Molecular structures of several complexes have been confirmed by X-ray crystallography. Self-assembly patterns via non-covalent intermolecular interactions have been also investigated. In the following chapters, we have described all these observations.

References

1 N.D. Chasteen (Ed.), *Vanadium in Biological Systems*, Kluwer, Dordrecht, 1990.

2. H. Sigel, A. Sigel (Eds.), *Metal Ions in Biological Systems*: *Vanadium and its Role in Life*, Vol. 31, Marcel Dekker, New York, 1995.
3. D. Rehder, *Coord. Chem. Rev*., 1999, **182**, 297.
4. R.R. Eady, *Coor. Chem. Rev.*, 2003, **237**, 23.
5. A. Butler, C.J. Carrano, *Coord. Chem. Rev*., 1991, **109**, 148.
6. R.N. Pau, in: M.J. Dilworth, A.R. Glenn (Eds.), *Biology and Biochemistry of Nitrogen Fixation*, Elsevier, Amsterdam, 1991, p. 37.
7. A. Butler, J.V. Walker, *Chem. Rev.*, 1993, **93**, 1937.
8. K.H. Thompson, J.H. McNeill, C. Orvig, *Chem. Rev*., 1999, **99**, 2561.
9. Y. Shechter, I. Goldwaser, M. Mironchik, M. Fridkin, D. Gefel, *Coord. Chem. Rev*., 2003, **237**, 3.
10. A.G.J. Ligtenbarg, R. Hage , B.L. Fering, *Coord. Chem. Rev.*, 2003, **237**, 89.
11. D. Rehder, *Inorg,. Chem. Commn*., 2003, **6**, 604.
12. C.D. Garner, E.M. Armstrong, R.E. Berry, R.L. Beddoes, D. Collison, J.J.A. Cooney, S.N. Ertok, M. Helliwell, *J. Inorg. Biochem*., 2000, **80**, 17.
13. M.R. Maurya, *J. Chem. Sci*., 2006, **118(6),** 503.
14. V. Conte, E.D. Funa, G. Licini, *Applied Catalysis A*, 1997, **157**, 335.

15. K.A. Jørgensen, *Chem Rev*., 1989, **89**, 435.
16. A. Kumar, Jr., S.K. Das, A. Kumar, *J. Catal*., 1997, **166**, 108
17. A. Butler, M.J. Clague, G.E. Meister, *Chem. Rev*., 1994, **94**, 625.
18. C. Slebodnick, B.J. Hamestra, V.L. Pecoraro, *Struct. Bond. (Berli*n) 1997, **89**, 51.
19. M.R. Maurya, *Coord. Chem. Rev*., 2003, **237**, 163.
20. L.J. Calviou, D. Collison, C.D. Garner, F.E. Mabbs, M.A. Passand, M. Pearson, *Polyhedron*, 1989, **8**, 1835.
21. M.R. Maurya, S. Khurana, *J. Chem. Res*.(S), 2002, 261
22. P.R. Klich, A.T. Daniher, P.R. Challen, D.B. McConville, W.J. Youngs, *Inorg. Chem*., 1996, **35**, 347.
23. J.K. Money, K. Folting, J.C. Huffmann, D. Collison, J. Temperley, F.E. Mabbs, G. Christou, *Inorg. Chem*., 1986, **25**, 4583.
24. S. Macedo-Ribeiro, W. Hemrika, R. Renirie, R. Wever, A. Messerschmidt, *J. Biol. Inorg. Chem*., 1999, **4**, 209.
25. S.K. Dutta, S.B. Kumar, S. Bhattacharyya, E.R.T. Tiekink, M. Chaudhury, *Inorg. Chem*., 1997, **36**, 4954.
26. S.K. Dutta, S. Samanta, S.B. Kumar, O.H. Han, P. Burckel, A.A. Pinkerton, M. Chaudhury, *Inorg. Chem*., 1999, **38**, 1982.
27. S.K. Dutta, S. Samanta, D. Ghosh, R.J. Butcher, M. Chaudhury, *Inorg. Chem*., 2002, **41**, 5555.
28. S. Samanta, D. Ghosh, S. Mukhopadhyay, A. Endo, T.J.R. Weakley, M. Chaudhury, *Inorg. Chem*., 2003, **42**, 1508.
29. S. Samanta, S. Mukhopadhyay, D. Mandal, R.J. Butcher, M. Chaudhury, *Inorg. Chem*., 2003, **42**, 6284.
30. M.R. Maurya, A. Kumar, A.R. Bhat, A. Azam, C. Bader, D. Rehder, *Inorg. Chem*., 2006, **45**, 1260.
31. N.R. Sangeetha, V. Kavita, S. Wocadlo, A.K. Powell, S. Pal, *J. Coord. Chem*., 2000, **51**, 55.

32. N.R. Sangeetha, S. Pal, *Bull. Chem. Soc. Jpn*., 2000, **73**, 357.
33. S.N. Pal, S. Pal, *J. Chem. Crystallogr*., 2000, **30,** 329.
34. S.N. Pal, S. Pal, *Acta Crystallogr. Sect. C*, 2001, **57**, 141.
35. S.N. Pal, K.R. Rahika, S. Pal, *Z. Anorg. Allg. Chem*., 2001, **627**, 1631.
36. P.J. Bosserman, D.T. Sawyer, *Inorg. Chem.*, 1982, **21**, 1545
37. G. Asgedom, A. Sreedhara, J. Kivikoski, C.P. Rao, *Polyhedron*, 1997, **16**, 643.
38. M.R. Maurya, S. Khurana, C. Schulzke, D. Rehder, *Eur. J. Inorg. Chem*., 2001, 779.
39. S.K. Dutta, S.B. Kumar, S. Bhattacharyya, E.R.T. Tieknick, M. Chaudhury, *Inorg. Chem.,* 1997, **36**, 4954.
40. Nishizawa. M, Hirotsu. K, Ooi. S, Saito. K, *J. Chem. Soc. Chem. Commun.,* 1979, 707.
41. S. Mondal, S.P. Rath, S. Dutta, A. Chakravorty, *J. Chem. Soc. Dalton Trans.*, 1996, 99.

Ternary complexes of oxovanadium(IV) with acetylacetone and N-(2-pyridyl)-N′-(5-R-salicylidene)hydrazines

2.1. Abstract

The reactions of one equivalent each of [VO(acac)$_2$] and N-(2-pyridyl)-N'-(5-R-salicylidene)hydrazines (HphsalR) (derived from 2-hydrazinopyridine and 5-substituted salicylaldehydes) in boiling acetonitrile under aerobic conditions provide ternary complexes of oxovanadium(IV) having the general formula [VO(phsalR)(acac)]. The complexes have been characterized by analytical, magnetic and spectroscopic measurements. The structures of two representative complexes have been determined by X-ray crystallography. In each structure, the metal centre is in a distorted octahedral N_2O_4 coordination sphere. The tridentate phsalR$^-$ coordinates the metal ion via the pyridine-N, the imine-N and the phenolate-O atoms in a meridional fashion. The remaining three coordinations sites are occupied by the bidentate O, O-donor acetylacetonate (acac$^-$) and the oxo group. In the crystal lattice, the molecules of each of the two complexes assemble to form one-dimensional supramolecular structure via intermolecular N–H$^{\cdots}$O=V hydrogen bond interaction. Electronic spectra collected using dimethylsulfoxide solutions of the complexes display a weak absorption within 643–720 nm due to d–d transition and some strong absorptions in the range 510–262 nm due to ligand-to-metal charge transfer and ligand centred transitions. The room temperature (298 K) effective magnetic moments of the complexes in the solid state are consistent with an S = 1/2 ground state of the metal ion in each complex. All the complexes display axial EPR spectra with well-resolved ^{51}V hyperfine

structure characteristic of an axially compressed octahedral coordination geometry around the metal centre.

2.2. Introduction

There are several examples of dioxovanadium(V) complexes which are synthesized under aerobic condition using aroylhydrazine based Schiff bases and [VO(acac)$_2$] as the precursors.[1-5] In this chapter, we have explored the synthetic chemistry using [VO(acac)$_2$] and an O,N,O-donor Schiff base system N-(2-pyridyl)-N′-(5-R-salicylidene)hydrazine (HphsalR, H represents the dissociable phenolic OH proton). In the deprotonated state (phsalR$^-$) can coordinate a metal ion via the pyridine-N, the imine-N and the phenolate-O atoms. However, under similar reaction conditions ternary complexes of oxovanadium(IV) have been isolated instead of dioxovanadium(V) complexes as observed before.[3-5] In the following account, we have described the syntheses and the physical properties of these ternary complexes having the general formula [VO(phsalR)(acac)]. The solid state molecular structures and self-assembly patterns of two representative complexes have been investigated by X-ray crystallography.

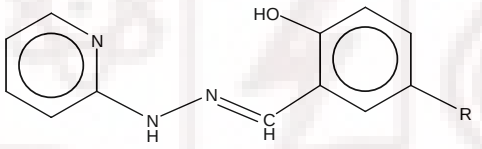

Hphsal (R = H)
HphsalOMe (R = OCH_3)
HphsalCl (R = Cl)
HphsalBr (R = Br)
HphsalNO_2 (R = NO_2)

2.3. Experimental

2.3.1. Materials

The Schiff bases were prepared in 70–80% yield by condensation reactions of 2-hydrazinopyridine with the corresponding 5-substituted salicylaldehyde in methanolic media.[6,7] Bis(acetylacetonato)oxovanadium(IV) was prepared by following a reported procedure.[8] All other chemicals and solvents used in this work were of analytical grade available commercially and were used without further purification.

2.3.2. Physical measurements

Microanalytical (C, H, N) data were obtained with a Thermo Finnigon Flash EA1112 series elemental analyzer. Infrared spectra were collected by using KBr pellets on a Jasco-5300 FT-IR spectrophotometer. A Shimadzu 3101-PC UV/vis/NIR spectrophotometer was used to record the electronic spectra. EPR spectra were recorded on a Jeol JES-FA200 spectrometer. Solution electrical conductivities were measured with a Digisun DI-909 conductivity meter. A Sherwood Scientific balance was used for magnetic susceptibility measurements. Diamagnetic corrections calculated from Pascal's constants[9] were used to obtain the molar paramagnetic susceptibilities.

2.3.3. Synthesis of [VO(phsal)(acac)] (1)

An acetonitrile solution (10 ml) of Hphsal (81 mg, 0.38 mmol) was added to an acetonitrile solution (25 ml) of [$VO(acac)_2$] (100 mg, 0.38 mmol). The mixture was heated on a water bath for 15–20 min. The resulting dark brown solution was kept in air at room temperature. Dark brown crystalline material separated in about 1–2 h was collected by filtration, washed with acetonitrile and finally dried in air. Yield, 65 mg (45%).

The other four complexes [VO(phsalOMe)(acac)] (**2**), [VO(phsalCl)(acac)] (**3**), [VO(phsalBr)(acac)] (**4**) and [$VO(phsalNO_2)$(acac)] (**5**) were synthesized from acetonitrile media using one mole equivalent each

of $[VO(acac)_2]$ and the corresponding Schiff base in 30–48% yields by following similar procedures as described above.

2.3.4. X-ray crystallography

Single crystals of both [VO(phsal)(acac)] (**1**) and [VO(phsalCl)(acac)] (**3**) were collected directly from the products precipitated in the synthetic reaction mixtures. In each case, unit cell parameters and the intensity data were obtained on a Bruker-Nonius SMART APEX CCD single crystal diffractometer, equipped with a graphite monochromator and a Mo $K\alpha$ fine-focus sealed tube (λ = 0.71073 Å) operated at 2.0 kW. The detector was placed at a distance of 6.0 cm from the crystal. Data were collected at 298 K with a scan width of 0.3º in ω and an exposure time of 15 sec/frame. The SMART software was used for data acquisition and the SAINT-Plus software was used for data extraction.[10] The absorption corrections were performed with the help of SADABS program.[11] The structures were solved by direct methods and refined on F^2 by full-matrix least-squares procedures. Both complexes crystallize in the space groups $P2_1/c$. All non-hydrogen atoms were refined using anisotropic thermal parameters. The hydrogen atoms were included in the structure factor calculations at idealized positions by using a riding model but not refined. The SHELX-97 programs[12] were used for structure solution and refinement. ORTEX6a[13] and Platon[14] packages were used for molecular graphics. Selected crystallographic data for both **1** and **3** are listed in Table 2.1.

Table 2.1. Crystallographic data for [VO(phsal)(acac)] (**1**) and [VO(phsalCl)(acac)] (**3**)

Complex	**1**	**3**
Chemical formula	$VC_{17}H_{17}N_3O_4$	$VC_{17}H_{16}N_3O_4Cl$
Formula weight	378.28	412.72
Crystal system	monoclinic	monoclinic
Space group	$P2_1/c$	$P2_1/c$
a (Å)	8.3504(15)	9.1819(10)
b (Å)	16.434(3)	15.9499(17)
c (Å)	12.2006(18)	12.3903(13)
β (°)	97.86(2)	91.221(2)
V (Å^3)	1658.5(5)	1814.2(3)
Z	4	4
ρ (g cm^{-3})	1.515	1.511
μ (mm^{-1})	0.626	0.722
Reflections collected	19001	14668
Reflections unique	3978	3569
Reflections [$I \geq 2\sigma(I)$]	3395	3121
R_1, wR_2 [$I \geq 2\sigma(I)$][a, b, c]	0.0626, 0.1427	0.0498, 0.1198
R_1, wR_2 [all data][b, c]	0.0737, 0.1487	0.0575, 0.1242
GOF on F^2	1.209	1.095
Largest peak and		

hole (e Å^3)	0.826, –0.261	0.449, –0.219

[a]$R_1 = \sum||F_o| - |F_c||/\sum|F_o|$. [b] w$R_2 = \{\sum[(F_o^2 - F_c^2)^2]/\sum[w(F_o^2)^2]\}^{1/2}$. [c] GOF = $\{\sum[w(F_o^2 - F_c^2)^2]/(n - p)\}^{1/2}$ where 'n' is the number of reflections and 'p' is the number of parameters refined.

2.5. Results and discussion

2.5.1. Synthesis and some properties

All the complexes were synthesized from acetonitrile media by reacting $[VO(acac)_2]$ and HphsalR in 1:1 mole ratio. The elemental analysis data are consistent with the general molecular formula [VO(phsalR)(acac)] (Table 2.2). Unlike previously reported complexes from our lab[3-5] there is no oxidation of the metal ion in the present reactions. Only one acetylacetonate of $[VO(acac)_2]$ has been replaced by phsalR^- and the ternary complexes are formed. The complexes are insoluble in common organic solvents except dimethylsulphoxide and dimethylformamide. In solutions, they are electrically non-conducting. The room temperature (298 K) magnetic moments of the complexes in the solid state are in the range 1.68–1.92 μ_B (Table 2.4). These values are consistent with an S = 1/2 ground state expected for the metal ion in mononuclear oxovanadium(IV) species.

Table 2.2. Elemental analysis data

Complex	**Found (Calc.) (%)**		
	C	H	N
[VO(phsal)(acac)] (**1**)	53.85 (53.98)	4.42 (4.53)	10.98 (11.11)
[VO(phsalOMe)(acac)] (**2**)	52.73 (52.95)	4.73 (4.69)	10.14 (10.29)
[VO(phsalCl)(acac)] (**3**)	49.22 (49.47)	4.05 (3.91)	9.89 (10.18)
[VO(phsalBr)(acac)] (**4**)	44.39 (44.66)	3.38 (3.53)	8.97 (9.19)
[VO(phsalNO_2)(acac)] (**5**)	47.98 (48.24)	3.75 (3.81)	13.15 (13.24)

2.5.2. Spectroscopic properties

Infrared spectra of the complexes display a strong band in the range 1622–1634 cm^{-1}. The origin of this band is most probably the C=N stretch of the tridentate Schiff base ligand.[1-3,15,16] A broad band centered at ~3400 cm^{-1} is attributed to the N–H stretch of the hydrazine fragment of the ligand. Two medium to strong bands observed in the ranges 1512–1553 and 1582–1601 cm^{-1} are most likely due to the coupled C=C and C=O stretches of the acetylacetonate moiety.[17] In all the spectra, the V=O stretch appears as a strong band within 928–949 cm^{-1} (Table 2.4). These values are consistent with the V=O stretching frequencies reported for distorted octahedral oxovanadium(IV) species.[18,19]

The dimethylsulfoxide solutions of the complexes have been used to record the electronic spectra. The main features of all the spectra are quite similar. A representative spectrum is shown in Fig. 2.1 and the spectral data are given in Table 2.3. There are two major absorptions within the ranges 510–420 and 383–340 nm in the visible region. These are attributed to the ligand-to-metal charge transfer transitions (LMCT). The high energy absorption (275–262 nm) is most likely due to a transition involving ligand orbitals only. The complexes **1**–**3** show an additional weak absorption in the range 643–720 nm due to d-d transition.[18-20] For complexes **4** and **5** this absorption is probably obscured by the tail of the following LMCT band.

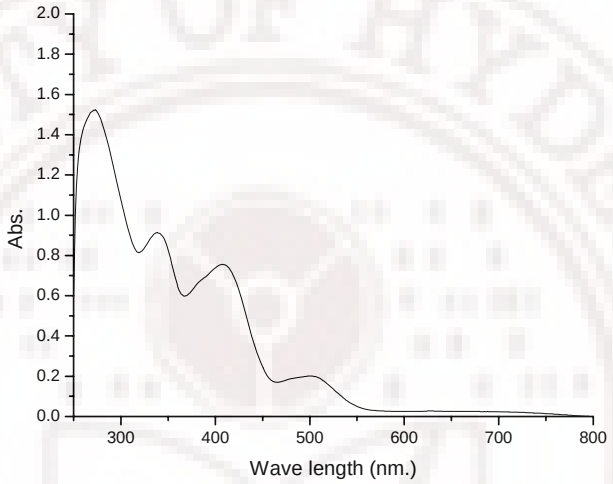

Fig. 2.1. Electronic spectrum of [VO(phsal)(acac)] (**1**) in dimethylsulphoxide solution.

Complex	**λ_{max} (nm) (10^{-3} x ε (M^{-1} cm^{-1}))**
[VO(phsal)(acac)] (**1**)	670[b] (0.09), 503 (1.8), 480[b] (1.7), 362 (1.8), 275[b] (2.9)
[VO(phsalOMe)(acac)] (**2**)	720 (0.03), 510 (1.9), 489[b] (1.8), 383 (2.1), 267 (3.4)
[VO(phsalCl)(acac)] (**3**)	643 (0.03), 420 (0.7), 340 (0.9), 275[b] (1.3)
[VO(phsalBr)(acac)] (**4**)	510 (2.4), 488[b] (2.2), 370 (1.8), 265[b] (5.9)
[VO(phsalNO_2)(acac)] (**5**)	500 (5.2), 485[b] (5.1), 356 (7.6), 262[b] (5.5)

[a] In dimethylsulfoxide solution.
[b] Shoulder.

EPR spectra of the complexes have been collected using powdered samples as well as dimethylsulfoxide solutions. At room temperature (298 K) the powdered samples of **1** and **5** display an isotropic signal at g = 1.98 and 2.0, respectively. Interestingly the powdered samples of complexes **2**–**4** at 298 K display well resolved axial spectra with ^{51}V (I = 7/2) hyperfine structure having $g_{\|}$ ~ 1.94 ($A_{\|}$ ~ 178 G) and $g_{\perp}$ ~ 1.98 ($A_{\perp}$ ~ 60 G). Lowering of temperature to 123 K makes the signals more sharp for **2**–**4**. In the case of **1**, a similar well resolved axial spectrum is observed at 123 K instead of the isotropic signal observed at room temperature. On the other hand, for **5** the hyperfine structure due to the metal centre is reasonably resolved for the $g_{\|}$ component and partially resolved for the $g_{\perp}$ component. The observation of the isotropic signal for **1** and **5** at room temperature could be due to several factors such as spin-spin interaction, exchange interactions, spin-lattice relaxation and dynamic Jahn-Teller effect. Considering that the metal ion is coordinatively saturated in all the complex molecules (**1**–**5**) which differ only by the substituent on the tridentate ligand and the observation of the resolved spectrum at low temperature, it appears that one of the last two factors or both are responsible for the different behavior of **1** and **5**. The spectra of the complexes in frozen (123 K) dimethylsulfoxide solutions are grossly identical and very similar with the powder phase spectra observed at 298 and 123 K for **2**–**4** and at 123 K for **1**. The frozen solution spectral parameters are listed in Table 2.4 and a representative spectrum is shown in Fig. 2.2. The $g_{\|} < g_{\perp}$ and $A_{\|} > A_{\perp}$ relationships for all the complexes are consistent with an axially compressed octahedral geometry around the vanadium (IV) centre with the unpaired electron in the d_{xy} orbital.[21,22]

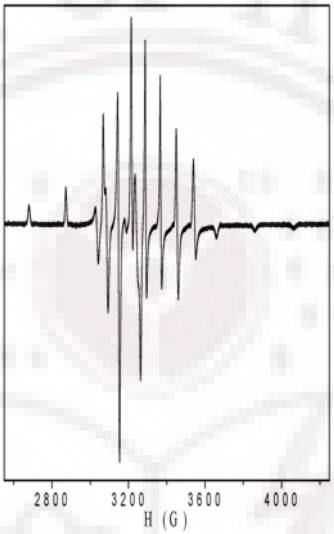

Fig. 2.2. EPR spectrum of [VO(phsalCl)(acac)] (**3**) in frozen (123 K) dimethylsulfoxide solution.

Table 2.4. Magnetic susceptibility[a], infrared [b] and EPR [c] spectroscopic data

Complex	μ_{eff} (μ_B)	$\nu_{V=O}$ (cm^{-1})	$g_{\|}(A_{\|}$ (G))	$g_{\perp}(A_{\perp}$ (G))
[VO(phsal)(acac)] (**1**)	1.78	928	1.95 (178)	1.99 (66)
[VO(phsalOMe)(acac)] (**2**)	1.72	943	1.99 (179)	1.99 (65)
[VO(phsalCl)(acac)] (**3**)	1.82	945	1.93 (198)	1.99 (73)
[VO(phsalBr)(acac)] (**4**)	1.68	949	1.95 (178)	1.99 (73)
[VO(phsalNO_2)(acac)] (**5**)	1.92	937	1.95 (178)	1.99 (67)

[a] In 298 K.
[b] In KBr disk.

[c] In frozen (123 K) dimethylsulfoxide solution.

2.5.3. Molecular structures of [VO(phsal)(acac)] (1) and [VO(phsalCl)(acac)] (3)

The molecular structures of **1** and **3** are depicted in Figs. 2.3 and 2.4., respectively. Bond parameters associated with the metal ions in both complexes are listed in Table 2.5. In each complex molecule, the metal centre is in a distorted octahedral N_2O_4 coordination sphere assembled by the pyridine-N, the imine-N and the phenolate-O donor phsalR^- (R = H or Cl), the O, O-donor acetylacetonate ($acac^-$) and the oxo group. The meridionally spaning tridentate ligand and one of the O-atom of $acac^-$ form a N_2O_2 square plane around the metal centre. The remaining two axial sites are occupied by the oxo group and the second O-atom of $acac^-$. The chelate bite angles are

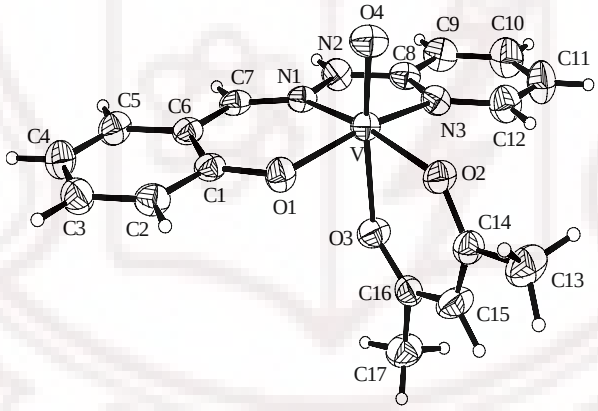

Fig. 2.3. Molecular structure of (a) [VO(phsal)(acac)] (**1**) with the atom labeling scheme. All non-hydrogen atoms are represented by their 40% probability thermal ellipsoids.

unexceptional and comparable in **1** and **3**. The V–N(pyridine), the V–N(imine) and the V=O bond lengths are very similar in both structures. However, the V–O(phenolate) bond length is slightly longer in **3** than that in **1**. This difference is possibly due to the electron withdrawing effect of the Cl-atom at the *para* position of the phenolate-O in **3**. Not surprisingly the two V–O bond lengths associated with the $acac^-$ ligand are different in both complexes. The V–O bond which is *trans* to the oxo group is significantly longer than the V–O bond which is *cis* to the oxo group (Table 2.5). The *cis* and *trans* V–O bond lengths observed in **1** and **3** are comparable with those reported for oxovanadium(IV) species containing $acac^-$ as ligand in the same orientation.[21,26] In general, all the metal to coordinating atom bond lengths in both **1** and **3** are within the ranges reported for octahedral vanadium(IV) species containing the same coordinating atoms.[18,19,21-23]

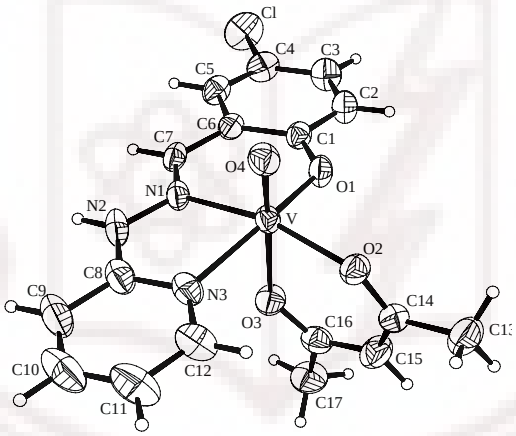

Fig. 2.4. Molecular structure of [VO(phsalCl)(acac)] (**3**) with the atom labeling scheme. All non-hydrogen atoms are represented by their 40% probability thermal ellipsoids.

Table 2.5. Selected bond lengths and angles for [VO(phsal)(acac)] (**1**) and [VO(phsalCl)(acac)] (**3**)

	1	**3**
Bond lengths (Å)		
V–N(1)	2.066(2)	2.066(2)
V–N(3)	2.121(2)	2.119(2)
V–O(1)	1.935(2)	1.9485(18)
V–O(2)	1.9837(18)	1.9787(18)
V–O(3)	2.182(2)	2.1769(19)
V–O(4)	1.6147(19)	1.6113(18)
Bond angles (°)		
N(1)–V–O(1)	88.72(8)	88.96(8)
N(1)–V–O(2)	165.96(8)	164.22(8)
N(1)–V–O(3)	83.52(8)	81.65(8)
N(1)–V–O(4)	99.05(9)	100.04(9)
N(1)–V–N(3)	76.57(9)	76.66(9)
N(3)–V–O(1)	158.55(8)	159.95(8)
N(3)–V–O(2)	97.02(9)	96.44(9)
N(3)–V–O(3)	78.40(8)	80.51(8)
N(3)–V–O(4)	96.30(10)	95.20(9)
O(1)–V–O(2)	93.70(8)	93.82(8)
O(1)–V–O(3)	84.57(8)	83.67(8)

O(1)–V–O(4)	101.44(10)	101.09(10)
O(2)–V–O(3)	82.94(8)	83.22(7)
O(2)–V–O(4)	94.03(9)	94.67(9)
O(3)–V–O(4)	173.47(10)	174.94(9)

2.5.4. Intermolecular hydrogen bonding and self-assembly

The type of complex molecules described in this work contain two major functionalities which can participate in intermolecular hydrogen bond interactions. These are the N–H group of the hydrazine fragment of the tridentate ligand and the metal coordinated oxo group. It may be noted that the acidity of the N–H proton increases significantly in aroyl- or arylhydrazine based Schiff bases when the adjacent imine–N is coordinated to a metal ion.[24] A similar situation is expected in the present series of complexes also. The vanadium (IV/V) bound oxo group is fairly strong basic centre and is known to participate in intermolecular weak C–H···O interactions.[7,23] Thus it is anticipated that the self-assembly of the molecules of both **1** and **3** in the crystal lattice will be guided by reasonably strong intermolecular N–H···O=V hydrogen bond interactions. Indeed this interaction is observed in both the structures. The N2···O4 distance and the N2–H···O4 angle are 2.909(3) Å and 177.4^{o} for **1** and 2.980(3) Å and 175.6^{o} for **3**. In each case, self-assembly of the complex molecules via these intermolecular N–H···O=V hydrogen bond interactions leads to one-dimensional supramolecular structure in the crystal lattice (Figure 2.6). There are no significant short contacts and hence no additional non-covalent interactions between the parallel one-dimensional structures.

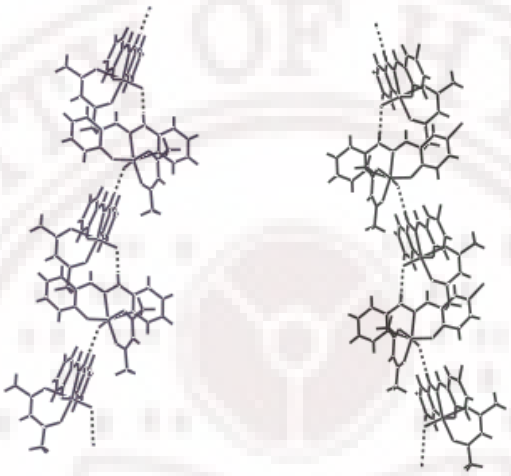

(a) (b)

Fig. 2.6. One-dimensional ordering of (a) [VO(phsal)(acac)] (**1**) and (b) [VO(phsalCl)(acac)] (**3**) in the crystal lattice.

2.6. Conclusion

The synthesis and physical properties of a new series of oxovanadium(IV) ternary complexes are described. The general formula of these complexes is [VO(phsalR)(acac)] where Hacac and HphsalR represent the bidentate acetylacetone and the tridentate Schiff base N-(2-pyridyl)-N′-(5-R-salicylidene)hydrazine, respectively. The identities of the complexes have been established by microanalytical, magnetic, spectroscopic and X-ray crystallographic methods. The complexes display ligand-field and ligand-to-metal charge transfer bands in the electronic spectra. The EPR spectra of the complexes are characteristic of an axially compressed d_{xy}^{1} configuration. The crystal structures show that the meridional pyridine-N, imine-N and phenolate-

O donor phsalR^{-}, the O,O-donor acac^{-} and the oxo group form a distorted N_2O_4 octahedron around the metal centre. In the crystal lattice, the complex molecules are self-organized to one-dimensional supramolecular structure via intermolecular N–H···O=V hydrogen bond interaction.

Supplementary material

Crystallographic data for [VO(phsal)(acac)] (**1**) and [VO(phsalCl)(acac)] (**3**) have been deposited with the Cambridge Crystallographic Data Centre (deposition numbers are CCDC 286182 and 286183 for 1 and 3, respectively).

2.8. References

1. N.R. Sangeetha, V. Kavita, S. Wocadlo, A.K. Powell, S. Pal, *J. Coord. Chem*., 2000, **51**, 55.
2. N.R. Sangeetha, S. Pal, *Bull. Chem. Soc. Jpn*., 2000, **73**, 357.
3. S.N. Pal, S. Pal, *J. Chem. Crystallogr*., 2000, **30**, 329.
4. S.N. Pal, S. Pal, *Acta Crystallogr. Sect. C*, 2001, **57**, 141.
5. S.N. Pal, K.R. Rahika, S. Pal, *Z. Anorg. Allg. Chem*., 2001, **627,** 1631.
6. M.F. Zady, J.L. Wong, *J. Org. Chem*, 1976, **41**, 2491.
7. C.C. Blanco, F.G. Sanchez, *Anal. Chem*., 1984, **56**, 2035.
8. R.A. Rowe, M.M. Jones, *Inorg. Synth*., 1957, **5**, 113.
9. W.E. Hatfield, in: E.A. Boudreaux, L.N. Mulay (Eds.), Theory and Applications of Molecular Paramagnetism, Wiley, New York, 1976, p. 491.
10. *SMART* version 5.630 and *SAINT*-plus version 6.45, Bruker-Nonius Analytical X-ray Systems Inc., Madison, WI, USA, 2003.
11. G.M. Sheldrick, *SADABS*, *Empirical Absorption Correction Program*, University of Göttingen, Göttingen, Germany, 1997.
12. G.M. Sheldrick, *SHELX-97, Structure Determination Software*, University of Göttingen, Göttingen, Germany, 1997.

13. P. McArdle, *J. Appl. Crystallogr*., 1995, **28**, 65.
14. A.L. Spek, *PLATON A Multipurpose Crystallographic Tool*, Utrecht University, Utrecht, The Netherlands, 2002.
15. A. Kumar, Jr., S.K. Das, A. Kumar, *J. Catal*., 1997, **166**, 108.
16. M.R. Maurya, *Coord. Chem. Rev*., 2003, **237**, 163.
17. K. Nakamoto, in: *Infrared and Raman Spectra of Inorganic and Coordination Compounds*, Wiley, New York, 1986, p. 259.
18. X. Li, M.S. Lah, V.L. Pecoraro, *Inorg. Chem*., 1988, **27**, 4657.
19. J.A. Bonadies, C.J. Carrano, *J. Am. Chem. Soc*., 1986, **108**, 4088.
20. C.J. Ballhausen, H.B. Gray, *Inorg. Chem*., 1962, **1**, 111.
21. P. Basu, S. Pal, A. Chakravorty, *J. Chem. Soc., Dalton Trans*., 1991, 3217.
22. J. Chakravarty, S. Dutta, A. Dey, A. Chakravorty, *J. Chem. Soc., Dalton Trans*., 1994, 557.
23. S.P. Anthony, L. Srikanth, T.P. Radhakrishnan, *Mol. Cryst. Liq. Cryst*., 2002, **381**, 133.
24. S.N. Pal, S. Pal, *J. Chem. Soc., Dalton Trans*., 2002, 2102.

Chapter 3

Dioxovanadium(V) complexes with N-(2-pyridyl)-N′-(5-R-salicylidene)hydrazines

3.1. Abstract

Dioxovanadium(V) complexes having the general formula $[VO_2(phsalR)]$ have been synthesized in 52–63% yields by reacting one mole equivalent each of $VOSO_4{\cdot}5H_2O$, 4-R-2-(pyridin-2-yl-hydrazonomethyl)-phenols (HphsalR, where R = H, OCH_3, Cl, Br and NO_2) and $N(C_2H_5)_3$ in water-acetonitrile (1:1.3) mixture. The complexes have been characterized by elemental analysis, magnetic and spectroscopic measurements. The physical properties of the complexes are consistent with the +5 oxidation state of the metal ion in them. The X-ray structure of a representative complex, $[VO_2(phsal)]$ (R = H) has been determined. The metal centre in $[VO_2(phsal)]$ is in square-pyramidal N_2O_3 coordination sphere. The monoanionic pyridine-N, imine-N and phenolate-O donor $phsal^-$ and one of the two oxo groups form the N,N,O,O basal plane and the other oxo group satisfies the fifth apical coordination site. This square-pyramidal molecules form dimeric units due to the participation of the oxo group at the basal plane in the V–O–V bridge formation. The structure of the dimeric species $[VO_2(phsal)]_2$ can be described as two edge-shared VN_2O_4 octahedra. In the crystal lattice, these dimeric units form infinite one-dimensional chain structure via intermolecular N–H···O=V hydrogen bonding interaction.

3.2. Introduction

In our attempts to prepare complexes of VO_2^+ with a N,N,O-donor Schiff base system N-(2-pyridyl)-N′-(5-R-salicylidene)hydrazine (HphsalR) using $[VO(acac)_2]$ as the precursor, we have isolated some ternary oxovanadium(IV) complexes of formula [VO(phsalR)(acac)]. In the previous chapter these ternary complexes have been described. To explore further the coordination chemistry of oxovanadium species with HphsalR, we have used $VOSO_4 \cdot 5H_2O$ as the precursor and isolated dioxovanadium(V) complexes with the general formula $[VO_2(phsalR)]$. In this chapter, we have described the synthesis, characterization and physical properties of these complexes. The molecular structure of a representative complex has been determined by X-ray crystallography.

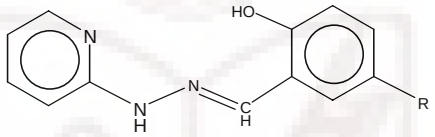

Hphsal (R = H)
HphsalOMe (R = OCH_3)
HphsalCl (R = Cl)
HphsalBr (R = Br)
HphsalNO_2 (R = NO_2)

3.3. Experimental

3.3.1. Materials

The Schiff bases (HphsalR) were prepared in as described in the preceding chapter. All other chemicals and solvents used in this work were of analytical grade available commercially and were used without further purification.

3.3.2. Physical measurements

Microanalytical (C, H, N) data were obtained with a Thermo Finnigon Flash EA1112 series elemental analyzer. Infrared spectra were collected by using KBr pellets on a Jasco-5300 FT-IR spectrophotometer. A Sherwood Scientific balance was used for magnetic susceptibility measurements. A Shimadzu 3101-PC UV/vis/NIR spectrophotometer was used to record the electronic spectra. The proton NMR spectra were recorded with the help of a Bruker 400 MHz spectrometer. A Jeol JES-FA200 spectrometer was used for EPR experiments. Solution electrical conductivities were measured with a Digisun DI-909 conductivity meter

3.3.3. Synthesis of $[VO_2(phsal)]$ (6*)*

An aqueous solution (15 ml) of $VOSO_4 \cdot 5H_2O$ (100 mg, 0.4 mmol) was added to an acetonitrile solution (20 ml) of Hphsal (85 mg, 0.4 mmol) and $N(C_2H_5)_3$ (0.07 ml, 51 mg, 0.5 mmol). The mixture was refluxed for 1h. The resulting brown solution was kept in air at room temperature for slow evaporation. Dark brown crystalline material separated in about 2 days was collected by filtration, washed with acetonitrile and finally dried in air. Yield, 60 mg (51%).

The other four complexes $[VO_2(phsalOCH_3)]$ (**7**), $[VO_2(phsalCl)]$ (**8**), $[VO_2(phsalBr)]$ (**9**) and $[VO_2(phsalNO_2)]$ (**10**) reported in this work were synthesized by using one mole equivalent each of $VOSO_4 \cdot 5H_2O$, $N(C_2H_5)_3$ and the corresponding Schiff base in 50–60% yields by following the same procedure as described above.

3.3.4. X-ray crystallography

Single crystal of $[VO_2(phsal)]$ (**6**) was collected directly from the product precipitated in the synthetic reaction mixture. The unit cell parameters and the intensity data were obtained on a Bruker-Nonius SMART APEX CCD single crystal diffractometer, equipped with a graphite monochromator and a Mo $K\alpha$ fine-focus sealed tube (λ = 0.71073 Å) operated at 2.0 kW. The detector was placed at a distance of 6.0 cm from the crystal. Data were collected at 298 K with a scan width of 0.3º in ω and an exposure time of 5 s/frame. The SMART software was used for data acquisition and the SAINT Plus software was used for data extraction.[1] The SADABS program[2] was used for the absorption correction. The complex crystallizes in the space group $P\bar{1}$. The structure was solved by direct method and refined on F^2 by full-matrix least-squares procedures. All non-hydrogen atoms were refined anisotropically. The hydrogen atom of the NH group in the hydrazine fragment of the ligand was located on a difference map and refined with $U_{iso}(H) = 1.2U_{eq}(N)$. The other hydrogen atoms were added at idealized positions by using a riding model. The SHELX-97 programs[3] were used for structure solution and refinement. The ORTEX6a[4] and Platon[5] packages were used for molecular graphics. Selected crystallographic data for **6** are listed in Table 3.1.

Table 3.1. Crystallographic data for $[VO_2(phsal)]$ (**6**)

Complex	**3**
Chemical formula	$VC_{12}H_{10}N_3O_3$
Formula weight	295.17
Crystal system	Triclinic
Space group	$P\ \bar{1}$
a (Å)	6.9432(13)
b (Å)	7.8457(15)
c (Å)	11.359(2)
α (°)	91.024(3)
β (°)	99.877(3)
γ (°)	101.149(3)
V (Å^3)	597.3(2)
Z	2
ρ (g cm^{-3})	1.641
μ (mm^{-1})	0.837
Reflections collected	6960
Reflections unique	2768
Reflections [$I \geq 2\sigma(I)$]	2260
Parameters	175
R_1, wR_2 [$I \geq 2\sigma(I)$][a, b, c]	0.0459, 0.1054
R_1, wR_2 [all data][b, c]	0.0598, 0.1113
GOF on F^2	1.080
Largest peak and hole (e Å^{-3})	0.506, –0.256

[a] $R_1 = \sum||F_o| - |F_c||/\sum|F_o|$. [b] $wR_2 = \{\sum[(F_o^2 - F_c^2)^2]/\sum[w(F_o^2)^2]\}^{1/2}$.
[c] GOF = $\{\sum[w(F_o^2 - F_c^2)^2]/(n - p)\}^{1/2}$ where 'n' is the number of reflections and 'p' is the number of parameters refined.

3.4. Results and discussion

3.4.1. Synthesis and some properties

The complexes were synthesized in moderate yields by reacting equimolar amounts of $VOSO_4 \cdot 5H_2O$, HphsalR and $N(C_2H_5)_3$ in water-acetonitrile mixture under aerobic condition. The elemental analysis data are consistent with the general molecular formula $[VO_2(phsalR)]$ (Table 3.2). The complexes are insoluble in common organic solvents except dimethylsulphoxide and dimethylformamide. In solutions, they are electrically non-conducting. The EPR silence and the room temperature magnetic susceptibilities indicate the diamagnetic character of these complexes. Thus the metal ion in each of the five complexes is in +5 oxidation state. Most likely during the formation of these complexes from oxovanadium(IV) starting material, the aerial oxygen acts as the oxidizing agent.

Table 3.2. Elemental analysis[a] data

Complex	**Found (Calc.) (%)**		
	C	**H**	**N**
$[VO_2(phsal)]$ (**6**)	48.72 (48.83)	3.35 (3.41)	14.18 (14.24)
$[VO_2(phsalOMe)]$(**7**)	47.83 (48.01)	3.62 (3.72)	12.79 (12.92)
$[VO_2(phsalCl)]$ (**8**)	43.65 (43.73)	2.71 (2.75)	12.66 (12.75)
$[VO_2(phsalBr)]$ (**9**)	38.41 (38.53)	2.45 (2.42)	11.15 (11.23)
$[VO_2(phsalNO_2)]$ (**10**)	42.14 (42.37)	2.38 (2.67)	16.33 (16.47)

[a] Calculated values are in parentheses.

3.4.2. Spectroscopic characteristics

The infrared spectra of **6**–**10** display a broad band centred at ~3400 cm^{-1}. This band is possibly due to the N–H stretch of the hydrazine fragment of the ligand.[6] The strong band observed in the range 1632–1636 cm^{-1} is assigned to the C=N stretch of the tridentate Schiff base ligand.[7-11,12] The complexes of dioxovanadium(V) display two strong to medium bands in the ranges 930–970 and 900–940 cm^{-1}. The higher energy band is assigned to the ν_{as} stretch and the lower energy band is assigned to ν_{s} stretch of the *cis*-VO_2^+ moiety.[9-11,13-16] The present series of complexes (**6–10**) display a strong and sharp band at ~942 cm^{-1}. This band is attributed to the ν_{as} stretch of the *cis*-VO_2^+ moiety. All the spectra show a very strong band at ~890 cm^{-1} with a shoulder at ~910 cm^{-1}. Perhaps the ν_{s} stretch of the *cis*-VO_2^+ unit is the origin of this shoulder. A representative spectrum is illustrated in Fig. 3.1.

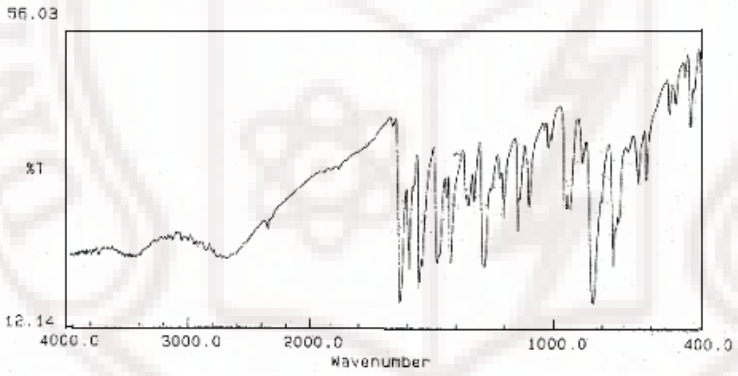

Fig. 3.1. Infrared spectrum of [VO_2(phsal)] (**6**) in KBr disk.

Electronic spectra were recorded using dimethylformamide solutions of **6**–**10**. The spectral profiles of all the complexes are very similar. A representative spectrum is shown in Fig. 3.2. The complexes display several absorptions in the wavelength range 512–270 nm (Table 3.3). The

absorptions in the range 512–350 nm are possibly due to the ligand-to-metal charge transfer transitions.[7-11,13-16] The highest energy absorption observed in the range 280–270 nm is most likely due to a ligand centred transition.

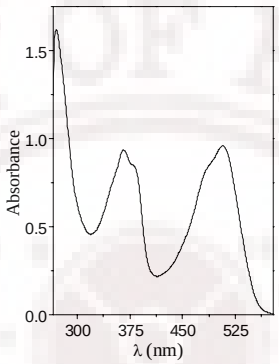

Fig. 3.2. Electronic spectrum of [VO_2(phsalCl)] (**8**) in dimethylformamide solution.

Table 3.3. Electronic spectroscopic[b] data

Complex	**λ_{max} (nm) (10^{-4} x ε (M^{-1} cm^{-1}))**
[VO_2(phsal)] (**6**)	505 (1.18), 480[c] (1.11), 418[c] (0.89), 380[c] (1.55), 360 (1.75), 280[c] (2.58)
[VO_2(phsalOMe)](**7**)	510 (1.09), 485[c] (0.99), 385[c] (1.16), 370 (1.31), 272 (2.13)
[VO_2(phsalCl)] (**8**)	510 (0.96), 480[c] (0.82), 385[c] (0.84), 365 (0.93), 270 (1.58)
[VO_2(phsalBr)] (**9**)	507 (1.60), 485[c] (1.38), 385[c] (1.50), 368 (1.66), 275 (2.59)
[VO_2(phsalNO_2)] (**10**)	512 (1.13), 488[c] (1.03), 375[c] (1.62), 350 (1.93), 275[c] (1.44)

[b] In dimethylformamide.
[c] Shoulder.

The dimethylsulphoxide-d_6 solutions of **6**–**10** were used to record the proton NMR spectra. The aromatic protons appear as multiplets in the range δ 8.5–6.8 ppm. The protons of the methyl group of the methoxy substituent in $[VO_2(phsalOCH_3)]$ (**7**) resonate as a singlet at δ 3.74 ppm. The –NH– proton of the hydrazine fragment in all the complexes appears as a broad singlet within δ 12.65–12.87 ppm. The azomethine (–CH=N–) proton is observed as a singlet in the range δ 8.55–8.59 ppm. We have also recorded ^{51}V NMR spectra of **6**–**10** in dimethylsulphoxide-d_6. All the complexes show a resonance between δ –549 and –555 ppm. These chemical shifts are comparable with those reported for similar dioxovanadium (V) complexes.[13,15-17]

3.4.3. Molecular structure of $[VO_2(phsal)]$ (6)

Dioxovanadium (V) complexes with planar tridentate ligands can have either trigonal-bipyramidal or square-pyramidal geometry.[9-11,13-15,17-19] In the solid state, trigonal-bipyramidal complexes can dimerise and form di(μ-oxo) bridged dinuclear species. Examples of such di (μ-oxo) bridged species are rare.[9,13,17-19] The structure of **6** is depicted in Fig. 3.3. The bond parameters associated with the metal ion are listed in Table 3.4. The metal ion is in a square-pyramidal N_2O_3 coordination sphere. One of the two oxo groups and the pyridine-N, the imine-N and the phenolate-O donor $phsal^-$ form the N_2O_2 basal plane (mean deviation 0.07 Å). The second oxo group satisfies the apical coordination site. As commonly observed for square-pyramidal complexes[7-9,13,17-21] the metal centre in **6** is displaced by 0.367(1) Å from the N_2O_2 basal plane toward the apical oxo group. The distortion of a square-pyramidal geometry toward a trigonal bipyramidal geometry can be indicated by the value of τ which is defined as (β–α)/60, where α is the smaller and β is the larger *trans* bond angles in the basal plane.[21] For a perfect square-pyramidal geometry the value of τ is zero and for an ideal trigonal bipyramidal geometry the value of τ is unity. In the case of **6**, the τ is found to be 0.02.

Thus the N_2O_3 coordination sphere in **6** is very close to an ideal square-pyramidal shape. As expected the V–O(phenolate) (1.8797(18) Å) and V–N(pyridine) (2.112(2) Å) bond lengths in **6** (Table 3.4) are shorter than these bond lengths (1.935(2) and 2.121(4) Å) observed in the previously reported ternary oxovanadium(IV) complex with $phsal^-$ (Chapter 2). However, the V–N(imine) bond length (2.1706(19) Å) in **6** is longer than that (2.066(2) Å) in [VO(phsal)(acac)]. This difference is possibly due to the greater *trans* effect of the oxo group in **6** compared to that of the acetylacetonate-O in [VO(phsal)(acac)]. In general, the V–O(phenolate), the V–N(pyridine) and the V–N(imine) bond lengths in **6** are comparable with the bond lengths observed in VO^{3+} and VO_2^+ complexes containing the same coordinating atoms.[7-11,13-19] In **6**, the V=O bond length (1.6736(17) Å) in the basal plane is significantly longer than the apical V=O bond length (1.600(2) Å). This is due to the formation of a centrosymmetric dimeric species via sharing of the basal plane oxo groups by the metal centres of two molecules of **6** (Fig.3.3). Such di(μ-oxo) bridged complexes formed by dimerisation of square-pyramidal dioxovanadium(V) species are not very common.[9,13,17-19] In $[VO_2(phsal)]_2$, the $V_2(\mu\text{-}O)_2$ unit is planar and unsymmetrical with respect to the V–O distances (V–O2, 1.6736(17) Å and V–O2a, 2.5193(19) Å). The V–O2–V(a) and the O2–V–O2a angles are 103.08(8) and 76.92(8)°, respectively. The metal···metal distance is 3.325(1) Å. The long V–O2a distance suggests weak coordination at the *trans* position to the apical oxo group. Thus the metal centres are in distorted octahedral N_2O_4 cordination spheres in $[VO_2(phsal)]_2$ and the dimeric species resembles two edge-shared octahedra.

(a)

(b)

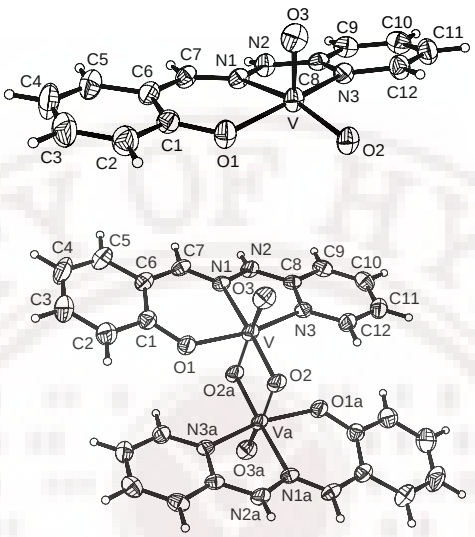

Fig. 3.3. Structure of (a) $[VO_2(phsal)]$ (**6**) with the atom labeling scheme (b) Centrosymmetric dimer of $[VO_2(phsal)]$ (**6**). All non-hydrogen atoms are represented by their 40% probability thermal ellipsoids.

Table 3.4. Selected bond lengths (Å) and angles (^{o}) for $[VO_2(phsal)]_2$(**6**)

Bond lengths			
V–O(1)	1.8797(18)	V–N(1)	2.1706(19)
V–O(2)	1.6736(17)	V–N(3)	2.112(2)
V–O(3)	1.600(2)	V–O(2a)	2.5193(19)
Bond angles			
O(1)–V–O(2)	102.27(8)	O(1)–V–O(3)	101.51(10)
O(1)–V–N(1)	83.06(8)	O(1)–V–N(3)	152.99(8)
O(1)–V–O(2a)	83.32(8)	O(2)–V–O(3)	107.55(9)
O(2)–V–N(1)	151.53(9)	O(2)–V–N(3)	93.05(8)
O(2)–V–O(2a)	76.92(8)	O(3)–V–N(1)	98.53(9)
O(3)–V–(N(3)	94.74(9)	O(3)–V–O(2a)	172.31(8)
N(1)–V–N(3)	73.22(8)	N(1)–V–O(2a)	75.97(6)
N(3)–V–O(2a)	78.62(7)	V–O(2a)–V	103.08(8)

Symmetry transformation used to generate the equivalent atoms: x, y, z + 1.

3.4.4. Intermolecular hydrogen bonding and self-assembly

The complexes (**6**–**10**) described in this work possess an acceptor as well as a donor group for conventional hydrogen bonding interaction. These are the metal coordinated oxo group and the N–H group of the hydrazine fragment of phsal^{-}. The vanadium(IV/V) bound oxo group is fairly strong basic centre and is known to participate in intermolecular conventional as well as non-conventional hydrogen bonding interactions.[11,22] It has been observed before that the acidity of the N–H proton increases significantly in aryl- or aroylhydrazine based Schiff bases when the adjacent imine-N is coordinated to a metal ion.[23,24] It may be noted that for the ternary oxovanadium(IV) complex of phsal^{-}, [VO(phsal)(acac)], the strong intermolecular N–H···O=V hydrogen bonding interaction plays the decisive role in

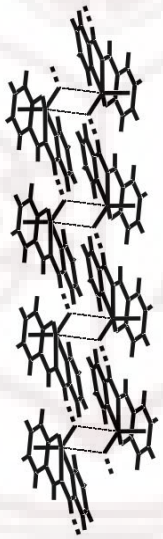

Fig. 3.4. One-dimensional ordering of the dimers of [VO_2(phsal)] (**6**) via intermolecular N(H···O=V) hydrogen bonds in the crystal lattice

providing the infinite one-dimensional supramolecular structure (Chapter 2). The same self-assembly pattern via intermolecular N–H···O=V hydrogen bonding interaction is also observed in the crystal lattice of **6** (Fig. 3.4). The dimeric species $[VO_2(phsal)]_2$ forms a one-dimensional chain structure due to the involvement of the N–H group of $phsal^-$ and the metal bound oxo group at the basal plane of the square-pyramidal monomeric complex molecule in intermolecular N–H···O=V hydrogen bonding interaction. The N2–H, H···O2 and N2···O2 distances and the N2–H···O2 angle are 0.82(3), 1.94(3) and 2.745(3) Å and 168(3)°, respectively. There is no other significant non-covalent interaction between the parallel one-dimensional structures.

3.5. Conclusion

A new series of dioxovanadium(V) complexes of general formula $[VO_2(phsalR)]$ (HphsalR = N-(2-pyridyl)-N′-(5-R-salicylidene)hydrazines has been synthesized. The complexes have been characterized with the help of microanalytical, magnetic, spectroscopic and X-ray crystallographic measurements. All the complexes are diamagnetic and NMR active. The electronic spectra of the complexes display several bands due to ligand-to-metal charge transfer and ligand centred transitions. The crystal structure of $[VO_2(phsal)]$ (R = H) reveals that the metal centre is in an essentially perfect square-planar N_2O_3 coordination sphere assembled by the pyridine-N, the imine-N and the phenolate-O donor planar $phsal^-$ and two oxo groups. Dimerisation of $[VO_2(phsal)]$ leads to the formation of a di(μ-oxo)-bridged species in which the metal centres are in two edge-shared distorted octahedral N_2O_4 coordination spheres. In the crystal lattice, these dimers form an intermolecular N–H···O=V hydrogen bond assisted one-dimensional supramolecular assembly.

Supplementary material

Crystallographic data for [VO_2(phsal)] (**6**) has been deposited with the Cambridge Crystallographic Data Centre (deposition number is CCDC 618872).

3.6. References

1. *SMART* version 5.630 and *SAINT*-plus version 6.45, Bruker-Nonius Analytical X-ray Systems Inc., Madison, WI, USA, 2003.
2. G.M. Sheldrick, *SADABS*, *Empirical Absorption Correction Program*, University of Göttingen, Göttingen, Germany, 1997.
3. G.M. Sheldrick, *SHELX-97*, *Structure Determination Software*, University of Göttingen, Göttingen, Germany, 1997.
4. P. McArdle, *J. Appl. Crystallogr*., 1995, **28**, 65.
5. A.L. Spek, *PLATON A Multipurpose Crystallographic Tool*, Utrecht University, Utrecht, The Netherlands, 2002.
6. W. Kemp, *Organic Spectroscopy*, Macmillan, Hampshire, 1987, p 66.
7. N.R. Sangeetha, V. Kavita, S. Wocadlo, A.K. Powell, S. Pal, *J. Coord. Chem.*, 2000, **51**, 55.
8. N.R. Sangeetha, S. Pal, *Bull. Chem. Soc. Jpn*., 2000, **73**, 357.
9. S.N. Pal, S. Pal, *J. Chem. Crystallogr*., 2000, **30,** 329.
10. S.N. Pal, S. Pal, *Acta Crystallogr. Sect. C*, 2001, **57**, 141.
11. S.N. Pal, K.R. Rahika, S. Pal, *Z. Anorg. Allg. Chem*., 2001, **627**, 1631.
12. S.G. Sreerama, S. Pal, *Inorg. Chem*., 2005, **44**, 6299.
13. X. Li, M.S. Lah, V.L. Pecoraro, *Inorg. Chem*., 1988, 27, 4657.
14. X.-M. Zhang, X.-Z. You, X. Wang, *Polyhedron*, 1996, **15**, 1793.

15. A.G.J. Ligtenbarg, A.L. Spek, R. Hage, B.L. Feringa, *J. Chem. Soc., Dalton Trans.*, 1999, 659.
16. M.R. Maurya, S. Khurana, C. Schulzke, D. Rehder, *Eur. J. Inorg. Chem*., 2001, 779.
17. C.A. Root, J.D. Hoeschele, C.R. Cornman, J.W. Kampf, V.L.Pecoraro, *Inorg. Chem.*, 1993, **32**, 3855.
18. L.M. Mokry, C.J. Carrano, *Inorg. Chem*., 1993, **32**, 6119
19. C.A. Duncan, E.P. Copeland, I.A. Kahwa, A. Quick, D.J. Williams, *J. Chem. Soc*., *Dalton Trans*., 1997, 917.
20. B.F. Hoskins, F.D. Whillans, *Coord. Chem. Rev*., 1972, **9**, 365.
21. A.W. Addison, T.N. Rao, J. Reedijk, J. van Rijn, G.C. Verschoor, *J. Chem. Soc*., *Dalton Trans*., 1984, 1349.
22. S.P. Anthony, L. Srikanth, T.P. Radhakrishnan, *Mol. Cryst. Liq. Cryst*., 2002**,** **381**, 133.
23. B. Mondal, S. Chakraborty, P. Munshi, M.G. Walawalkar, G.K. Lahiri, J. *Chem.Soc., Dalton Trans*., 2000, 2327.
24. S.N. Pal, S. Pal, *J. Chem. Soc., Dalton Trans*., 2002, 2102.

Oxomethoxovanadium(V) complexes derived from thiobenzhydrazide

4.1. Abstract

A family of complexes containing the $\{VO(OMe)\}^{2+}$ motif with the O, N, S-donor Schiff bases (H_2tbhsR) derived from thiobenzhydrazide and 5-substituted salicylaldehydes has been described. Reactions of $[VO(acac)_2]$ with H_2tbhsR in methanol provide the complexes having the general formula [VO(OMe)(tbhsR)] (R = H, OMe, Cl, Br and NO_2) in 40–53% yields. Microanalytical, various spectroscopic (IR, UV-vis and NMR) and electrochemical measurements have been used for the characterization of the complexes. All the complexes are redox active and display a near reversible metal centred reduction in the potential range 0.20 to 0.47 V (vs. Ag/AgCl). The trend in these potential values reflects the polar effect of the substituent on the salicylidene fragment of $tbhsR^{2-}$. The X-ray crystal structures of all the complexes have been determined. In each of the complexes where R = H, OMe, Cl and Br, the metal ion is in a distorted square-pyramidal O_3NS coordination sphere assembled by the O,N,S-donor $tbhsR^{2-}$, the methoxo and the oxo groups. The complex where R = NO_2, crystallizes as a hexacoordinated species due to coordination of a methanol O-atom at the vacant sixth site. The bond parameters associated with the metal ions and the physical properties of the complexes are consistent with the +5 oxidation state of the metal ion in all the complexes. Scrutiny of crystal packing reveals dimeric, one-dimensional and two-dimensional self-assembled structures via intermolecular C–H···O and O–H···O interactions. The two-dimensional network contains the cyclic tetramer of methanol.

4.2. Introduction

In our lab, we have been working on complexes of pentavalent vanadium with hydrazine based Schiff bases for quite some time.[1-6] Tridentate benzoic acid (5-R-2-hydroxy-benzylidene)-hydrazides (H_2L) belong to this class of Schiff bases. In methanolic media, reactions of H_2L (R = OMe and Cl) and bis(acetylacetonato)oxovanadium(IV) afford complexes containing the oxomethoxovanadium(V) motif.[1] In these complexes, the phenolate-O, the imine-N and the deprotonated amide-O donor L^{2-} and the methoxo group constitute an O_3N square-plane around the metal centre and the oxo group occupies the apical position. In the solid state, when the substituent (R) on L^{2-} is an electron releasing group such as OMe the square-pyramidal units dimerise and form a methoxo bridged species $[LVO(\mu\text{-}OMe)_2VL]$. On the other hand, when L^{2-} contains an electron withdrawing substituent such as Cl or it is unsubstituted,[7] the complexes crystallize as [VOL(OMe)(MeOH)] where the sixth coordination site is occupied by the methanol O-atom. In this chapter, we have reported the syntheses, physical properties and X-ray structures of a family of vanadium(V) complexes containing the $\{VO(OMe)\}^{2+}$ unit with thiobenzoic acid (5-R-2-hydroxy-benzylidene)-hydrazides (H_2tbhsR, R = H, OMe, Cl, Br and NO_2) which are the thio analogues[8] of H_2L.

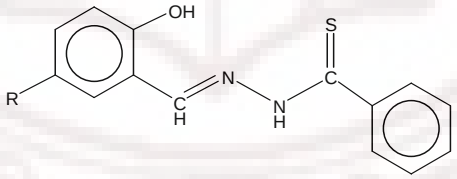

H_2tbhs (R = H)
H_2tbhsCl (R = Cl)
H_2tbhsBr (R = Br)
H_2tbhsOMe (R = OMe)
H_2tbhsNO_2 (R = NO_2)

4.3. Experimental

4.3.1. Materials

Bis(acetylacetonato)oxovanadium(IV)[9] and thiobenzhydrazide[10] were prepared by following reported procedures. The Schiff bases (H_2tbhsR) were prepared by condensation reactions of thiobenzhydrazide with the corresponding 5-substituted salicylaldehyde in ethanolic media.[8] All other chemicals and solvents used in this work were of analytical grade available commercially and were used without further purification.

4.3.2. Physical measurements

Microanalytical (C, H, N) data were obtained with a Thermo Finnigon Flash EA1112 series elemental analyzer. Infrared spectra were collected on a Jasco-5300 FT-IR spectrophotometer. A Sherwood Scientific balance was used for magnetic susceptibility measurements. A Shimadzu 3101-PC UV/vis/NIR spectrophotometer was used to record the electronic spectra. The ^{1}H($Si(CH_3)_4$ as internal standard) and ^{51}V ($VOCl_3$ as external standard) NMR spectra were recorded with the help of a Bruker 400 MHz NMR spectrometer. A Jeol JES-FA200 spectrometer was used for EPR experiments. Solution electrical conductivities were measured with a Digisun DI-909 conductivity meter. A CH-Instruments model 620A electrochemical analyzer was used for cyclic voltammetric experiments with acetonitrile solutions of the complexes containing tetrabutylammonium perchlorate (TBAP) as the supporting electrolyte. The three electrode measurements were carried out at 298 K under dinitrogen atmosphere with a platinum disk working electrode, a platinum wire auxiliary electrode and an Ag/AgCl reference electrode. Under identical condition the Fc^{+}/Fc couple was observed at 0.30 V. The potentials reported in this work are uncorrected for junction contributions.

4.3.3. Synthesis of [VO(OMe)(tbhs)] (11)

A methanol solution (15 ml) of [$VO(acac)_2$] (53 mg, 0.2 mmol) was added to a methanol solution (15 ml) of H_2tbhs (51 mg, 0.2 mmol). The mixture was heated on a steam bath for 15 min. The resulting brown solution was kept in air at room temperature for slow evaporation. The dark brown crystalline material separated in about 2–3 days was collected by filtration, washed with methanol and finally dried in air. Yield, 30 mg (43%)

The other four complexes [VO(OMe)(tbhsOMe)] (**12**), [VO(OMe)(tbhsCl)] (**13**), [VO(OMe)(tbhsBr)] (**14**) and [$VO(OMe)(tbhsNO_2)$] (**15**) reported in this work were synthesized by using one mole equivalent each of [$VO(acac)_2$] and the corresponding Schiff base in 40–53% yields by following the same procedure as described above.

4.3.2. X-ray Crystallography

For all the crystals, the unit cell parameters and the intensity data were obtained on a Bruker-Nonius SMART APEX CCD single crystal X-ray diffractometer, equipped with a graphite monochromator and a Mo $K\alpha$ fine-focus sealed tube (λ = 0.71073 Å) operated at 2.0 kW. The detector was placed at a distance of 6.0 cm from the crystal. Data were collected at 298 K with a scan width of 0.3º in ω and an exposure time of 5 s/frame. The SMART software was used for data acquisition and the SAINT-Plus software was used for data extraction.[11] The SADABS program[12] was used for the absorption correction. The structures were solved by direct methods and refined on F^2 by full-matrix least-squares procedures. All non-hydrogen atoms were refined anisotropically. The hydrogen atoms of **11–14** were added at idealized positions by using a riding model. The hydrogen atoms of the hydroxyl groups of the methanol molecules in [**15**(MeOH)]·MeOH were located on a difference map and refined isotropically. The remaining hydrogen atoms were treated similarly as described for **11–14**. The SHELX-97 programs[13] of the

WinGX package[14] were used for structure solution and refinement. The ORTEX6a[15] and Platon[16] packages were used for molecular graphics. Selected crystallographic data for all the structures are listed in Table 4.1 and Table 4.2.

Table 4.1. Selected crystallographic data for [VO(OMe)(tbhsR)] (**11** (R=H), **12** (R=OMe), **13** (R=Cl))

Complex	**11**	**12**	**13**
Empirical formula	$VC_{15}H_{13}N_2O_3S$	$VC_{16}H_{15}N_2O_4S$	$VC_{15}H_{12}N_2O_3ClS$
Formula mass (g mol^{-1})	352.27	382.30	386.72
Crystal system	Monoclinic	Monoclinic	Monoclinic
Space group	$P2_1/n$	$P2_1/n$	$P2_1/c$
a (Å)	7.412(3)	6.4840(7)	13.993(4)
b (Å)	11.448(4)	19.424(2)	7.672(2)
c (Å)	17.865(3)	13.1867(15)	15.855(4)
β (°)	96.380(6)	92.394(2)	105.798(4)
V ($Å^3$)	1506.5(8)	1659.3(3)	1637.7(7)
Z	4	4	4
ρ (g cm^{-3})	1.553	1.530	1.568
μ (mm^{-1})	0.810	0.746	0.910
Reflections Collected	13836	19074	18187
Reflections unique	2646	3969	3895
Reflections ($I \geq 2\sigma(I)$)	2466	3113	2487
Parameters	200	219	209
GOF on F^2	1.411	1.137	1.128
R_1, wR_2 ($I \geq 2\sigma(I)$)	0.0867, 0.1652	0.0607, 0.1321	0.0865, 0.1649
R_1, wR_2 (all data)	0.0954, 0.1683	0.0794, 0.1408	0.1415, 0.1851
Largest peak, hole (e $Å^{-3}$)	0.460, –0.377	0.485, –0.248	0.613, –0.454

[a] $R_1 = \sum||F_o| - |F_c||/\sum|F_o|$, [b] $wR_2 = \{\sum[(F_o^2 - F_c^2)^2]/\sum[w(F_o^2)^2]\}^{1/2}$, [c] GOF = $\{\sum[w(F_o^2 - F_c^2)^2]/(n - p)\}^{1/2}$ where 'n' is the number of reflections and 'p' is the number of parameters refined.

Table 4.2. Selected crystallographic data for **14** (R=Br) and [VO(OMe)(tbhsNO$_2$)(MeOH)].MeOH ([**15** (MeOH)].MeOH

Complex	**14**	**[15(MeOH)].MeOH**
Empirical formula	$VC_{13}H_{12}N_2O_3BrS$	$VC_{17}H_{20}N_3O_7S$
Formula mass (g mol^{-1})	431.18	461.36
Crystal system	Monoclinic	Triclinic
Space group	$P2_1/c$	$P\bar{1}$
a (Å)	13.9212(12)	9.130(2)
b (Å)	7.8122(7)	11.190(3)
c (Å)	15.8620(14)	11.810(3)
α (^{o})	90	100.841(4)
β (^{o})	105.327(2)	108.038(4)
γ (^{o})	90	111.815(4)
V (Å^3)	1663.7(3)	1000.4(4)
Z	4	2
ρ (g cm^{-3})	1.721	1.532
μ (mm^{-1})	3.137	0.645
Reflections collected	18670	11566
Reflections unique	3970	4646
Reflections ($I \geq 2\sigma(I)$)	2454	3934
Parameters	209	273
GOF on F^2	1.010	1.034
R_1, wR_2 ($I \geq 2\sigma(I)$)	0.0508, 0.1060	0.0390, 0.0997
R_1, wR_2 (all data)	0.0973, 0.1231	0.0474, 0.1045
Largest peak, hole (e Å^{-3})	0.788, –0.276	0.302, –0.247

[a] $R_1 = \sum||F_o| - |F_c||/\sum|F_o|$, [b] $wR_2 = \{\sum[(F_o^2 - F_c^2)^2]/\sum[w(F_o^2)^2]\}^{1/2}$, [c] GOF = $\{\sum[w(F_o^2 - F_c^2)^2]/(n - p)\}^{1/2}$ where 'n' is the number of reflections and 'p' is the number of parameters refined.

4.4. Results and discussion

4.4.1. Synthesis and characterization

Reactions of equimolar amounts of bis(acetylacetonato)oxovanadium(IV) and H_2tbhsR in methanol under aerobic conditions afford the complexes in moderate yields. The elemental analysis data (Table 4.3) are consistent with the general molecular formula [VO(OMe)(tbhsR)] (**11** (R = H), **12** (R = OMe), **13** (R = Cl), **14** (R = Br) and **15** (R = NO_2)). The solubility of the complexes in methanol is very poor. However, they are highly soluble in other organic solvents such as acetonitrile, dichloromethane and chloroform. In solution, neither of **11–15** is electrically conducting. The complexes are diamagnetic and EPR silent. Thus the metal ion in each of these five complexes is in the +5 oxidation state. The low potentials for the vanadium(V)/vanadium(IV) couple (*vide infra*) suggest that in all likelihood the aerial oxygen acts as the oxidant for the oxidation of the metal centre during the synthesis of these complexes from oxovanadium(IV) starting material.

Table 4.3. Elemental analysis[a] data

Complex	**Found (Calc.) (%)**		
	C	**H**	**N**
[VO(OMe)(tbhs)] (**11**)	50.92 (51.14)	3.65 (3.72)	7.76 (7.95)
[VO(OMe)(tbhsOMe)](**12**)	50.14 (50.27)	3.82 (3.95)	7.18 (7.33)
[VO(OMe)(tbhsCl)] (**13**)	46.31 (46.59)	2.98 (3.13)	7.10 (7.24)
[VO(OMe)(tbhsBr)] (**14**)	41.55 (41.78)	2.63 (2.81)	6.39 (6.50)
[VO(OMe)(tbhsNO_2)] (**15**)	45.14 (45.35)	2.83 (3.04)	10.43 (10.58)

[a] Calculated values are in parentheses.

4.4.2. Spectroscopic properties

Infrared spectra of **11–15** in KBr disks do not display any band assignable to the O–H and N–H stretches observed for the free Schiff bases.[8] Thus both phenolic and the thioamide protons are dissociated and the dianionic ligand ($tbhsR^{2-}$) binds the metal centre via the phenolate-O, the imine-N and the thioenolate-S in each complex. This type of coordination mode of $tbhsR^{2-}$ has been confirmed by X-ray structure determination of all the complexes (*vide infra*). Weak coordination of methanol at *trans* to the oxo group is not uncommon in the complexes of $\{VO(OMe)\}^{2+}$ with tridentate ligands when these are synthesized or crystallized in methanol.[1,7,23,24] Absence of the O–H stretch also indicates that there is no coordinated methanol molecule in **11–15**. The moderately strong band observed in the range 1622–1586 cm^{-1} is attributed to the conjugate C=N–N=C moiety of the ligand.[1-8,22] The V=O stretch appears as a medium to strong band in the range 995–984 cm^{-1} (Table 4.4).[1,7,] A representative spectrum is shown in Fig. 4.1.

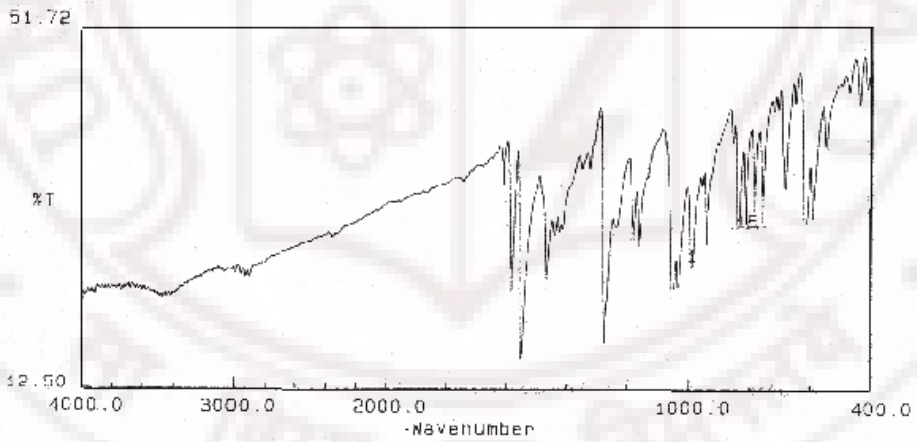

Fig. 4.1. Infrared spectrum of [VO(OMe)(tbhsOMe)](**12**) in KBr disk.

Electronic spectra of the complexes were recorded using brown acetonitrile solutions of the complexes. The spectral profiles of **11–15** are very similar. Four strong absorptions are observed in the wavelength range 435–220 nm (Table 4.4, Fig. 4.2). The lower energy absorptions are ascribable to the ligand-to-metal charge transfer transitions and the higher energy absorptions are likely to be due to ligand centred transitions.[1–7,17–22,24] Interestingly there is an overall blue-shift particularly for the first two band positions with the increase of electron withdrawing ability of the substituent (R) on tbhsR^{2-}. Such shift of band positions due to the variation of the polar effect of the substituent (R) on the ligand has been observed before.[19-21,25-28]

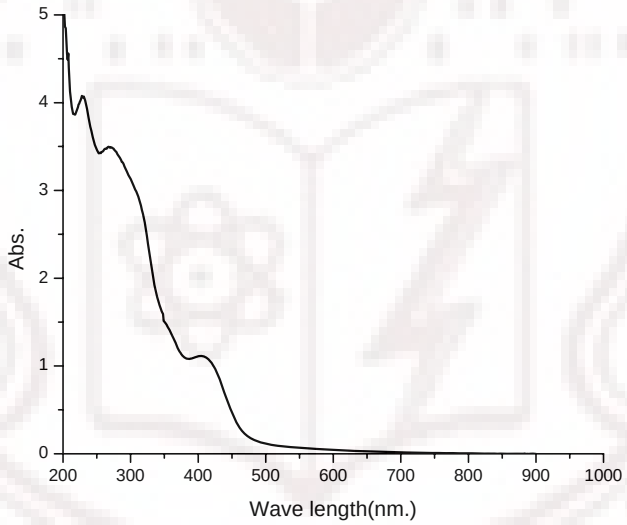

Fig. 4.2. Electronic spectrum of [VO(OMe)(tbhs)] (**11**) in acetonitrile solution

The $CDCl_3$ solutions of **11**–**15** were used to record the ^{1}H as well as ^{51}V NMR spectra. The aromatic protons appear as multiplets in the range δ 8.1–7.0 ppm. The methyl protons of the methoxo group resonate as a singlet near δ 3.5 ppm. The singlet observed at δ 3.86 ppm in the spectrum of **12** is

attributed to the protons of the methyl group of the methoxy substituent on the salicylidene fragment of the tridentate ligand. The azomethine (–CH=N–) proton is observed as a singlet at δ ~8.1 ppm. The ^{51}V NMR spectra of **11**–**15** display a strong resonance between δ –373 and –382 ppm (Table 4.4). These chemical shifts are not unusual for complexes containing the monooxovanadium(V) unit particularly when the metal centre is coordinated to a soft centre such as S^-.[18,22,29]

Table 4.4. Spectroscopic (IR [a], UV–VIS[b] and ^{51}V NMR [c]) data

Complex	$\nu_{V=O}$(cm^{-1})	λ_{max}(nm)(10^{-3}×ε(M^{-1}cm^{-1}))	δ(ppm)
[VO(OMe)(tbhs)](**11**)	984	412(5.3), 333[d](11.7), 284(25.5), 230[d](26.4)	–380
[VO(OMe)(tbhsOMe)(**12**)	990	435(8.6), 360[d](12.7), 282(33.8), 240[d](32.4)	–373
[VO(OMe)(tbhsCl)(**13**)	995	407(11.0), 325[d](27.1), 270(34.6), 230(40.1)	–379
[VO(OMe)(tbhsBr)(**14**)	993	410(4.4), 340[d](17.9), 278(28.5), 230[d](36.9)	–382
[VO(OMe)(tbhsNO_2)](**15**)	992	400[d](7.5), 330[d](17.3), 293(20.1), 220[d](18.8)	–379

[a] In KBr disk.
[b] In acetonitrile.
[c] In $CDCl_3$.
[d] Shoulder.

4.4.3. Electrochemical properties

Electron transfer properties of **11–15** in acetonitrile solutions were studied by cyclic voltammetry. All the complexes display a near reversible reduction response in the potential range 0.20 to 0.47 V (vs. Ag/AgCl). A representative cyclic voltammogram is shown in Fig. 4.3 and the potential data are listed in Table 4.5. This response is assigned to the vanadium(V)–vanadium(IV) couple. The one-electron nature of this couple is ascertained by comparing the current heights with known one-electron redox processes under identical conditions.[1,30,31] The trend in the $E_{1/2}$ values of this vanadium(V)–vanadium(IV) couple (Table 4.5) reflects the effect of the electronic nature of the substituents (R) on the salicylidene fragment of $tbhsR^{2-}$. For the most electron withdrawing substituent (R = NO_2, complex **15**) the reduction of the metal centre occurs at the highest potential while for the most electron releasing substituent (R = OMe, complex **12**) it occurs at the lowest potential. A satisfactory linear relationship is observed (Fig. 4.3) when the $E_{1/2}$ values are plotted against the Hammett constants (σ_p)[32] of the substituents. Thus as the V–O(phenolate) bond strength increases with the increase of the electron releasing ability of the substituent (R) at the *para* position with respect to the phenolate-O, the vanadium(V) to vanadium(IV) reduction becomes more and more difficult. There is a significant anodic shift of the potentials for **11–13** compared to the potentials (–0.15 V (R = H), –0.25 V (R = OMe) and –0.04 V (R = Cl)) of the same couple for the analogous oxomethoxovanadium(V) complexes with the O,N,O-donor benzoic acid (5-R-2-hydroxy-benzylidene)-hydrazides.[1,7] Thus the hard phenolate-O coordination in the latter complexes is more efficient compared to the soft thioenolate-S coordination in **11**–**13** for stabilization of vanadium(V).

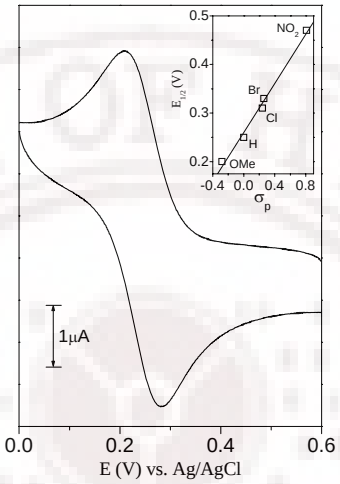

Fig. 4.3. Cyclic voltammogram (scan rate 50 mVs^{-1}) of [VO(OMe)(tbhs)] (**11**) in acetonitrile solution (0.1 M TBAP). Inset: Correlation between the $E_{1/2}$ values for the vanadium(V)–vanadium(IV) couple and the Hammett substituent constants. The straight line represents a linear least-squares fit.

Table 4.5. Cyclic voltammetric[a] data

Complex	$E_{1/2}$[b] **(V)**	ΔE_p[c] **(mV)**
[VO(OMe)(tbhs)] (**11**)	0.25	70
[VO(OMe)(tbhsOMe)] (**12**)	0.20	80
[VO(OMe)(tbhsCl)] (**13**)	0.31	80
[VO(OMe)(tbhsBr)] (**14**)	0.33	70
[VO(OMe)(tbhsNO_2)] (**15**)	0.47	80

[a] In acetonitrile (298 K) at a scan rate of 50 mVs^{-1}.
[b] $E_{1/2} = (E_{pa} + E_{pc})/2$, where E_{pa} and E_{pc} are anodic and cathodic peak potentials, respectively.
[c] $\Delta E_p = E_{pa} - E_{pc}$.

4.4.4. Molecular structures

Single crystals of **11–14** suitable for X-ray structure determination were collected from the crystalline material obtained during their synthesis. Complexes **11** and **12** crystallize in the space group $P2_1/n$ while complexes **13** and **14** crystallize in the space group $P2_1/c$. In each case, the asymmetric unit contains one complex molecule. The same space group, similar unit cell parameters and the structures indicate that **13** and **14** are isomorphous. The structure of **11** synthesized by a different procedure has been reported earlier.[33] The unit cell and bond parameters of the previous structure are very similar with those observed in this work. In the case of **15**, crystals obtained from the synthetic reaction mixture are not suitable for the determination of a decent structure. Crystals obtained from the reaction mixture of **15** have two types of morphologies which are irregular blocks and needles. A block type crystal provided an orthorhombic unit cell of dimensions a = 16.697(2)Å, b = 49.701(5)Å, c = 7.8837(8)Å, V = 6542.2(1)Å^3. The data collected indicate the space group C2*mb*. However, the structure could not be solved possibly due to twining problem. A monoclinic cell of dimensions a = 26.233(7)Å, b = 7.885(2)Å, c = 16.727(5)Å, b = 108.580(5)Å, V = 3279.5(6)Å^3 was obtained with a needle shaped crystal. In this case, the structure could be solved in the space group $P2_1/c$. The asymmetric unit contains two square-pyramidal molecules of **15**. Anisotropic refinement of all non-hydrogen atoms and the inclusion of all hydrogen atoms by riding model provided R_1 value as ~0.25 [IP ≥ 2r(I)]. None of the two molecules has a coordinated methanol molecule trans to the oxo group. But for each of them there is a large peak between the metal centre (at a distance of ~1.5Å) and the coordinated phenolate-O (at a distance of ~1.2Å). Inclusion of these two peaks in the refinement though causes some decrease in the R factors, but there is no significant change in their positions and several atoms become non-positive definite indicating the poor quality of the data. Better crystals were obtained only when the amorphous solid obtained by rapid evaporation of a dichloromethane solution

of **15** was dissolved in methanol and allowed to evaporate slowly. In this process, the complex crystallizes in the space group $P\bar{1}$ and the asymmetric unit contains a hexacoordinated molecule [VO(OMe)(tbhsNO$_2$)(MeOH)] ([**15**(MeOH)]) and a methanol molecule.

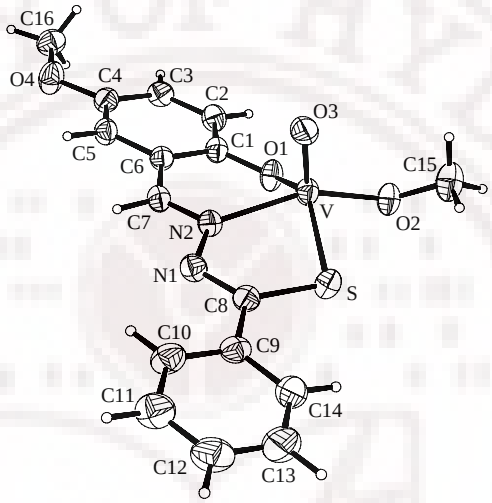

Fig. 4.4. Molecular structure of (a) [VO(OMe)(tbhsOMe)] (**12**) with the atom labeling scheme. All non-hydrogen atoms are represented by their 30% probability thermal ellipsoids.

The molecular structures of **11–14** are very similar. A representative structure is shown in Fig. 4.4. The structure of [**15**(MeOH)] is shown in Fig.4.5. Selected bond parameters for **11**–**14** are listed in Table 4.4 and those for [**15**(MeOH)] are given in Table 4.5. In **11–14**, the metal centres are in distorted square-pyramidal O_3NS coordination spheres. The O,N,S-donor tbhsR^{2-} and the methoxo group constitute a satisfactory O_2NS basal plane (mean deviations: 0.14–0.19 Å) and the oxo group occupies the apical position. The displacement of the metal centre from the basal plane toward the apical oxo group is in the range 0.47–0.52 Å. The *cis* bond angles are in the range 77.05(7)–111.67(11)^o, while the *trans* bond angles are within

137.24(8)–157.00(18)^{o} (Table 4.4). The extent of distortion of a square-pyramidal geometry toward a trigonal-bipyramidal geometry can be measured by the value of τ which is defined as $(\beta-\alpha)/60$, where α is the smaller and β is the larger *trans* bond angles in the basal plane.[41] For an ideal square-pyramidal geometry τ is zero and for an ideal trigonal-bipyramidal geometry τ is unity. The value of τ is found to be within 0.23–0.33 for **11–14**. Thus the O_3NS coordination spheres in **11–14** are closer to the square-pyramidal shape than the trigonal bipyramidal shape. The main difference between the molecular structures of **11**–**14** and that of [**15**(MeOH)] is the coordination of a methanol molecule at the vacant sixth coordination site which is *trans* to the oxo group.

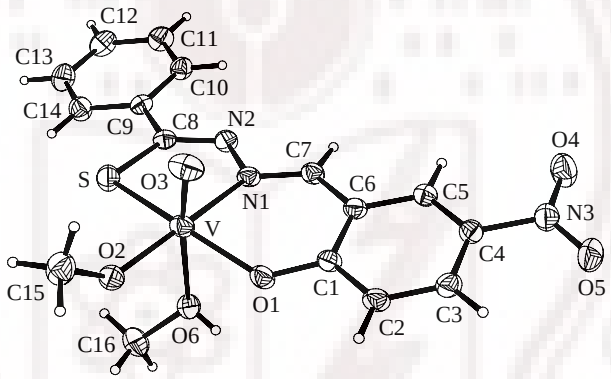

Fig. 4.5. Molecular structure of [VO(OMe)(tbhsNO$_2$)(MeOH)] ([**15**(MeOH)]) with the atom labeling scheme. All non-hydrogen atoms are represented by their 30% probability thermal ellipsoids.

Possibly the relatively less electron density at the metal centre in **15** due to the strong electron withdrawing effect of the nitro substituent on the tridentate ligand prompts the coordination of the solvent molecule during recrystallization. Here the *cis* bond angles are in the range 74.98(6)–103.37(6)^{o} (Table 4.5). The *trans* O=V–O(methanol) bond angle (173.65(7)^{o}) is almost linear compared to the other two *trans* angles (152.56(5) and 161.95(6)^{o}). Here also the metal centre is displaced from the

O_2NS square-plane toward the oxo group. However, the displacement is noticeably less (0.32 Å) compared to that in **11**–**14**. This smaller displacement is possibly due to the coordination of the methanol molecule. The orientation of the methoxo methyl in [**15**(MeOH)] is toward the oxo group side perhaps due to steric constrain imposed by the metal coordinated methanol (Fig. 4.5). The opposite is observed in **11**, **13** and **14**. Curiously the orientation of the methoxo methyl in **12** is in the same direction as observed for [**15**(MeOH)]

Table 4.4. Selected bond lengths (Å) and bond angles (^{o}) for [VO(OMe)(tbhsR)] (**12**)

Bond parameters	**11** (R = H)	**12** (R = OMe)	**13** (R = Cl)	**14** (R = Br)
V–S	2.3269(17)	2.3332(10)	2.3329(16)	2.3372(12)
V–N(1)	2.107(4)	2.134(2)	2.116(4)	2.108(3)
V–O(1)	1.841(4)	1.823(2)	1.842(4)	1.844(3)
V–O(2)	1.769(4)	1.756(2)	1.733(3)	1.736(3)
V–O(3)	1.576(4)	1.575(2)	1.593(4)	1.597(3)
S–C(8)	1.757(5)	1.748(3)	1.752(5)	1.751(4)
N(2)–C(8)	1.281(7)	1.295(4)	1.295(6)	1.282(4)
S–V–N(1)	77.42(12)	77.05(7)	77.33(11)	77.53(8)
S–V–O(1)	140.67(14)	137.24(8)	141.94(14)	142.04(10)
S–V–O(2)	85.34(14)	85.21(8)	85.88(13)	85.88(9)
S–V–O(3)	106.00(17)	107.28(9)	107.40(16)	107.41(12)
N(1)–V–O(1)	84.27(17)	83.57(9)	84.06(15)	84.08(11)
N(1)–V–O(2)	154.15(19)	156.73(11)	157.00(18)	156.94(12)
N(1)–V–O(3)	96.1(2)	93.52(10)	94.27(18)	94.58(13)
O(1)–V–O(2)	97.60(18)	100.00(9)	100.33(17)	99.98(12)
O(1)–V–O(3)	110.4(2)	111.67(11)	106.8(2)	106.92(15)
O(2)–V–O(3)	107.2(2)	106.18(11)	105.8(2)	105.70(15)

Table 4.5. Selected bond lengths (Å) and bond angles (°) for [VO(OMe)(tbhsNO$_2$)(MeOH)]·MeOH (**15** (MeOH))

V–S	2.3687(8)	V–O(2)	1.7669(13)
V–N(1)	2.1514(15)	V–O(3)	1.5727(16)
V–O(1)	1.8818(14)	V–O(6)	2.3981(16)
S–C(8)	1.7332(18)	N(2)–C(8)	1.288(2)
S–V–N(1)	77.78(5)	N(1)–V–O(6)	81.90(5)
S–V–O(1)	152.56(5)	O(1)–V–O(2)	103.37(6)
S–V–O(2)	89.48(5)	O(1)–V–O(3)	100.93(8)
S–V–O(3)	99.92(7)	O(1)–V–O(6)	74.98(6)
S–V–O(6)	82.57(5)	O(2)–V–O(3)	101.97(8)
N(1)–V–O(1)	83.53(6)	O(2)–V–O(6)	83.84(6)
N(1)–V–O(2)	161.95(6)	O(3)–V–O(6)	173.65(7)
N(1)–V–O(3)	92.87(7)		

The C–S and C–N bond lengths (Tables 4.4 and 4.5) are consistent with the thioenolate form of the thioamide functionality of tbhsR^{2-}.[17-22,33] The other intraligand bond parameters are normal. The V–S(thioenolate), the V–N(imine) and the V–O(phenolate) bond lengths (Tables 4.4 and 4.5) in all the complexes are comparable with the bond lengths reported for vanadium(V) complexes with similar tridentate ligands.[17-22,33] A reasonable linear correlation of the V–O(phenolate) bond lengths in **11**–**15** with the Hammett constants (σ_p)[32] of the substituents indicates the decrease of bond strength with the increase of electron withdrawing effect of the substituent. This observation is consistent with the electrochemical behavior of **11–15** in solution (*vide supra*). The V–OMe bond lengths are within the range reported for oxomethoxovanadium(V) species.[1,7,13,23,24,33] The V=O bond lengths are

unexceptional.[1-7,23,24,33] However, the V=O bond lengths are slightly longer in the isomorphous pair **13** and **14** compared to that in **11** and **12** (Table 4.4). Involvement of the oxo group of both **13** and **14** in two intermolecular hydrogen bonds (*vide infra*) may be partially responsible for this elongation. As commonly observed in analogous species, the elongated V–O(methanol) bond *trans* to the oxo group in [VO(OMe)(tbhsNO_2)(MeOH)] indicates weak coordination of the methanol.[1,7,23,24]

4.4.5. Intermolecular hydrogen bonding

In these complexes, the metal coordinated O-atoms particularly the oxo group[5,6,35,36] and the O-atoms of the ligand substituents (OMe and NO_2) can participate in intermolecular hydrogen bonds as acceptors. In the case of [**15**(MeOH)]·MeOH, the methanol molecules are also capable of forming strong intermolecular hydrogen bonds. We have investigated the self-assembly patterns via intermolecular hydrogen bonding and other non-covalent interactions in the crystal lattices of all the structures. Interestingly no significant non-covalent interaction has been found in the case of **11**. In the rest of the species, other than hydrogen bonding (D···A distance ≤ 3.5 Å) no other noteworthy non-covalent interaction has been noticed (Table 4.6).

The self-assembly of **12** via the C–H···O interaction involving the methyl C–H (C15–H) of the metal coordinated methoxo group and the oxo group (O3) leads to a one-dimensional supramolecular structure in the crystal lattice (Fig.4.6(b)). The isomorphous species **13** and **14** form the same type of discrete dimeric species through a pair of reciprocal C–H···O···H–C hydrogen bonding motif. The dimeric structure of **14** is illustrated in Fig. 4.6(a). The azomethine C–H (C7–H) and the C–H (C5–H) *ortho* to the chloro or bromo substituent on the salicylidene fragment of tbhsR^{2-} act as the donors and the metal bound oxo group (O3) acts as the acceptor in this C–H···O···H–C motif. It may be noted that the hydrogen atoms of C7–H and C5–H are more positive

in character compared to the other hydrogen atoms due to metal coordination at the azomethine N-atom and the presence of electron withdrawing substituent at C4, respectively.

The host-guest type of species [**15**(MeOH)]·MeOH is expected to show a more intricate self-assembly pattern compared to that of **12–14** due to the presence of the methanol molecules. In fact the methanol molecules form hydrogen bonds only within themselves. The hydroxyl groups (O6–H and O7–H) of both metal coordinated and the guest methanol molecules act as acceptor as well as donor in four O–H···O interactions and provide a unique

Table 4.6. Geometrical parameters for intermolecular hydrogen bonds

Complex	**D···A**	**$d_{(D\cdots A)}$ [Å]**	**D–H···A [°]**
12	C(15)···O(3)[a]	3.400(4)	178
13	C(5)···O(3)[b]	3.296(6)	137
	C(7)···O(3)[b]	3.200(6)	135
14	C(5)···O(3)[b]	3.361(5)	136
	C(7)···O(3)[b]	3.199(4)	134
[**15**(MeOH)]·MeOH	O(6)···O(7)[c]	2.705(3)	161(3)
	C(2)···O(1)[d]	3.440(3)	162
	C(15)···O(4)[e]	3.422(4)	153

Symmetry transformations used to generate equivalent atoms:
[a] 1+x, y, z.
[b] –x, 2–y, –z.
[c] –x, 1–y, 2–z.
[d] 1–x, 1–y, 2–z.
[e] x, y, –1+z.

example for cyclic tetramer[37-40] in the solid state (Fig. 4.6(c)). This cyclic tetramer of methanol acts as a bridge between the two square-pyramidal

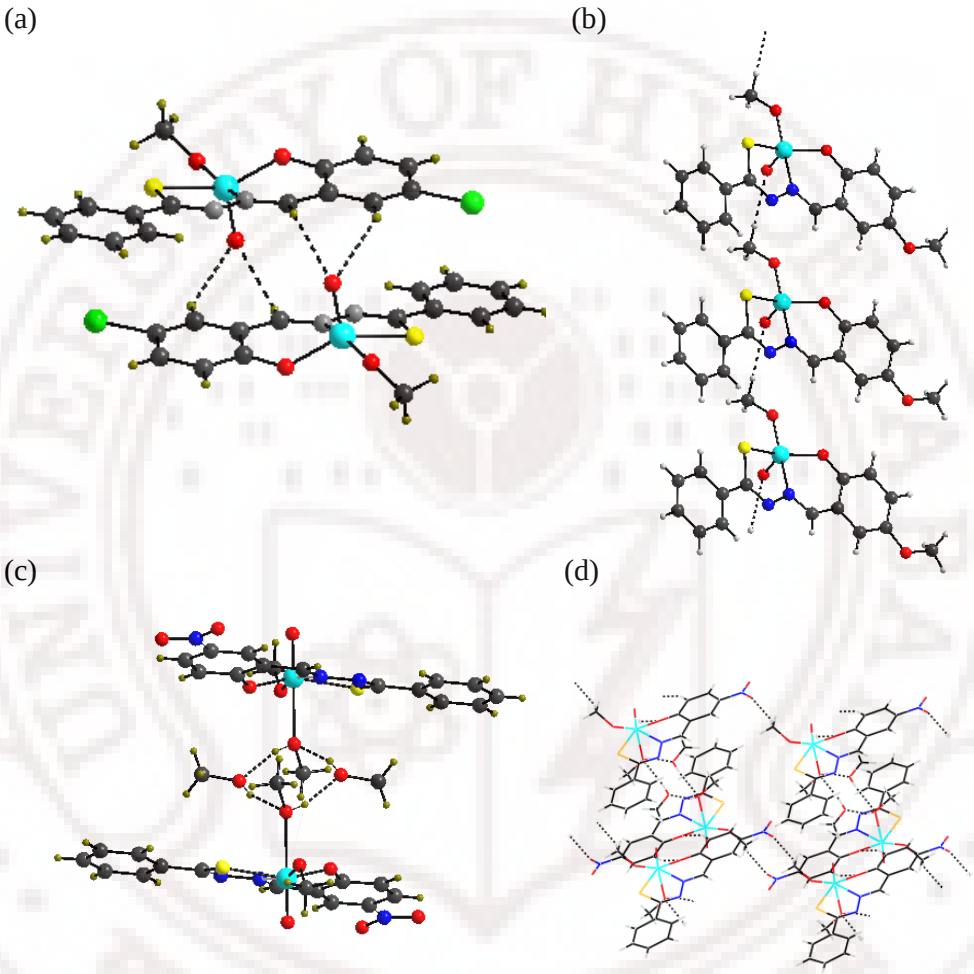

Fig. 4.6. (a) Dimer of [VO(OMe)(tbhsBr)] (**14**) through C–H···O···H–C hydrogen bonding motif. (b) One-dimensional ordering of [VO(OMe)(tbhsOMe)] (**12**) via C–H···O interaction. (c) The C–H···O interaction assisted one-dimensional ordering of the dimer of [**15**(MeOH)]·MeOH containing the cyclic tetramer of methanol. (d) Two-dimensional network of [**15**(MeOH)]·MeOH.

complex units and a dimer of [**15**(MeOH)]·MeOH is formed. These dimers are connected by a pair of reciprocal C–H···O interactions involving the metal coordinated phenolate-O (O1) and the C–H (C2–H) *ortho* to O1 and form a one-dimensional chain like structure (Fig. 4.6(b)). In these parallel chains, the host molecules are involved in another pair of reciprocal C–H···O interactions with the host molecules of the adjacent chains. One of the nitro group O-atoms (O4) and the methyl C–H (C15–H) of the metal coordinated methoxo group participate in this C–H···O interaction. As a result, a two-dimensional network of [**15**(MeOH)] formed (Fig. 4.6(d)).

4.5. Conclusion

Using the tridentate Schiff bases (H_2tbhsR) prepared from thiobenzhydrazide and 5-substituted salicylaldehydes, a series of oxomethoxovanadium(V) complexes having the general formula [VO(OMe)(tbhsR)] has been synthesized. The dianionic tbhsR^{2-} coordinates the metal ion via the phenolate-O, the imine-N and the thioenolate-S atoms. The complexes are redox active and display a near reversible metal centred reduction. The potential of the vanadium(V)-vanadium(IV) couple is sensitive to the electronic nature of the substituent on the salicylidene fragment of the tridentate ligand. X-ray structures of the complexes where R = H, OMe, Cl and Br determined using crystals obtained directly from the synthetic reaction mixtures show a square-pyramidal coordination geometry for all these complexes. However, recrystallization of the complex where R = NO_2 from methanol has provided a solvated hexacoordinated species [VO(OMe)(tbhsNO_2)(MeOH)]·MeOH. Investigations of the intermolecular non-covalent interactions in the solid state reveal different types of non-classical C–H···O and classical O–H···O hydrogen bonding interactions in these structures. Self-assembly via these interactions leads to a one-dimensional array of the complex where R = OMe and discrete hydrogen

bonded dimers for the complexes where R = Cl and Br. A two-dimensional network which involves cyclic tetramers of methanol is observed for the solvated hexacoordinated species.

Supplementary material

CCDC 648292, 648293, 648294, 648295, 648296 contain the supplementary crystallographic data for the crystals (**11**), (**12**), (**13**), (**14**) and (**15**). These data can be obtained free of charge from The Cambridge Crystallographic Data Centre via www.ccdc.cam.ac_uk/data_request/cif.

4.6. References

1. N.R. Sangeetha, V. Kavita, S. Wocadlo, A.K. Powell, S. Pal, *J. Coord. Chem.*, 2000, **51**, 55.
2. N.R. Sangeetha, S. Pal, *Bull. Chem. Soc. Jpn.*, 2000, **73**, 357.
3. S.N. Pal, S. Pal, *J. Chem. Crystallogr.*, 2000, **30**, 329.
4. S.N. Pal, S. Pal, *Acta Crystallogr. Sect. C*, 2002, **57**, 141.
5. S.N. Pal, K.R. Radhika, S. Pal, *Z. Anorg. Allg. Chem.*, 2001, **627**, 1631.
6. A. Sarkar, S. Pal, *Polyhedron*, 2007, **26**, 1205.
7. S.P. Rath, S. Mondal, A. Chakravorty, *Inorg. Chim. Acta*, 1997, **263**, 247.
8. N.K. Singh, D.K. Singh, J. Singh, *Indian J. Chem. Sect. A*, 2001, **40**, 1064.
9. R.A. Rowe, M.M. Jones, *Inorg. Synth.*, 1957, **5**, 113.
10. K.A. Jensen, C. Pedersen, *Acta Chem. Scand.*, 1961, **15,** 1097.
11. *SMART* version 5.630 and *SAINT*-plus version 6.45, Bruker-Nonius Analytical X-ray Systems Inc., Madison, WI, USA, 2003.
12. G.M. Sheldrick, *SADABS*, Program for Area Detector Absorption Correction, University of Göttingen, Göttingen, Germany, 1997.
13. G.M. Sheldrick, *SHELX-97*, Structure Determination Software, University of Göttingen, Göttingen, Germany, 1997.
14. L.J. Farrugia, *J. Appl. Crystallogr.*, 1999, **32,** 837.

15. P. McArdle, J. Appl. Crystallogr., 1995, **28**, 65.
16. A.L. Spek, *PLATON*, A Multipurpose Crystallographic Tool, Utrecht University, Utrecht, The Netherlands, 2002.
17. S.K. Dutta, S.B. Kumar, S. Bhattacharyya, E.R.T. Tiekink, M. Chaudhury, *Inorg. Chem.*, 1997, **36**, 4954.
18. S.K. Dutta, S. Samanta, S.B. Kumar, O.H. Han, P. Burckel, A.A. Pinkerton, M. Chaudhury, *Inorg. Chem*., 1999, **38**, 1982.
19. S.K. Dutta, S. Samanta, D. Ghosh, R.J. Butcher, M. Chaudhury, *Inorg. Chem*., 2002, **41**, 5555.
20. S. Samanta, D. Ghosh, S. Mukhopadhyay, A. Endo, T.J.R. Weakley, M. Chaudhury, *Inorg*. *Chem*., 2003, **42**, 1508.
21. S. Samanta, S. Mukhopadhyay, D. Mandal, R.J. Butcher, M. Chaudhury, *Inorg. Chem*., 2003, **42**, 6284.
22. M.R. Maurya, A. Kumar, A.R. Bhat, A. Azam, C. Bader, D. Rehder, *Inorg. Chem.*, 2006, **45**, 1260.
23. K. Nakajima, M. Kojima, K. Toriumi, K. Saito, J. Fujita, *Bull. Chem. Soc. Jpn*., 1989, **62**, 760.
24. M.R. Maurya, S. Agarwal, C. Bader, M. Ebel, D. Rehder, *Dalton Trans*., 2005, 537.
25. R.N. Mukherjee, O.A. Rajan, A. Chakravorty, *Inorg. Chem.*, 1982, **21**, 785.
26. J.W. Pyrz, A.L. Roe, L.J. Stern, L. Que, Jr., *J. Am. Chem. Soc*., 1985, **107,** 614.
27. S.N. Pal, J. Pushparaju, N.R. Sangeetha, S. Pal, *Trans. Met. Chem*., 2000, **25,** 529.
28. S.N. Pal, S. Pal, *Z. Anorg. Allg. Chem*., 2002, **628**, 2091.
29. D. Rehder, C. Weidemann, A. Duch, W. Priebsch, *Inorg. Chem*., 1988, **27**, 584.
30. S.G. Sreerama, S. Pal, *Eur. J. Inorg. Chem.*, 2004, 4718.
31. R. Raveendran, S. Pal, *Inorg. Chim. Acta*, 2006, **359**, 3212.
32. J. March, in: Advanced Organic Chemistry, 4th ed., Wiley, New York, 1992, p. 280.

33. W. Bansse, E. Ludwig, E. Uhlemann, F. Weller, K. Dehnicke, W. Herrmann, *Z. Anorg. Allg. Chem.*, 1992, **613**, 36.
34. A.W. Addison, T.N. Rao, J. Reedijk, J. van Rijn, G.C. Verschoor, *J. Chem. Soc., Dalton Trans*., 1984, 1349.
35. S.P. Anthony, L. Srikanth, T.P. Radhakrishnan, *Mol. Cryst. Liq. Cryst*., 2002, **381**, 133.
36. A. Sarkar, S. Pal, *Polyhedron*, 2006, **25**, 1689.
37. R.W. Larsen, M.A. Suhm, *J. Chem. Phys*., 2006, **125**, 154314.
38. G. Brink, L. Glasser, *J. Comput. Chem*., 2004, **2**, 14.
39. Y. Yamaguchi, N. Yasutake, M. Nagaoka, *J. Phys. Chem. A*, 2002, **106**, 404.
40. J.R. Dixon, W.O. George, Md.F. Hossain, R. Lewis, J.M. Price, *J. Chem. Soc., Faraday Trans*., 1997, **93**, 3611.

An unsymmetric chiral trapped valence complex of $\{OV(\mu\text{-}O)VO\}^{3+}$

5.1. Abstract

In acetonitrile, reaction of bis(acetylacetonato)oxovanadium(IV) ([$VO(acac)_2$]) and acetylhydrazine ($CH_3CONHNH_2$) in 2:1 mole ratio provides a novel unsymmetrical chiral mixed-valent triply bridged dinuclear vanadium(IV/V) complex having the formula [(Hdmpz)OV(μ-acac)(μ-O)(μ-O_2CCH_3)VO(acac)] (Hdmpz = 3,5-dimethylpyrazole). The molecular structure of the complex has been confirmed by X-ray crystallography. It crystallizes in the chiral space group $P2_12_12_1$ indicating a spontaneous resolution in the crystal. The complex is one-electron paramagnetic and redox active. It displays V(V)V(IV) to V(V)V(V) oxidation and V(V)V(IV) to V(IV)V(IV) reduction responses. The crystal structure and the EPR measurements reveal the trapped-valent character of the complex in solid state as well as in solution phase. Circular dichroism spectroscopic measurement with a powdered sample reveals that the bulk material is not racemic. In solution, existence of both enantiomers of the complex is demonstrated by Pfeiffer effect using *l*- and *d*-arabinose as environmental substances.

5.2. Introduction

Complexes of the mixed-valent $\{OV(\mu\text{-}O)VO\}^{3+}$ core are of particular interest for their molecular and electronic structures. Structurally characterized complexes containing the $\{OV(\mu\text{-}O)VO\}^{3+}$ core are very few.[1–12] In all these complexes, the metal ions are bridged by only the oxo group and they are symmetric with respect to the ligands bonded to them. Only in one case, the two ligands attached to the two metal centres differ in the substituents attached to them.[12] The reported structures have been

scrutinized and it has been found that the delocalization of the unpaired 3d electron over the vanadium centres depend on the geometry of the $\{OV(\mu\text{-}O)VO\}^{3+}$ core in these complexes.[7,12] An *anti* linear configuration of the core facilitates very effective overlap of the d_{xy} metal orbitals via oxo bridge p_x orbital and a full delocalization of the unpaired electron.[1,5,9] For an *anti* bent configuration, both localized and delocalized electronic structures are found. In these cases, the π-basicity of the equatorial coordinating atoms plays important role in deciding the electronic structure.[8] Complexes with the *syn* bent $\{OV(\mu\text{-}O)VO\}^{3+}$ core are rare and they have localized electronic structure.[6,10,12] The lone example for a complex of $\{OV(\mu\text{-}O)VO\}^{3+}$ with a configuration in between *syn* and *anti* has also localized electronic structure.[8] It is interesting to note that in the EPR time scale except for two cases[7,9] the remaining solid state valence-trapped species display delocalized electronic structure in the solution phase. In this chapter, we report the synthesis, characterization and crystal structure of a complex containing the mixed-valent *syn*-$\{OV(\mu\text{-}O)VO\}^{3+}$ core, [(Hdmpz)OV(μ-acac)(μ-O)(μ-O_2CCH_3)VO(acac)] (Hdmpz = 3,5-dimethylpyrazole). This complex is chiral and truly unsymmetric with respect to the coordination environment around the two metal centres. Unlike the previously reported divanadium(IV/V) complexes, the present complex contains two additional bridges between the vanadium centres. The complex is valence trapped in the solid as well as in the solution phase. It is redox active and displays V(V)V(IV) to V(V)V(V) oxidation and V(V)V(IV) to V(IV)V(IV) reduction responses. We also report the optical resolution of the complex in solution by using the Pfeiffer effect.[13]

5.3. Experimental

5.3.1. Materials

Bis(acetylacetonato)oxovanadium(IV)[14] and acetylhydrazine[15] were prepared by following reported procedures. All other chemicals and solvents

used in this work were of analytical grade available commercially and were used without further purification.

5.3.2. Physical measurements

A Thermo Finnigon Flash EA1112 series elemental analyzer was used for the elemental (C, H, N) analysis. Room temperature (298 K) magnetic susceptibility was measured using a Sherwood Scientific balance. A diamagnetic correction calculated from Pascal's constants[16] was used to obtain the molar paramagnetic susceptibility. A Digisun DI-909 conductivity meter was used to measure the solution electrical conductivity. Infrared spectrum was recorded by using a KBr pellet on a Nicolet 5700 FT-IR spectrophotometer. Electronic spectra were recorded with the help of a Cary 100 Bio UV/vis spectrophotometer. A Jeol JES-FA200 spectrometer was used to record the X-band EPR spectra. The circular dichroism spectra were recorded on a Jasco J810 spectropolarimeter. A CH-Instruments model 620A electrochemical analyzer was used for the cyclic voltammetric experiments with methanol solution of the complex containing tetrabutylammonium perchlorate (TBAP) as supporting electrolyte. The three electrode measurements were carried out at 298 K under a dinitrogen atmosphere with a platinum disk or a glassy carbon working electrode, a platinum wire auxiliary electrode and an Ag/AgCl reference electrode. The potentials reported in this work are uncorrected for junction contributions.

5.3.3. Synthesis of [(Hdmpz)OV(μ-acac)(μ-O)(μ-O_2CCH_3)VO(acac)]

An acetonitrile solution (10 ml) of acetylhydrazine (74 mg, 1 mmol) was added to an acetonitrile solution (15 ml) of [$VO(acac)_2$] (530 mg, 2 mmol) and the mixture was heated on water bath for 15 minutes. The resulting brown solution was allowed to evaporate in air at room temperature. The brown needle shaped crystalline complex with a very little yellow powdery material separated in about 1-2 days, was collected by filtration. The solid thus

obtained was treated with acetonitrile (10 ml) to dissolve the complex and then filtered to remove the insoluble powdery material. Slow evaporation of the clear filtrate at room temperature in air provided the pure dark brown crystalline complex. A single crystal for X-ray structure determination was collected from this material. Yield was 250 mg (50%). $V_2C_{17}H_{25}N_2O_9$ (503.27): calcd. C 40.57, H 5.01, N 5.57; found C 40.28, H 4.87, N 5.31. Selected IR bands in KBr [cm^{-1}]: 3270 (m), 1582 (s), 1557 (s), 1530 (s), 1433 (m), 1362 (m), 1238 (s), 1144 (m), 986 (s), 965 (m), 801 (m), 673 (m), 586 (w), 465 (w), 422 (w). Electronic spectroscopic data in CH_3OH: λ_{max} [nm] (ε [M^{-1} cm^{-1}]) = 535 sh (150), 330 sh (2690), 275 (3140).

5.3.4. X-ray crystallography

The unit cell parameters and the intensity data were obtained on a Bruker-Nonius SMART APEX CCD single crystal diffractometer, equipped with a graphite monochromator and a Mo $K\alpha$ fine-focus sealed tube (λ = 0.71073 Å) operated at 2.0 kW. The detector was placed at a distance of 6.0 cm from the crystal. Data were collected at 298 K with a scan width of 0.3º in ω and an exposure time of 10 sec/frame. The SMART software was used for data acquisition and the SAINT-Plus software was used for data extraction.[17] The absorption correction was performed with the help of SADABS program.[18] The structure was solved in the space group $P2_12_12_1$ by direct method and refined on F^2 by full-matrix least-squares procedures. The non-hydrogen atoms were refined using anisotropic thermal parameters. The H-atom of the N–H group in Hdmpz was located in a difference Fourier map and refined with $U_{iso}(H) = 1.2U_{eq}(N)$. All other hydrogen atoms were included in the structure factor calculations at idealized positions by using a riding model. The SHELX-97 programs[19] available in the WinGX package[20] were used for structure solution and refinement. The ORTEX6a[21] and and Platon[22] packages were used for molecular graphics. Selected crystal and refinement data are listed in Table 5.1.

Table 5.1. Crystallographic data for $[V_2O_3(O_2CCH_3)(acac)_2(Hdmpz)]$(**16**)

Complex	**16**
Empirical Formula	$V_2C_{17}H_{25}N_2O_9$
Formula mass (g mol^{-1})	503.27
Crystal system	Orthorhombic
Space group	$P2_12_12_1$
a [Å]	7.9322(19)
b [Å]	14.024(3)
c [Å]	20.541(5)
V [$Å^3$]	2285.0(9)
Z	4
ρ (g cm^{-3})	1.463
μ (mm^{-1})	0.865
Reflections collected	16244
Reflections unique	4483
Reflections ($I \geq 2\sigma(I)$)	3925
Parameters	281
GOF on F^2	1.021
R_1, wR_2 ($I \geq 2\sigma_I$)	0.0372, 0.0832
R_1, wR_2 (all data)	0.0451, 0.0868
Largest peak, hole (e $Å^{-3}$)	0.283, –0.241

[a] $R_1 = \sum||F_o| - |F_c||/\sum|F_o|$. [b] $wR_2 = \{\sum[(F_o^2 - F_c^2)^2]/\sum[w(F_o^2)^2]\}^{1/2}$.
[c] GOF = $\{\sum[w(F_o^2 - F_c^2)^2]/(n - p)\}^{1/2}$ where 'n' is the number of reflections and 'p' is the number of parameters refined.

5.4. Results and Discussion

5.4.1. Synthesis and Characterization

The dinuclear complex, [(Hdmpz)OV(μ-acac)(μ-O)(μ-O_2CCH_3)VO(acac)], has been synthesized by reacting one mole equivalent of acetylhydrazine and two mole equivalents of bis(acetylacetonato)oxovanadium(IV) ([$VO(acac)_2$]) in acetonitrile under aerobic condition. We have repeated this reaction several times and each of these repetitions provided the complex in very similar (45–50%) yield. Thus the synthetic procedure is reproducible. It is known that the reaction of acetylacetone with hydrazine produces 3,5-dimethylpyrazole (Hdmpz).[23] In all probability the dissociation of a part of [$VO(acac)_2$] and the hydrolysis of acetylhydrazine provide acetylacetone and hydrazine, respectively for the formation of the Hdmpz in the reaction mixture. The source of the bridging acetate group is the acetic acid produced in the hydrolysis of acetylhydrazine. The oxygen in air is responsible for the oxidation of a part of the vanadium(IV) to vanadium(V) during synthesis of the complex. If the reaction of [$VO(acac)_2$] with acetylhydrazine is performed in dry acetonitrile under nitrogen atmosphere the complex does not form. This observation corroborates to a certain extent the above described pathway for the formation of the complex. However, despite our several attempts we could not synthesize the complex using [$VO(acac)_2$], Hdmpz and various salts of acetate as starting materials. The elemental analysis data are consistent with the dinuclear molecular formula. The complex is electrically non-conducting in solution. The room temperature (298 K) effective magnetic moment (1.70 μ_B) of the complex in powder phase suggests the presence of an unpaired electron.

5.4.2. Description of the Molecular Structure

The complex crystallizes in the chiral space group $P2_12_12_1$. The molecular structure with the atom numbering scheme is shown in Fig. 5.1. The bond parameters associated with the two metal centers are listed in Table 5.2. Both metal centers are in distorted octahedral coordination geometry. The *cis* and *trans* bond angles are in the ranges 73.36(8)–104.16(12)^o and 156.98(9)–177.5(1)^o, respectively. The first metal center V(1) is in O_6 and the second metal center V(2) is in NO_5 coordination sphere. Although hexacoordinated, but the metal center is significantly displaced towards the terminal oxo group in each case. The displacement of V(1) from the square-plane formed by O(1), O(2), O(5) and O(8) (mean deviation 0.04 Å) is 0.297(1) Å and that of V(2) from the square-plane formed by N(1), O(4), O(6) and O(8) (mean deviation 0.10 Å) is 0.286(1) Å. The metal centers are bridged by the oxo group, one acetylacetonate O-atom and the acetate. The bond lengths involving the bridging oxo group O(8), the O-atoms of the bridging acetate O(5) and O(6), and the terminal oxo groups O(7) and O(9) are significantly shorter at V(1) than at V(2) (Table 5.2). These bond lengths clearly indicate a trapped-valence situation where V(1) is in +5 oxidation state and V(2) is in +4 oxidation state. However, the variations in the bond lengths involving the O-atoms of the two acetylacetonate ligands are not straightforward with respect to the above oxidation state assignment due to the differences in their positions and the coordination modes (Fig. 5.1, Table 5.2). The V(1)–O(1) bond length (1.981(2) Å) *trans* to the acetate O-atom is comparable with the V(2)–O(4) bond length (1.988(2) Å). Most likely the strong intramolecular N(2)–H···O(1) hydrogen bond involving the Hdmpz N–H group (Fig. 5.1) is the primary reason for the lengthening of the V(1)–O(1) bond to a value which is comparable with the V(2)–O(4) bond length. The N(2)–H, H···O(1) and N(2)···O(1) distances and the N(2)–H···O(1) angle are 0.83(3), 2.12(4) and 2.934(4) Å and 165(4)^o, respectively. For the bridging acetylacetonate O-atom O(3), the V–O bond

length (2.357(2) Å) is significantly longer at V(1) than that (2.196(2) Å) at V(2). For both the metal centers, O(3) is *trans* to the terminal oxo groups. Most likely a stronger *trans* influence by the short V=O bond at V(1) compared to that by the long V=O bond at V(2) on O(3) causes this difference. Similarly the shorter V(1)–O(8) bond (1.777(2) Å) than the V(2)–O(8) bond (1.888(2) Å) causes the long V(1)–O(2) (2.012(2) Å) and the short V(2)–O(4) (1.988(2) Å) bonds as both O(2) and O(4) are *trans* to the bridging oxo group O(8). Thus the V_2O_2 core is not symmetric with respect to the V–O bond lengths and it is folded along the O(3)---O(8) line due to the additional acetate bridge. The fold angle is 20.4(1)^o. The V–O–V bridge angle at the acetylacetonate O-atom O(3) is 87.54(7)^o while that at the oxo bridge O(8) is 118.7(1)^o. The O(7)–V(1)···V(2)–O(9) torsion angle is 3.3(2)^o. Thus the $\{OV(\mu\text{-}O)VO\}^{3+}$ core has a near perfect *syn* bent configuration with V(1)···V(2) distance as 3.1522(8) Å.

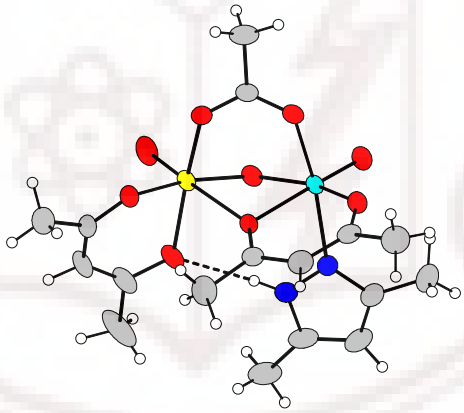

Fig. 5.1. Molecular structure of [(Hdmpz)OV(μ-acac)(μ-O)(μ-O_2CCH_3)VO(acac)] with the atom labeling scheme. All non-hydrogen atoms are represented by their 30% probability thermal ellipsoids.

Table 5.2. Selected bond lengths (Å) and angles (°) for $[V_2O_3(O_2CCH_3)(acac)_2(Hdmpz)]$(**16**)

16	**Bond parameters**	**16**	**Bond parameters**
V(1)–O(1)	1.981(2)	V(2)–N(1)	2.127(3)
V(1)–O(2)	2.012(2)	V(2)–O(3)	2.196(2)
V(1)–O(3)	2.357(2)	V(2)–O(4)	1.988(2)
V(1)–O(5)	1.988(2)	V(2)–O(6)	2.026(2)
V(1)–O(7)	1.577(2)	V(2)–O(8)	1.888(2)
V(1)–O(8)	1.777(2)	V(2)–O(9)	1.592(2)
O(1)–V(1)–O(2)	85.28(9)	N(1)–V(2)–O(3)	83.55(9)
O(1)–V(1)–O(3)	83.24(9)	N(1)–V(2)–O(4)	90.61(10)
O(1)–V(1)–O(5)	162.64(10)	N(1)–V(2)–O(6)	169.43(10)
O(1)–V(1)–O(7)	97.35(12)	N(1)–V(2)–O(8)	91.23(10)
O(1)–V(1)–O(8)	94.76(9)	N(1)–V(2)–O(9)	94.01(11)
O(2)–V(1)–O(3)	85.91(8)	O(3)–V(2)–O(4)	81.88(9)
O(2)–V(1)–O(5)	83.21(9)	O(3)–V(2)–O(6)	86.00(8)
O(2)–V(1)–O(7)	96.55(11)	O(3)–V(2)–O(8)	75.53(8)
O(2)–V(1)–O(8)	159.09(9)	O(3)–V(2)–O(9)	177.03(10)
O(3)–V(1)–O(5)	83.03(8)	O(4)–V(2)–O(6)	86.36(9)
O(3)–V(1)–O(7)	177.5(1)	O(4)–V(2)–O(8)	156.98(9)
O(3)–V(1)–O(8)	73.36(8)	O(4)–V(2)–O(9)	99.88(11)
O(5)–V(1)–O(7)	96.82(12)	O(6)–V(2)–O(8)	87.67(8)
O(5)–V(1)–O(8)	91.43(9)	O(6)–V(2)–O(9)	96.48(10)
O(7)–V(1)–O(8)	104.16(12)	O(8)–V(2)–O(9)	102.88(11)

5.4.3. Intermolecular Interactions and Self-assembly

We have investigated the self-assembly pattern of [(Hdmpz)OV(μ-acac)(μ-O)(μ-O_2CCH_3)VO(acac)] in the crystal via intermolecular non-covalent interactions. Vanadium(IV/V) bound oxo groups are known to participate as acceptor in intermolecular hydrogen bonding interactions to provide various types of self-assembled networks.[24–28] Here also the bridging oxo atom O(8) and one of the two terminal oxo atoms O(9) are involved in two intermolecular C–H···O interactions with the methyl groups belonging to the Hdmpz and acetylacetonate, respectively. The C(17)···O(8) and the C(5)···O(9) distances are 3.328(5) and 3.411(4) Å, respectively. The C(17)–H···O(8) and the C(5)–H···O(9) angles are 146 and 147°, respectively. Both interactions generate right handed helical structures (Fig. 5.2). The helix formed due to the C(5)–H···O(9) interaction propagates along the *b*-axis and that formed by the C(17)–H···O(8) interaction propagates along the *c*-axis. These two essentially mutually perpendicular C–H···O interactions form a two-dimensional assembly of the complex molecules (Fig. 5.3). There is no other significant non-covalent interaction between these layered structures.

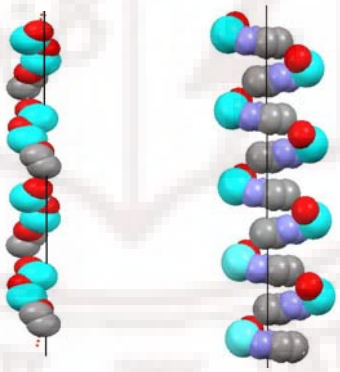

Fig. 5.2. The right-handed helices along the (a) *b*- and (b) *c*-axis formed via intermolecular C(5)–H···O(9) and C(17)–H···O(8) interactions, respectively. For clarity only the HC(5)C(4)O(2)V(1)O(8)V(2)O(9) and HC(17)C(16)N(2)N(1)V(2)O(8) atoms are shown in (a) and (b), respectively.

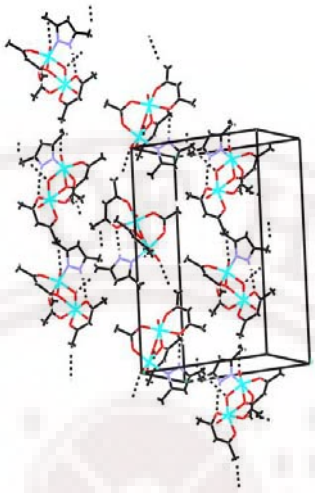

Fig. 5.3. Two dimensional network of [(Hdmpz) OV(μ-acac)(μ-O)(μ-O_2CCH_3)VO(acac)](**16**).

5.4.4. Electrochemical Properties

The electron transfer behavior of the complex in methanol solution has been examined with the help of cyclic voltammetry. It displays two irreversible responses at the cathodic and the anodic sides of Ag/AgCl reference electrode (Fig. 5.4). The former was observed at a platinum electrode while the latter was observed at a glassy carbon electrode. The one electron nature of each of these two responses is corroborated by comparing the peak current with known one electron transfer processes under identical conditions.[28,29] The response at the cathodic side ($E_{1/2}$ = −0.21 V, ΔE_p = 270 mV) is assigned to the V(IV)V(V) → V(IV)V(IV) reduction and that ($E_{1/2}$ = 0.43 V, ΔE_p = 480 mV) at the anodic side is assigned to the V(IV)V(V) → V(V)V(V) oxidation.

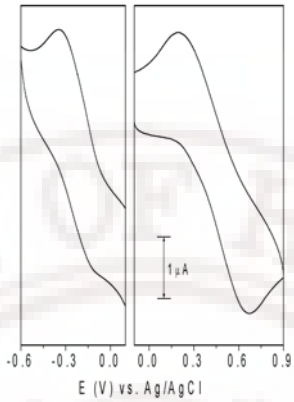

Fig. 5.4. Cyclic voltammograms (scan rate 50 mVs^{-1}) of [(Hdmpz)OV(μ-acac)(μ-O)(μ-O_2CCH_3)VO(acac)] in methanol (0.1 M TBAP) at 298 K

5.4.5. Spectroscopic Properties

The complex displays three strong overlapping bands at 1582, 1557 and 1530 cm^{-1} in the infrared spectrum. The highest frequency band is assigned to the asymmetric stretching of the bridging acetate group, while the following two bands are assigned to the coupled C⋯C and C⋯O stretching modes of the acetylacetonate ligands.[30,31] The medium intensity band observed at 1433 cm^{-1} is attributed to the symmetric stretching mode of the bridging acetate.[30,31] The N–H stretch of the Hdmpz appears as a broad band at 3270 cm^{-1}. A strong and a medium intensity band are observed at 986 and 965 cm^{-1}, respectively. These are assigned to the stretching frequencies of the two unsymmetrical terminal V=O bonds. Observation of such two V=O stretching modes for trapped-valent complexes of $\{V_2O_3\}^{3+}$ core has been reported before.[7,12]

The electronic spectrum of the complex in methanol solution displays a low intensity broad shoulder centered at 535 nm. The origin of this broad shoulder is presumably a combination of more than one ligand-field transitions.[7–12] Following this weak absorption a shoulder at 330 nm and a

strong absorption at 275 nm are observed. These are assigned to the ligand-to-metal charge transfer and ligand centered transitions. The complex does not display any low energy absorption that can be attributed to the intervalence transfer transition. The absence of intervalence band indicates the trapped valent character of the complex in solution.

The EPR spectra of the complex in methanol at 298 K and at 120 K are depicted in Fig. 5.5. The room temperature spectrum displays the clear eight line ^{51}V (I = 7/2) hyperfine structure. The g_{iso} and A_{iso} values are 1.984 and 97 x 10^{-4} cm^{-1}, respectively. Thus as observed in the electronic spectrum, the observation of the eight line spectrum instead of the fifteen line spectrum further corroborates the rare valence localized situation in solution phase for a complex of $\{V_2O_3\}^{3+}$ core.[7,9,12] The frozen solution spectrum displays a typical well resolved axial spectrum having $g_{\|}$ = 1.947 ($A_{\|}$ = 168 x 10^{-4} cm^{-1}) and $g_{\perp}$ = 1.986 ($A_{\perp}$ = 63 x 10^{-4} cm^{-1}).[8–10] It is well established that the parameters particularly the hyperfine constants obtained from the EPR spectra of oxovanadium(IV) complexes can be used to determine the type and number of the metal coordinating moieties with the help of the additivity relationship.[32] We have calculated the $A_{\|}$ value for the present valence localized complex from the contributions to it by the equatorial coordinating atoms of the tetravalent metal center V(2) namely the acetate-O, the acetylacetonate-O, the pyrazole-N and the bridging oxo group (Fig. 5.1). Due to unavailability of the data for the pyrazole-N and the bridging oxo group, we have used the values for the imidazole-N and OH^-, respectively.[32] The calculated $A_{\|}$ value (164.5 x 10^{-4} cm^{-1}) is very close to its value (168 x 10^{-4} cm^{-1}) determined from the frozen solution EPR spectrum of the complex.

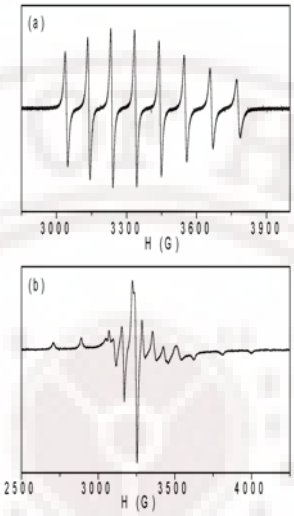

Fig. 5.5. X-band EPR spectra of [(Hdmpz)OV(μ-acac)(μ-O)(μ-O_2CCH_3)VO(acac)] in methanol at (a) 298 K and (b) 120 K.

5.4.6. Chirality of the Complex

The asymmetric molecules of [(Hdmpz)OV(μ-acac)(μ-O)(μ-O_2CCH_3)VO(acac)] crystallize in the chiral space group $P2_12_12_1$. Thus there is a spontaneous resolution in the crystal of the complex. The chiral molecules self assemble to a two-dimensional layered structure composed of two mutually perpendicular right-handed helices formed via intermolecular C–H···O interactions (*vide supra*). To verify whether the bulk crystalline material is optically enriched or racemic we have used the circular dichroism (CD) spectroscopy. The spectrum was collected with a powdered sample taken in silicone oil. Interestingly the powdered crystalline material is CD active (Fig. 5.6). Hence there is not only spontaneous resolution in the single crystal but as a whole the crystalline bulk material is also enriched by a single enantiomeric form.

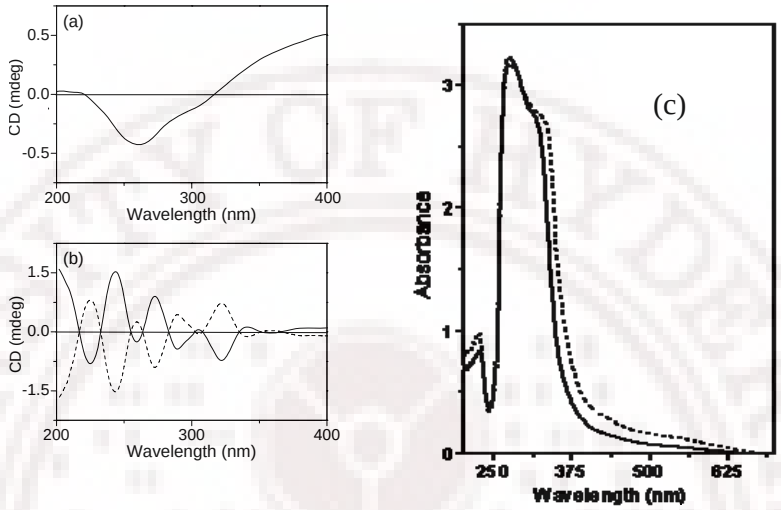

Fig. 5.6. (a) CD spectra of [(Hdmpz)OV(μ-acac)(μ-O)(μ-O_2CCH_3)VO(acac)]: powdered sample and (b) in solution with *d*-arabinose (—) and *l*-arabinose (--). (c) Electronic spectra of pure [(Hdmpz)OV(μ-acac)(μ-O)(μ-O_2CCH_3)VO(acac)] (—) and with *d*-arabinose (---) in dimethylsulfoxide.

As expected in solution the complex is CD inactive due to racemization. However, with the help of Pfeiffer effect[13] optical resolution of the complex in solution have been achieved. In this effect, the racemate equilibrium is shifted in favor of one enantiomer in presence of an enantiopure chiral compound as the environment substance. We have used *l*- and *d*-forms of arabinose (tetrahydro-pyran-2,3,4,5-tetraol) as the environment substance which are insoluble in methanol but soluble in dimethylsulfoxide. The electronic spectra of the complex in methanol and in dimethylsulfoxide are essentially identical. Thus the complex is not decomposed in dimethylsulfoxide. The dimethylsulfoxide solution of the complex is CD inactive but in presence of *l*- or *d*-arabinose it is CD active. The complex and arabinose were dissolved in dimethylsulfoxide in 1:2 mole ratio, allowed to

stay for 12 h to attain the equilibrium and then the CD spectra were recorded. These spectra (Fig. 5.6) clearly show the presence of the two enantiomeric forms of the complex in solution. The O–H groups of arabinose can form hydrogen bonds with the oxo groups present in the complex.[36] Hence the enantiomeric enrichment of the complex in solution most likely occurs due to the formation of its hydrogen bonded aggregate with *l*- or *d*-arabinose. Formation of such aggregates is also indicated by a small but definite red shift of the electronic spectrum of the complex in presence of *l*- or *d*-arabinose (Fig. 5.6 (c)).

5.5. Conclusion

A novel unsymmetrical complex of the (μ-oxo)dioxovanadium(IV,V) core, $\{OV(\mu\text{-}O)VO\}^{3+}$, containing an acetate and an acetylacetonate as two additional bridges between the metal centers has been synthesized and characterized. The complex, [(Hdmpz)OV(μ-acac)(μ-O)(μ-O_2CCH_3)VO(acac)], crystallizes in the chiral space group $P2_12_12_1$ and the crystal structure revealed a valence localized $\{OV(\mu\text{-}O)VO\}^{3+}$ core with a near perfect *syn* configuration and a very small V–O–V angle ($118.7(1)^o$). In the crystal lattice, self-assembly of the chiral complex molecules via two intermolecular C–H···O interactions leads to a two dimensional structure composed of two mutually perpendicular right-handed helices. This complex provides the rare example for a divanadium(IV,V) species having a valence localized electronic structure in fluid solution at ambient temperature. It is very likely that the valence delocalization is prevented primarily by the very different coordination environment of the two metal centers. CD spectroscopic measurements with the powdered sample showed that the crystallization of the chiral complex from racemic solution results into optically enriched bulk material. The presence of both enantiomers of the

complex in solution has been demonstrated via chiral discrimination activated by enantiopure arabinose as an environment substance.

Supplementary material

Crystallographic data for the complex, [(Hdmpz)OV(μ-acac)(μ-O)(μ-O_2CCH_3)VO(acac)], has been deposited with the Cambridge Crystallographic Data Centre (deposition number is CCDC-705100)

5.6. References

1. M. Nishizawa, K. Hirotsu, S. Ooi, K. Saito, *J. Chem. Soc., Chem. Commun.*, 1979, 707.
2. P. Blanc, C. Madic, J. –P. Launay, *Inorg. Chem.*, 1982, **21**, 2923.
3. F. Babonneau, C. Sanchez, J. Livage, J. –P. Launay, M. Daoudi, Y. Jeannin, *Nouv. J. Chem.*, 1982, **6**, 353.
4. A. Kojima, K. Okajaki, S. Ooi, K. Saito, *Inorg. Chem.*, 1983, **22**, 1168.
5. J. –P. Launay, Y. Jeannin, M. Daoudi, *Inorg. Chem.*, 1985, **24**, 1052.
6. J.C. Pessoa, J.A. L. Silva, A.L. Vieira, L. Vilas-Boas, P. O'Brien, P. Thornton, *J. Chem. Soc. Dalton Trans.*, 1992, 1745.
7. D. Schultz, T. Weyhermüller, K. Weighardt, B. Nuber, *Inorg. Chim. Acta*, 1995, **40**, 217.
8. S. Mondal, P. Ghosh, A. Chakravorty, *Inorg. Chem.*, 1997, **36**, 59.
9. M. Mahroof-Tahir, A.D. Keramidas, R.B. Goldfarb, O.P. Anderson, M.M. Miller, D.C. Crans, *Inorg. Chem.*, 1997, **36**, 1657.
10. S.K. Dutta, S.B. Kumar, S. Bhattacharyya, E.R.T. Tiekink, M. Chaudhury, *Inorg. Chem.*, 1997, **36**, 4954.
11. R.A. Holwerda, B. R. Whittlesey, M. J. Nilges, *Inorg. Chem.*, 1998, **37**, 64.
12. S.K. Dutta, S. Samanta, S.B. Kumar, O.H. Han, P. Burckel, A.A. Pinkerton, M. Chaudhury, *Inorg. Chem.*, 1999, **38**, 1982.
13. P. Pfeiffer, K. Quehl, *Ber.*, 1931, **64**, 2667.

14. R.A. Rowe, M.M. Jones, *Inorg. Synth.*, 1957, **5**, 113.
15. L.L. Koh, O.L. Kon, K.W. Loh, Y.C. Long, J.D. Ranford, A.L.C. Tan, Y.Y. Tjan, *J. Inorg. Biochem.*, 1998, **72**, 155.
16. W.E. Hatfield, *Theory and Applications of Molecular Paramagnetism* (Eds.: E.A. Boudreaux, L. N. Mulay), Wiley, New York, 1976, p. 491.
17. *SMART 5.630 and SAINT-plus 6.45*, Bruker-Nonius Analytical X-ray Systems Inc., Madison, WI, USA, 2003.
18. G.M. Sheldrick, *SADABS Program for area detector absorption correction*, University of Göttingen, Göttingen, Germany, 1997.
19. G.M. Sheldrick, *SHELX-97 Programs for Crystal Structure Analysis*, University of Göttingen, Göttingen, Germany, 1997.
20. L.J. Farrugia, *J. Appl. Crystallogr.*, 1999, **32**, 837.
21. P. McArdle, *J. Appl. Crystallogr.*, 1995, **28**, 65.
22. A.L. Spek, *PLATON A Multipurpose Crystallographic Tool*, Utrecht University, Utrecht, The Netherlands, **2002**.
23. R.H. Wiley, P.E. Hexner, *Org. Synth. Coll.*, 1963, **4**, 351.
24. S.N. Pal, K.R. Radhika, S.Pal, *Z. Anorg. Allg. Chem***.,** 2001, **627,** 1631.
25. S.P. Anthony, L. Srikanth, T.P. Radhakrishnan, *Mol. Cryst. Liq. Cryst.*, **2002**, **381**, 133.
26. A. Sarkar, S. Pal, *Polyhedron*, 2006, **25**, 1689.
27. A. Sarkar, S. Pal, *Polyhedron*, 2007, **26**, 1205.
28. A. Sarkar, S. Pal, *Inorg. Chim. Acta*, 2008, **361**, 2296.
29. S.G. Sreerama, S. Pal, *Inorg. Chem.*, 2005, **44**, 6299.
30. H.J. Mok, J.A. Davis, S. Pal, S.K. Mandal, W.H. Armstrong, *Inorg. Chim. Acta*, 1997, **263**, 385.
31. K. Nakamoto, *Infrared and Raman Spectra of Inorganic and Coordination Compounds*, Wiley, New York, 1986, pp. 232–233 and 259-260.
32. T.S. Smith II, R. LoBrutto, V.L. Pecoraro, *Coord. Chem. Rev.*, 2002, **228**, 1.
33. V. Shivaiah, T. Arumuganathan, S.K. Das, *Inorg. Chem. Commun.*, 2004, **7**, 367.

Divanadium(V) complexes with acetylacetone aroylhydrazones

6.1. Abstract

In acetonitrile, reactions of bis(acetylacetonato)oxovanadium(IV) ([$VO(acac)_2$]) with 4-*R*-benzoylhydrazine in 1:1 mole ratio provide coordinatively symmetrical complexes (**17**–**21**) of the $\{OV(\mu\text{-}O)VO\}^{4+}$ motif in 40–47% yields. On the other hand, in methanol the same reactants provide complexes (**22**–**26**) containing the $\{OV(\mu\text{-}OMe)_2VO\}^{4+}$ core in 37–50% yields. In both series of complexes, the ligand is the O,N,O-donor deprotonated Schiff base system acetylacetone aroylhydrazone formed by template condensation of $acac^-$ with 4-*R*-benzoylhydrazine (R = H, Cl, OMe, NO_2 and NMe_2). All the complexes have been characterized by elemental analysis, magnetic and spectroscopic (IR, UV-vis and NMR) measurements. Molecular structures of three representative complexes (**20**, **22** and **23**) have been determined by X-ray crystallography. In each complex, the dianionic planar ligand is coordinated to the metal centre via the enolate-O, the imine-N and the O-atom of the deprotonated amide functionality. Cyclic voltammetric measurements in dichloromethane revealed that complexes **17**–**21** are redox inactive, while complexes **22**–**26** display a metal centred reduction in the potential range –0.06 to 0.32 V (vs. Ag/AgCl).

6.2. Introduction

In an attempt to prepare a $\{V_2O_3\}^{4+}$ complex, we have treated $[VO(acac)_2]$ with acetylhydrazine in acetonitrile under aerobic condition expecting a template reaction for the formation of the tridentate ligand expected from condensation of Hacac and acetylhydrazine. However, instead of the target complex, an unsymmetrical chiral trapped-valent complex, $[(Hdmpz)OV^{IV}(\mu\text{-acac})(\mu\text{-O})(\mu\text{-}O_2CCH_3)V^{V}O(acac)]$ (**16**) (Hdmpz = 3,5-dimethylpyrazole) has been isolated.[1] Complex has been described in the previous chapter. To explore whether analogous unsymmetrical complexes of $\{OV(\mu\text{-O})VO\}^{3+}$ core can be prepared or not, we have reacted various 4-susbstituted benzoylhydrazines with $[VO(acac)_2]$ in acetonitrile in presence of air. However, all the reactions yielded the original target species, the coordinatively symmetrical divanadium(V) complexes, [(acacbhR)OV(μ-O)VO(acacbhR)] (**17**–**21**). When the reactions were conducted in methanol dimeric oxomethoxovanadium(V) species, $[(acacbhR)OV(\mu\text{-}OMe)_2VO(acacbhR)]$ (**22**–**26**), were obtained. Herein, we describe the syntheses, characterization and physical properties of these two series of divanadium(V) complexes.

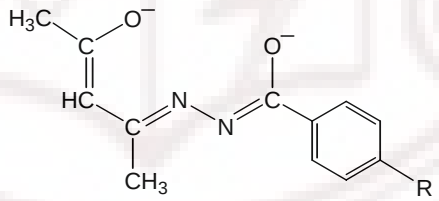

H_2acacbhR

(R = H, Cl, Ome, NO_2 and NMe_2)

6.3. Experimental

6.3.1. Materials

Bis(acetylacetonato)oxovanadium(IV)[2] was prepared by following a reported procedure. All other chemicals and solvents used in this work were of analytical grade available commercially and were used without further purification

6.3.2. Physical measurements

Microanalytical (C, H, N) data were obtained with the help of a Thermo Finnigon Flash EA1112 series elemental analyzer. Solution electrical conductivities were measured with a Digisun DI-909 conductivity meter. Magnetic susceptibility measurements were performed with a Sherwood Scientific balance. A Jasco-5300 FT-IR spectrophotometer was used to record the infrared spectra. Electronic spectra were recorded on a Shimadzu 3101-PC UV/vis/NIR spectrophotometer. The ^{1}H ($Si(CH_3)_4$ as internal standard) and ^{51}V ($VOCl_3$ as external standard) NMR spectra were collected with the help of a Bruker 400 MHz NMR spectrometer. A CH-Instruments model 620A electrochemical analyzer was used for cyclic voltammetric measurements with dichloromethane solutions of the complexes containing tetrabutylammonium perchlorate (TBAP) as the supporting electrolyte. The three electrode measurements were carried out at 298 K under dinitrogen atmosphere with a platinum disk working electrode, a platinum wire auxiliary electrode and an Ag/AgCl reference electrode. Under identical condition the Fc^{+}/Fc couple was observed at 0.38 V. The potentials reported in this work are uncorrected for junction contributions.

6.3.3. Synthesis of $[V_2O_3(acacbh)_2]$ (17)

An acetonitrile solution (15 ml) of $[VO(acac)_2]$ (0.53 g, 2 mmol) was added to an acetonitrile solution (15 ml) of benzoylhydrazine (0.27 g, 2 mmol)

and the mixture was heated on a steam bath for 15 min. The brown solution thus obtained was kept in air at room temperature for slow evaporation. In about 2–3 days the complex was obtained as a brown crystalline material. It was collected by filtration and dried in air. Yield was 0.25 g (43%).

The complexes $[V_2O_3(acacbhCl)_2]$ (**18**), $[V_2O_3(acacbhOMe)_2]$ (**19**), $[V_2O_3(NO_2)_2]$ (**20**) and $[V_2O_3(NMe)_2]$ (**21**) were synthesized by using one mole equivalent each of $[VO(acac)_2]$ and the corresponding 4-*R*-benzhydrazide in 40–47% yields by following the same procedure as described above.

The dimeric oxomethoxovanadium(V) complexes $[VO(OMe)(acacbh)]_2$ (**22**), $[VO(OMeacacbhCl)()]_2$ (**23**), $[VO(OMe)(acacbhOMe)]_2$ (**24**), $[VO(OMe)(acacbhNO_2)]_2$ (**25**) and $[VO(OMe)(NMe_2)]_2$ (**26**) were also prepared from one mole equivalent each of $[VO(acac)_2]$ and the corresponding 4-*R*-benzhydrazide in 37–50% yields by following the same procedure as described for **17** except for the solvent used as the reaction medium. For these complexes the reactions were conducted in methanol instead of acetonitrile.

6.3.4. X-ray crystallography

Single crystals of $[V_2O_3(acacbhNO_2)_2]$ (**20**) were grown by slow evaporation of an acetonitrile solution of complex. For both $[VO(OMe)(acacbhH)]_2$ (**22**) and $[VO(OMe)(acacbhCl)]_2$ (**23**), the single crystals were collected from the products obtained during their syntheses. The unit cell parameters and the intensity data for all the crystals were obtained on a Bruker-Nonius SMART APEX CCD single crystal X-ray diffractometer, equipped with a graphite monochromator and a Mo $K\alpha$ fine-focus sealed tube (λ = 0.71073 Å) operated at 2.0 kW. The detector was placed at a distance of 6.0 cm from the crystal. Data were collected at 298 K with a scan width of 0.3º in ω and an exposure time of 10 s/frame. The SMART software was used for data acquisition and the SAINT-Plus software was used for data

extraction.[3] The absorption corrections were performed with the help of the SADABS program.[4] The structures were solved by direct methods and refined on F^2 by full-matrix least-squares procedures. All non-hydrogen atoms were refined anisotropically. The hydrogen atoms were added at idealized positions by using a riding model. The SHELX-97 programs[5] of the WinGX package[6] were used for structure solution and refinement. The ORTEX6a[7] and Platon[8] packages were used for molecular graphics. Selected crystallographic data are summarized in Table 6.1.

Table 6.1. Selected crystal data for (**20**), (**22**) and (**23**)

Complex	**20**	**22**	**23**
Empirical formula	$V_2C_{24}H_{22}N_6O_{11}$	$V_2C_{26}H_{30}N_4O_8$	$V_2C_{26}H_{28}N_4O_8Cl_2$
Formula mass (g mol^{-1})	672.36	628.42	697.30
Crystal system	Orthorhombic	Orthorhombic	Monoclinic
Space group	*P*na2$_1$	*P*bca	*P*2$_1$/c
a (Å)	25.727(3)	10.990(2)	8.5913(9)
b (Å)	7.6471(9)	12.304(2)	12.4005(12)
c (Å)	14.1843(16)	21.216(4)	14.1496(14)
α (^{o})	90	90	90
β (^{o})	90	90	100.826(2)
γ (^{o})	90	90	90
V (Å^3)	2790.6(5)	2868.7(9)	1480.6(3)
Z	4	4	2
ρ (g cm^{-3})	1.600	1.455	1.564
μ (mm^{-1})	0.740	0.705	0.866
Reflections collected	19668	11859	13379
Reflections unique	3906	2771	2902
Reflections ($I \geq 2\sigma(I)$)	1625	2545	2521
Parameters	392	184	193
GOF on F^2	0.964	1.387	1.042
R_1, wR_2 ($I \geq 2\sigma(I)$)	0.0773, 0.1774	0.0780, 0.1544	0.0329, 0.0886
R_1, wR_2 (all data)	0.1867, 0.2518	0.0848, 0.1573	0.0385, 0.0923
Lar gest peak, hole (e Å^{-3})	0.687, –0.342	0.538, –0.385	0.288, –0.273

[a] $R_1 = \sum||F_o| - |F_c||/\sum|F_o|$. [b] $wR_2 = \{\sum[(F_o^2 - F_c^2)^2]/\sum[w(F_o^2)^2]\}^{1/2}$. [c] GOF = $\{\sum[w(F_o^2 - F_c^2)^2]/(n-p)\}^{1/2}$ where 'n' is the number of reflections and 'p' is the number of parameters refined.

6.5. Results and discussion

6.5.1. Synthesis and some properties

The synthetic procedures for both series of complexes, $[V_2O_3(acacbhR)_2]$ (**17**–**21**) and $[VO(OMe)(acacbhR)]_2$ (**22**–**26**), are essentially identical except for the solvent used as the reaction medium. In acetonitrile, the $\{V_2O_3\}^{4+}$ core is stabilized, while the $\{VO(OMe)\}^{2+}$ unit is preferred in methanol. In both cases, $[VO(acac)_2]$ and acid hydrazide (1:1 mole ratio) were used as starting materials. The ligands are thus formed due to template reactions between one of the metal coordinated acetylacetonate in $[VO(acac)_2]$ and the corresponding acid hydrazide. As the complexes are formed only under aerobic condition, the oxygen in air acts as the oxidant for the oxidation of the metal centre from +4 to +5 state. The microanalysis data for the complexes are listed in Table 6.2. The data are satisfactory with their molecular formulae. All the complexes are electrically non-conducting in solution. The magnetic susceptibility measurements with powdered samples of **17**–**26** indicate their diamagnetic nature and confirm the +5 oxidation state of the metal centre in each complex.

Table 6.2. Elemental analysis data

Complex	Found (calc.) (%)		
	C	**H**	**N**
17	49.37 (49.50)	3.98 (4.15)	9.49 (9.62)
18	44.15 (44.26)	3.38 (3.40)	8.51 (8.60)
19	48.39 (48.61)	4.16 (4.39)	8.53 (8.72)
20	42.54 (42.87)	3.09 (3.30)	12.27 (12.50)
21	50.12 (50.31)	4.97 (5.13)	12.39 (12.57)
22	49.41 (49.69)	4.64 (4.81)	8.72 (8.91)
23	44.45 (44.78)	3.92 (4.05)	7.91 (8.03)
24	48.63 (48.85)	4.74 (4.98)	7.98 (8.14)
25	43.29 (43.47)	3.77 (3.93)	11.56 (11.70)
26	50.28 (50.43)	5.53 (5.64)	11.64 (11.76)

6.5.2. Spectroscopic properties

Infrared spectra of the complexes in KBr disks do not display the characteristic bands associated with the C=O and the N–H functionalities of the free Schiff base system H_2acacbhR. The spectra of (**16**) and (**24**) are shown in Fig. 6.1.Thus in each complex both the acetylacetone and the amide fragments of the metal coordinated tridentate ligand are in enolate form. All the complexes display a strong band within 1601–1585 cm^{-1}. This band is attributed to the C=N–N=C fragment of the ligand.[9-15] Complexes **17**–**21** display a strong and a moderately strong band in the ranges 999–947 and 864–804 cm^{-1}, respectively. Such bands are typical of complexes containing

the $\{OV(\mu\text{-}O)VO\}^{4+}$ core.[10,19-23] The higher energy strong band is assigned to the V=O stretching, while the origin of the lower energy band is the asymmetric stretching of the V–O–V bridge. The V=O stretching observed within 998–984 cm^{-1} for complexes **22**–**26** is comparable with that reported for complexes of the $\{VO(OMe)\}^{2+}$ unit.[9,15,16]

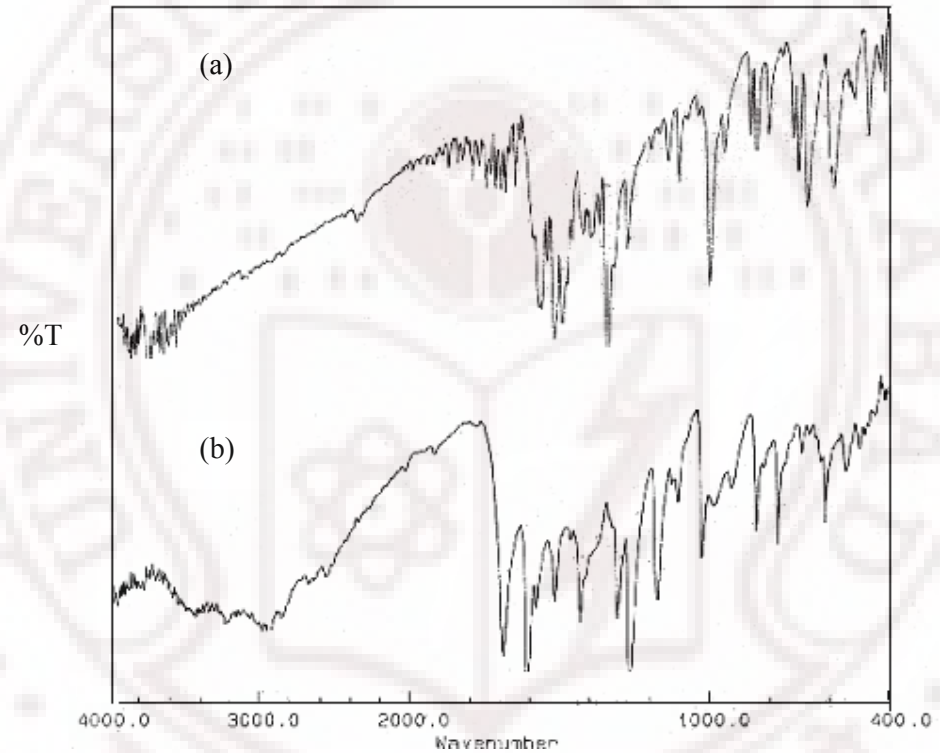

Fig. 6.1. Infrared spectra of (a) (**16**) and (b) (**24**) in KBr disks.

Electronic spectra of **17**–**26** were collected using their chloroform solutions. Representative spectra of both series of complexes are shown in Fig 6.2. The data are summarized in Table 6.3. The spectral profiles of the complexes are very similar. The spectra of (**20**) and (**22**) are illustrated in Fig.

6.2. All of them display two strong absorptions in the wavelength range 440–327 nm. These are likely to be due to the ligand-to-metal charge transfer transitions.[10,19-23] The very intense absorption observed within 290–260 nm is believed to be due to ligand centred transition.

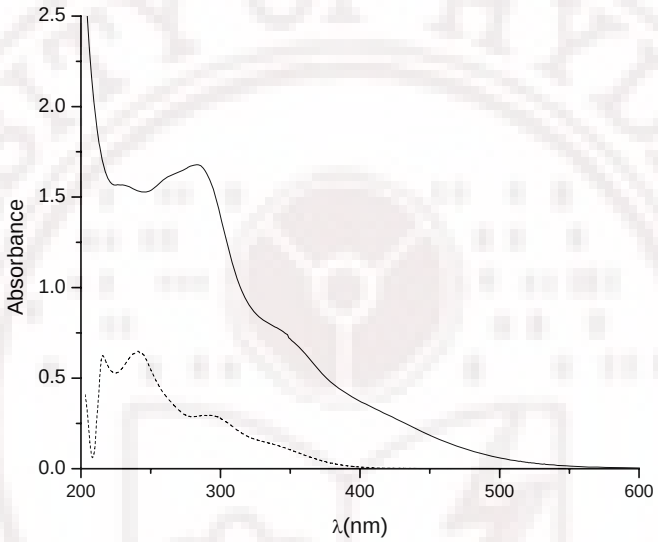

Fig. 6.2. Electronic spectra of (**20**) (····) and (**22**) (–) in chloroform.

The proton NMR spectra of all the complexes were collected in $CDCl_3$. The spectra of **17**–**21** display two singlets in the ranges δ 2.01–2.09 ppm and δ 3.34–3.48 ppm. These are assigned to the protons of the two methyl groups present in the acetylacetone fragment of the tridentate ligand. The –CH= proton of the acetylacetone fragment appears as a singlet within δ 5.15–5.75 ppm. The aromatic protons are observed in the range δ 7.0–8.3 ppm. For complexes **19** and **21** the methyl protons of the OMe and NMe_2 substituents on the aroyl fragments of the ligands are observed as singlets at δ 3.83 and 2.51 ppm, respectively. For complexes **22**–**26** the acetylacetone methyl groups appear as singlets within δ 2.01–2.17 ppm and δ 3.45–3.51 ppm. These complexes display an additional singlet within δ 3.75–3.92 ppm. This

signal has been assigned to the methyl protons of the metal coordinated methoxo group. The –CH= proton of the acetylacetone fragment resonates as a singlet within δ 5.29–5.32 ppm. The aromatic protons appear in the range δ 7.0–8.1 ppm. The methyl protons of the OMe and NMe_2 substituents on the aroyl fragments of the ligands in complexes **24** and **26** resonate as singlet at δ 3.49 and 2.55 ppm, respectively. Chloroform solutions of the complexes were used to record the ^{51}V NMR spectra (Table 6.3.). Complexes **17**–**21** display a strong resonance within δ –485 to –515 ppm. On the other hand, complexes **22**–**26** show a similar resonance between δ –484 to –510 ppm. These chemical shifts are comparable with that observed for oxidic pentavalent vanadium complexes having oxygen and nitrogen donor ligands.[23]

Table 6.3. Electronic[a] and ^{51}V NMR spectroscopic data

Complex	λ_{max} (nm) (10^{-3} x ε (M^{-1} cm^{-1}))	δ (ppm)
17	430[b] (2.4), 355 (5.1), 265 (13.2)	–515
18	425[b] (7.5), 350 (5.1), 260 (12.1)	–510
19	435[b] (2.0), 350 (5.3), 261 (13.3)	–487
20	430[b] (1.9), 355 (4.2), 268 (9.1)	–497
21	440[b] (2.0), 348 (4.8), 265 (11.3)	–485
22	420[b] (2.9), 340[b] (7.8), 286 (16.9)	–484
23	407[b] (4.7), 345[b] (10.7), 285 (22.7)	–509
24	410[b] (3.0), 345[b] (5.8), 265 (13.5)	–487
25	400[b] (7.2), 327[b] (16.9), 290 (19.9)	–487
26	440[b] (1.5), 345[b] (4.9), 265 (12.1)	–510

[a] In chloroform.
[b] Shoulder.

6.5.3. Electrochemical Properties

Electron transfer properties of all the complexes in dichloromethane have been examined with the help of cyclic voltammetry. Complexes **17**–**21** do not show any response, while complexes **22**–**26** display a reduction couple in the potential range –0.06 to 0.32 V. A representative cyclic voltammogram is shown in Fig. 6.3. and the potential data are listed in Table 6.4. The current heights of this couple are comparable with known one-electron redox processes under identical conditions.[1,9,15,28,29] Thus, this reduction is assigned to the vanadium(V) → vanadium(IV) reduction. The effect of the electronic nature of the substituent (*R*) present on the tridentate ligand is clearly reflected on the trend of the $E_{1/2}$ values for this reduction. The $E_{1/2}$ has the highest value for complex **25** containing the most electron withdrawing substituent NO_2, while it has the lowest value for complex **26** having most electron releasing substituent NMe_2 (Table 6.4.). The plot of the $E_{1/2}$ values against the Hammett substituent constants (σ_p)[30] shows a satisfactory linear relationship between them (Fig. 6.3.). Thus the vanadium(V) to vanadium(IV) reduction becomes easier as the V–O(amide) bond strength decreases with the increase of the electron withdrawing ability of the substituent (R) at the *para* position of the aroyl moiety. The variation of the bond strength is clearly reflected by the relatively shorter V–O(amide) bond length (1.916(3) Å) in **22** (R = H) compared to that (1.9245(14) Å) in **23** (R = Cl) (Table 6.6.).

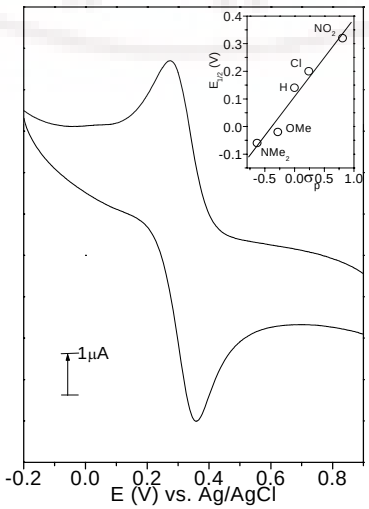

Fig. 6.3. Cyclic voltammogram (scan rate 50 mVs^{-1}) of (**25**) in dichloromethane (0.1 M TBAP). Inset: Correlation between the $E_{1/2}$ values for the vanadium(V)–vanadium(IV) reduction and the Hammett substituent constants. The straight line represents a linear least-squares fit.

Table 6.4. Cyclic voltammetric[a] data

Complex	$E_{1/2}$[b] (V)	ΔE_p[c] (mV)
22	0.14	90
23	0.20	80
24	–0.02	190
25	0.32	80
26	–0.06	110

[a] In dichloromethane (298 K) at a scan rate of 50 mVs^{-1}.
[b] $E_{1/2} = (E_{pa} + E_{pc})/2$, where E_{pa} and E_{pc} are anodic and cathodic peak potentials, respectively.
[c] $\Delta E_p = E_{pa} - E_{pc}$.

6.5.4 Molecular structures

$[V_2O_3(acacbhNO_2)_2]$ (**20**) crystallizes in the space group $Pna2_1$, while $[VO(OMe)(acacbh)]_2$ (**22**) and $[VO(OMe)(acacbhCl)]_2$ (**23**) crystallize in the space groups $Pbca$ and $P2_1/c$, respectively. In the case of **20**, the asymmetric unit contains a whole molecule of the complex. On the other hand, for each of **22** and **23**, the complex molecule has crystallographically imposed inversion symmetry and hence the asymmetric unit contains half of the dimeric molecule. The molecular structures of $[V_2O_3(acacbhNO_2)_2]$ (**20**), $[VO(OMe)(acacbh)]_2$ (**22**) and $[VO(OMe)(acacbhCl)]_2$ (**23**) are depicted in Figs. 6.3, 6.4(a) and 6.4(b), respectively. The C=C (1.29(2)–1.350(6) Å) and the C–O (1.315(2)–1.324(19) Å) bond lengths in the $-HC=C(O^-)-$ fragment[16-18,24,25] and the N=C (1.290(3)–1.305(17) Å) and the C–O (1.30(2)–1.317(5) Å) bond lengths in the $-N=C(O^-)-$ fragment[9-15,16-18,24-26] indicate the enolate form of both acetylacetone and the amide moieties of the ligands in all the three structures. Selected bond parameters associated with the metal ion for **20** are listed in Table 6.5. and that for **22** and **23** are listed in Table 6.6.

Although the two halves of the molecule of **20** are coordinatively symmetrical, but they are crystallographically inequivalent (Fig. 6.4). Each of the two metal centres is in essentially ideal square-pyramidal O_4N coordination environment. The O,N,O-donor $(acacbhNO_2)^{2-}$ together with the bridging oxo group form the O_3N square-base (mean deviations 0.05 and 0.06 Å) and the terminal oxo group satisfies the apical site. The value of τ defined as $(\beta-\alpha)/60$, where α is the smaller and β is the larger *trans* bond angles in the basal plane, reflects the extent of distortion of a square-pyramidal geometry toward a trigonal-bipyramidal geometry. A value of zero indicates an ideal square-pyramidal geometry, while a value of unity is expected for an ideal trigonal-bipyramidal geometry.[27] The value of τ is found to be 0.08 and 0.09 for V1 and V2, respectively. The dihedral angle between the two basal planes is 56.1(3)°. The V1···V2 distance, V–O–V bridge angle and the O=V···V=O torsion angle are 2.995(3) Å, 109.7(4)° and 77.6(7)°, respectively. Both metal centres are displaced from the basal plane toward the apical oxo group. These

displacements are 0.443(8) and 0.462(7) Å for V1 and V2, respectively. The V–O(enolate), V–N(imine) and V–O(amide) bond lengths are comparable with the bond lengths observed in vanadium(V) complexes having the same coordinating atoms.[1,9-15,21,26] The V–O(bridging) and the V=O bond lengths are within the range reported for complexes containing the $\{V_2O_3\}^{4+}$ core.[10,19-23]

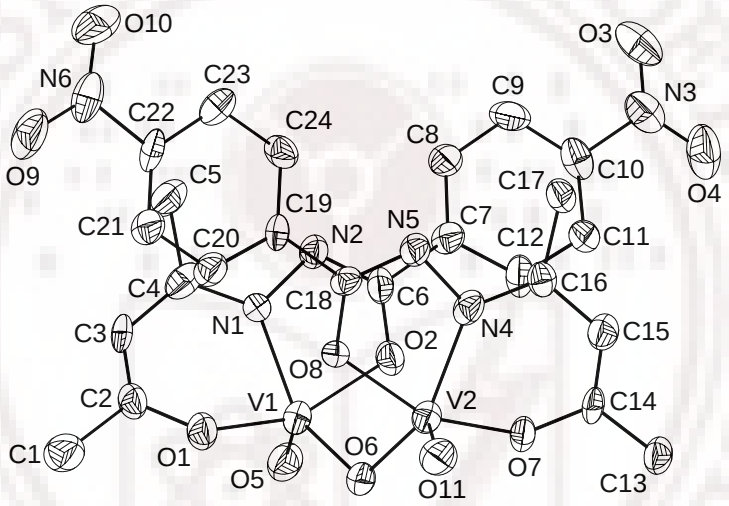

Fig. 6.4. Molecular structure of (**20**) with the atom labeling scheme. All non-hydrogen atoms are represented by their 25% probability thermal ellipsoids. Hydrogen atoms are omitted for clarity

The inverse symmetry related monomeric units of both **22** and **23** are square-pyramidal. The O,N,O-donor $(acacbhR)^{2-}$ (R = H and NO_2) and the methoxo O-atom constitute the O_3N basal plane and the oxo group occupies the apical site. The τ values are 0.02 and 0.05 for the monomers of **22** and **23**, respectively. The metal centre is displaced from the square-base toward the apical oxo group by 0.351(2) Å in the case of **22** and by 0.340(1) Å in the case of **23**.

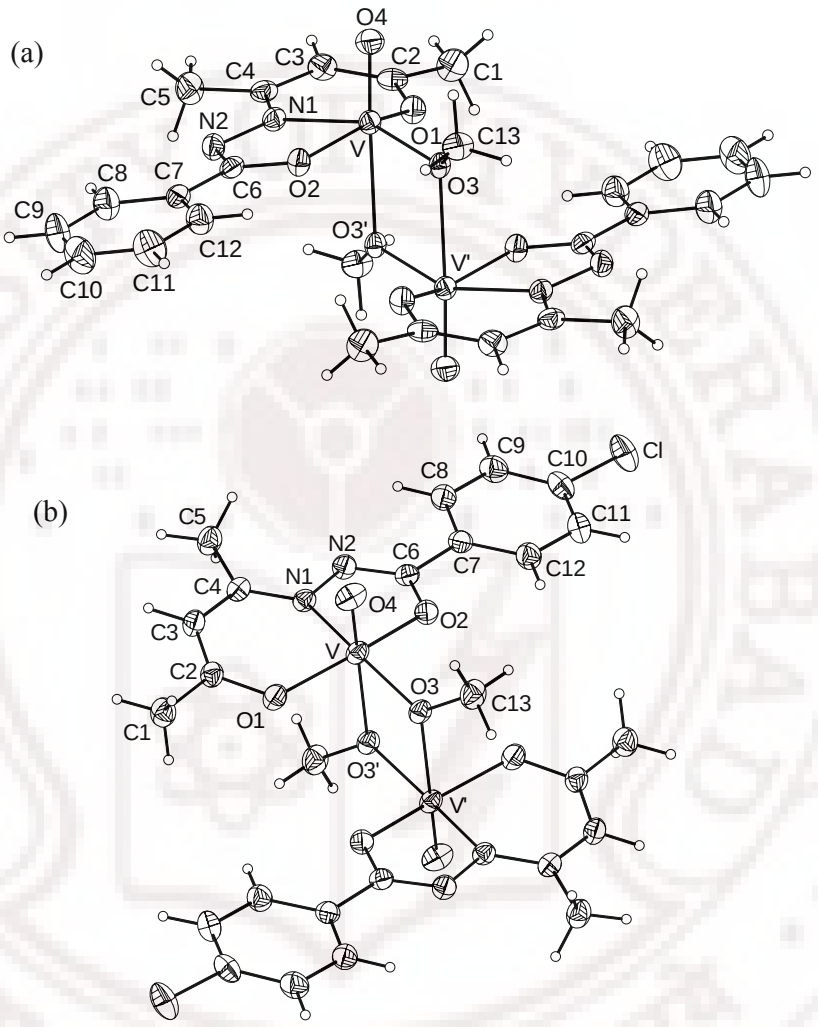

Fig. 6.5. Molecular structure of (a) (**22**) and (b) (**23**) with the atom labeling scheme. All non-hydrogen atoms are represented by their 30% probability thermal ellipsoids.

Two of these square-pyramidal units form a dimeric aggregate via reciprocal coordination of the methoxo O-atom at the *trans* position of the oxo

group (Figs. 6.5(a) and 6.5(b)). As a result the metal centres in each dimeric complex becomes hexacoordinated. Thus the geometry of the dimeric species can be described as edge shared two distorted octahedra. The V···V distances (3.403(1) Å in **22** and 3.3945(7) Å in **23**) and the V–O–V bridges angles (106.21(12)^{o} in **22** and 106.43(6)^{o} in **23**) are very similar in the two complexes. The V=O and the short and long V–O(methoxo) bond lengths are unexceptional.[9,15,26] The V–O(enolate), V–N(imine) and V–O(amide) bond lengths are similar to those observed for **20** and pentavalent vanadium complexes with ligands having similar coordinating centres.[1,9-15,21,26]

Table 6.5. Selected bond lengths (Å) and bond angles (^{o}) for (**20**)

V(1)–O(1)	1.845(10)	V(2)–O(6)	1.844(11)
V(1)–O(2)	1.936(10)	V(2)–O(7)	1.854(9)
V(1)–O(5)	1.594(13)	V(2)–O(8)	1.934(9)
V(1)–O(6)	1.818(11)	V(2)–O(11)	1.551(13)
V(1)–N(1)	2.054(13)	V(2)–N(4)	2.038(15)
O(1)–V(1)–O(2)	152.0(6)	O(6)–V(2)–O(7)	102.9(6)
O(1)–V(1)–O(5)	102.3(7)	O(6)–V(2)–O(8)	84.6(5)
O(1)–V(1)–O(6)	102.6(6)	O(6)–V(2)–O(11)	108.0(6)
O(1)–V(1)–N(1)	84.3(5)	O(6)–V(2)–N(4)	145.5(5)
O(2)–V(1)–O(5)	101.4(6)	O(7)–V(2)–O(8)	151.2(5)
O(2)–V(1)–O(6)	84.8(5)	O(7)–V(2)–O(11)	101.5(6)
O(2)–V(1)–N(1)	75.7(5)	O(7)–V(2)–N(4)	83.7(5)
O(5)–V(1)–O(6)	106.5(6)	O(8)–V(2)–O(11)	102.4(6)
O(5)–V(1)–N(1)	103.4(6)	O(8)–V(2)–N(4)	75.3(5)
O(6)–V(1)–N(1)	147.0(5)	O(11)–V(2)–N(4)	103.6(6)

Table 6.6. Selected bond lengths (Å) and bond angles (^{o}) for (**22**)[a] and (**23**)[b]

Bond parameters	22	23
V–O(1)	1.859(3)	1.8575(14)
V–O(2)	1.916(3)	1.9245(14)
V–O(3)	1.829(3)	1.8212(12)
V–O(4)	1.587(3)	1.5791(15)
V–N(1)	2.082(3)	2.0811(15)
V–O(3)′	2.404(3)	2.3953(14)
O(1)–V–O(2)	153.37(14)	152.91(6)
O(1)–V–O(3)	103.59(12)	104.14(6)
O(1)–V–O(4)	100.26(16)	99.02(8)
O(1)–V–N(1)	84.43(13)	83.95(6)
O(1)–V–O(3)′	79.94(12)	79.82(6)
O(2)–V–O(3)	89.10(12)	89.47(6)
O(2)–V–O(4)	99.38(16)	100.41(8)
O(2)–V–N(1)	75.00(13)	75.02(6)
O(2)–V–O(3)′	81.35(11)	81.84(6)
O(3)–V–O(4)	103.37(15)	103.45(7)
O(3)–V–N(1)	154.78(13)	156.01(6)
O(3)–V–O(3)′	73.79(12)	73.57(6)
O(4)–V–N(1)	98.53(15)	97.38(7)
O(4)–V–O(3)′	177.08(14)	176.32(6)
N(1)–V–O(3)′	84.39(12)	86.00(5)
V–O(3)–V′	106.21(12)	106.43(6)

Symmetry transformations used to generate equivalent atoms:
[a] –x + 2, –y + 1, –z
[b] –x, –y + 1, –z + 2

6.6. Conclusion

Two series of divanadium(V) complexes containing the $\{OV(\mu\text{-}O)VO\}^{4+}$ and the $\{OV(\mu\text{-}OMe)_2VO\}^{4+}$ motifs are described. The ligands are tridentate deprotonated 4-R-benzoic acid (1-methyl-3-oxo-butylidene)-hydrazides formed in situ during the synthesis of the complexes from bis(acetylacetonato)oxovanadium(IV) with 4-R-benzoylhydrazine. The complexes of $\{OV(\mu\text{-}O)VO\}^{4+}$ were obtained from acetonitrile, whereas the complexes of $\{OV(\mu\text{-}OMe)_2VO\}^{4+}$ were obtained from methanol. Both series of complexes are diamagnetic and electrically non-conducting in solution. The microanalysis and spectroscopic characteristics are consistent with their molecular formulae. The molecular structures of one oxo bridged complex and two dimethoxo bridged complexes have been confirmed by X-ray crystallography. The complexes of $\{OV(\mu\text{-}O)VO\}^{4+}$ do not show any redox response in dichloromethane. On the other hand, dimeric oxomethoxo species display a substituent sensitive vanadium(V) $\rightarrow$ vanadium(IV) reduction.

Supplementary material

CCDC 715732, 715733 and 715734 contain the supplementary crystallographic data for the crystals **20**, **22** and **23**. These data can be obtained free of charge from The Cambridge Crystallographic Data Centre via www.ccdc.cam.ac.uk/data_request/cif.

6.7. References

1. A. Sarkar, S. Pal, *Eur. J. Inorg. Chem*., 2009, 622.
2. R.A. Rowe, M.M. Jones, *Inorg. Synth*., 1957, **5**, 113.
3. *SMART version 5.630* and *SAINT-plus version 6.45*, Bruker-Nonius Analytical X-ray Systems Inc., Madison, WI, USA, 2003.
4. G.M. Sheldrick, *SADABS*, Program for Area Detector Absorption Correction, University of Göttingen, Göttingen, Germany, 1997.

5. G.M. Sheldrick, *SHELX-97*, Structure Determination Software, University of Göttingen, Göttingen, Germany, 1997.
6. L.J. Farrugia, *J. Appl. Crystallogr*., 1999, **32**, 837.
7. P. McArdle, *J. Appl. Crystallogr*., 1995, **28**, 65.
8. A.L. Spek, *PLATON,* A Multipurpose Crystallographic Tool, Utrecht University, Utrecht, The Netherlands, 2002.
9. N.R. Sangeetha, V. Kavita, S. Wocadlo, A.K. Powell, S. Pal, *J. Coord. Chem*., 2000, **51**, 55.
10. N.R. Sangeetha, S. Pal, *Bull. Chem. Soc. Jpn*., 2000, **73**, 357.
11. S.N. Pal, S. Pal, *J. Chem. Crystallogr*., 2000, **30**, 329.
12. S.N. Pal, S. Pal, *Acta Crystallogr. Sect.C,* 2001, **57**, 141.
13. S.N. Pal, K.R. Radhika, S. Pal, *Z. Anorg. Allg. Chem*., 2001, **627**, 1631.
14. A. Sarkar, S. Pal, *Polyhedron*, 2007, **26**, 1205.
15. A. Sarkar, S. Pal, *Inorg. Chim. Acta.,* 2008, **361**, 2296.
16. N.R. Sangeetha, C.K. Pal, P. Ghosh, S. Pal, *J. Chem. Soc., Dalton Trans*., 1996, 3293.
17. A. Mukhopadhyay, G. Padmaja, S.N. Pal, S. Pal, *Inorg. Chem. Commun*., 2003, **6**, 381.
18. S. Das, G.P. Muthukumaragopal, S.N. Pal, S. Pal, *New J. Chem*., 2003, **27**, 1102.
19. S. Dutta, P. Basu, A. Chakravorty, *Inorg. Chem*., 1993, **32**, 5343.
20. J. Dai, S. Akiyama, M. Munakata, M. Mikuriya, *Polyhedron*, 1994, **13**, 2495.
21. R. Dinda, P. Sengupta, S. Ghosh, T.C.W. Mak, *Inorg. Chem*., 2002, **41**, 1684.
22. M.R. Maurya, A. Kumar, A.R. Bhat, A. Azam, C. Bader, D. Rehder, *Inorg. Chem*., 2006, **45**, 1260.
23. P.B. Chatterjee, S. Bhattacharya, A. Audhya, K.-Y. Choi, A. Endo, M. Chaudhury, *Inorg. Chem*., 2008, **47**, 4891
24. S. Das, S. Pal, *J. Mol. Struct*., 2005, **741**, 183.
25. A. Mukhopadhyay, S. Pal, *Eur. J. Inorg. Chem*., 2006, 4879.
26. S.P. Rath, S. Mondal, A. Chakravorty, *Inorg. Chim. Acta,* 1997, **263**, 247.

27. A.W. Addison, T.N. Rao, J. Reedijk, J. van Rijn, G.C. Verschoor, *J. Chem. Soc., Dalton Trans*., 1984, 1349.
28. S.G. Sreerama, S. Pal, *Inorg. Chem*., 2005, **44**, 6299.
29. R. Raveendran, S. Pal, *Inorg. Chim. Acta,* 2006, **359**, 3212.
30. J. March, in: Advanced Organic Chemistry, 4th ed., Wiley, New York, 1992, p. 280.

Divanadium(V) and trapped valence linear tetravanadium(IV,V,V,IV) complexes with N,N′-bis(diacetyl)hydrazine

7.1. Abstract

In acetonitrile-water mixture, reactions of the dinucleating Schiff base N,N′-bis(diacetyl)hydrazine (H_2diah), bis(acetylacetonato)oxovanadium(IV) ([$VO(acac)_2$]), and a monodentate N-coordinating heterocycle (hc) in 1:2:2 mol ratio provide yellow divanadium(V) complexes of formula [(hc)O_2V(μ-diah)VO_2(hc)] (**27** (hc = imidazole (Himdz)), **28** (hc = pyrazole (Hpyz)), and **29** (hc = 3,5-dimethyl pyrazole (Hdmpyz))). On the other hand, in the same solvent mixture reactions of the same reagents in 1:4:2 mole ratio produce green linear tetravanadium(IV,V,V,IV) complexes of formula [$(acac)_2$OV(μ-O)VO(hc)(μ-diah)(hc)OV(μ-O)$VO(acac)_2$] (**30** (hc = imidazole (Himdz)), **31** (hc = pyrazole (Hpyz)), and **32** (hc = 3,5-dimethyl pyrazole (Hdmpyz))). The complexes (**27–32**) have been characterized by elemental analysis, magnetic susceptibility, various spectroscopic and electrochemical measurements. X-ray crystal structures of **27**, **29**, and **32** have been determined. In all three structures, the diazine ligand $diah^{2-}$ is in *trans* configuration. Metal centered bond parameters are consistent with the localized electronic structure of the *trans*-bent $\{OV(\mu\text{-}O)VO\}^{3+}$ core in the solid state. The pentavalent metal centers in **27**, **29**, and **32** are in distorted trigonal bipyramidal N_2O_3 coordination environment, while the terminal tetravalent metal centers in **32** are in distorted octahedral O_6 coordination sphere. The eight line EPR spectra of the tetravanadium species (**30**–**32**) in dimethylsulfoxide at ambient temperature indicate the rare valence localized electronic structure in fluid phase. All the complexes are redox active and display metal centered electron

transfer processes in dimethylsulfoxide solution. A reduction within −0.78 to −0.94 V (vs. Ag/AgCl) is observed for the divanadium(V) species (**27**–**29**), while a reduction and an oxidation are observed in the potential ranges −0.82 to −0.90 V and 0.96 to 1.12 V (vs. Ag/AgCl), respectively for the tetravanadium species (**30**–**32**).

7.2. Introduction

In chapter 5, we have described a coordinatively unsymmetrical complex of the mixed valence *syn*-$\{OV(\mu\text{-}O)VO\}^{3+}$ core.[1] This complex is of trapped valence character in the solid state as well as in solution at ambient temperature. Among the structurally characterized dinuclear complexes containing the $\{OV(\mu\text{-}O)VO\}^{3+}$ core reported in literature,[2] example for such coordinative unsymmetry and valence localized electronic structure in both solid and fluid state is non-existent. Compared to dinuclear species tetranuclear complexes composed of two $\{OV(\mu\text{-}O)VO\}^{3+}$ units are extremely rare. To the best of our knowledge only three structurally characterized complexes of this type are known.[3] Each of these species is with a pair of dinucleating ligands. The dinucleating ligand contains two tripodal ends connected by a spacer having one or two additional coordinating sites. The tripodal ends of each ligand bind two $\{OV(\mu\text{-}O)VO\}^{3+}$ units and as a result these complexes have cyclic structures. In one of these three complexes, the metal centers of the $\{OV(\mu\text{-}O)VO\}^{3+}$ cores are coordinatively unsymmetrical[3b] and in the remaining two complexes they are symmetrical.[3a,c] All these complexes are trapped valence in the solid state. However, EPR studies of only one of them is reported and at ambient temperature in solution the complex has valence delocalized electronic structure.[3b] In this chapter, we have described a series of dinuclear dioxovanadium(V) complexes with the dianionic deprotonated O,N,NO-donor Schiff base N,N′-bis(diacetyl)hydrazine as the bridging ligand and monodentate N-donor

heterocycles (imidazole, pyrazole, and 3,5-dimethyl pyrazole) as ancillary ligands and linear tetravanadium(IV,V,V,IV) complexes containing two trapped valence unsymmetrical $\{OV(\mu\text{-}O)VO\}^{3+}$ units formed due to the attachment of two bis(acetylacetonato)oxovanadium(IV) molecules at the two ends of the dinuclear species. In the following account, we have described the synthesis, characterization and electron transfer properties of these complexes. Molecular structures of represantative dinuclear dioxovanadium(V) and tetravanadium(IV,V,V,IV) complexes have been confirmed by single crystal X-ray diffraction analysis.

7.3. Experimental

7.3.1. Materials

Bis(acetylacetonato)oxovanadium(IV)[4] was prepared by following a reported procedure. All other chemicals and solvents used in this work were of analytical grade available commercially and were used without further purification

7.3.2. Physical measurements

Elemental (C, H, N) alnalysis data were obtained with the help of a Thermo Finnigon Flash EA1112 series elemental analyzer. Solution electrical conductivities were measured using a Digisun DI-909 conductivity meter. Magnetic susceptibility measurements were performed with a Sherwood Scientific balance. Diamagnetic corrections calculated from Pascal's constants[5] were used to obtain the molar paramagnetic susceptibilities. Infrared spectra were collected by using KBr pellets on a Jasco-5300 FT-IR spectrophotometer. A Cary 100 Bio UV/vis spectrophotometer was used to record the electronic spectra. The ^{1}H ($Si(CH_3)_4$ as internal standard) and ^{51}V ($VOCl_3$ as external standard) NMR spectra were collected with the help of Bruker 200 MHz and 400 MHz NMR spectrometers, respectively. A CH-Instruments model 620A electrochemical analyzer was used for cyclic

voltammetric measurements with dimethylsulfoxide solutions of the complexes containing tetrabutylammonium perchlorate (TBAP) as the supporting electrolyte. The three electrode measurements were carried out at 298 K under dinitrogen atmosphere with a glassy carbon working electrode, a platinum wire auxiliary electrode and an Ag/AgCl reference electrode. Under identical condition the Fc^{+}/Fc couple was observed at 0.65 V. The potentials reported in this work are uncorrected for junction contributions.

7.3.3. Synthesis of [(Himdz)O_2V(μ-diah)VO_2(Himdz)] (27).2H_2O

A water solution (5 mL) of N,N′-bis(diacetyl)hydrazine (116 mg, 1.0 mmol) was added to an acetonitrile solution (25 mL) of imidazole (136 mg, 2 mmol) and [$VO(acac)_2$] (530 mg, 2 mmol) and the mixture was boiled under reflux for 6 h and then filtered. The clear filtrate thus obtained was kept at 5° C. Yellow crystalline complex separated in about 7 days was collected by filtration washed with acetonitrile and dried in air. Yield: 185 mg (41%). [λ_{max}, nm (ε, M^{-1} cm^{-1})]: 308 (9 250), 270 (6 300). ^{1}H NMR (200 MHz, in $(CD_3)_2SO$, δ/ppm): 2.50 (s, CH_3), 6.25, 7.60, 8.18 (s, s, s, Himdz C–H protons), 13.15 (s, br, N–H).

[(Hpyz)O_2V(μ-diah)VO_2(Hpyz)] (**28**) was synthesized in 48% yield by following an identical procedure as described for **27**·2H_2O except for the heterocycle being pyrazole instead of imidazole. UV-vis (in $(CH_3)_2SO$) [λ_{max}, nm (ε, M^{-1} cm^{-1})]: 309 (9 300), 277 (6 300). ^{1}H NMR (200 MHz, in $(CD_3)_2SO$, δ/ppm): 2.50 (s, CH_3), 6.26, 7.59, 9.68 (s, s, s, Hpyz C–H protons), 12.71 (s, br, N–H).

[(Hdmpyz)O_2V(μ-diah)VO_2(Hdmpyz)] (**29)** was synthesized by using 3,5-dimethylpyrazole as the heterocycle this complex was obtained in 47% yield by following the same procedure used for the previous two complexes. UV-vis (in $(CH_3)_2SO$) [λ_{max}, nm (ε, M^{-1} cm^{-1})]: 307 (15 500), 272 (14 800). ^{1}H NMR (200 MHz, in $(CD_3)_2SO$, δ/ppm): 2.11 (s, 5-CH_3 of Hdmpyz), 2.27

(s, 3-CH_3 of Hdmpyz), 2.52 (s, CH_3), 5.73 (s, Hdmpyz C–H proton), 12.03 (s, br, N–H).

$[(acac)_2OV(\mu\text{-}O)VO(Himdz)(\mu\text{-}diah)(Himdz)OV(\mu\text{-}O)VO(acac)_2]$ (**30**). was was prepared in 31% yield by following an identical procedure as described for **27**·$2H_2O$ using H_2diah, Himdz and $[VO(acac)_2]$ in 1:2:4 mol ratio. UV-vis (in $(CH_3)_2SO$) [λ_{max}, nm (ε, M^{-1} cm^{-1})]: 560^{sh} (50), 420^{sh} (90), 312 (20 900), 273^{sh} (16 800).

$[(acac)_2OV(\mu\text{-}O)VO(Hpyz)(\mu\text{-}diah)(Hpyz)OV(\mu\text{-}O)VO(acac)_2]$ (**31**) was synthesied by an identical procedure as described for 30 was used to prepare this complex in 26% yield using pyrazole instead of imidazole. UV-vis (in $(CH_3)_2SO$) [λ_{max}, nm (ε, M^{-1} cm^{-1})]: 575^{sh} (30), 415^{sh} (220), 313 (21 500), 273^{sh} (15 500)

$[(acac)_2OV(\mu\text{-}O)VO(Hdmpyz)(\mu\text{-}diah)(Hdmpyz)OV(\mu\text{-}O)VO(acac)_2]$ (**32**) was prepared in 32% yield using 3,5-dimethylpyrazole as the heterocycle and a procedure identical to that used for the previous two complexes. UV-vis (in $(CH_3)_2SO$) [λ_{max}, nm (ε, M^{-1} cm^{-1})]: 550^{sh} (120), 423^{sh} (230), 313 (21 200), 275^{h} (17 300).

7.3.4. X-ray crystallography

Single crystals of **27**·$2H_2O$, **29**, and **32** were collected directly from the products obtained during their syntheses. For each crystal, a Bruker-Nonius SMART APEX CCD single crystal diffractometer, equipped with a graphite monochromator and a Mo $K\alpha$ fine-focus sealed tube (λ = 0.71073 Å) operated at 2.0 kW was used to determine the unit cell parameters and to collect the intensity data. The detector was placed at a distance of 6.0 cm from the crystal. Data were collected at 298 K with a scan width of 0.3º in ω and an exposure time of 10 sec/frame. The SMART software was used for data acquisition and the SAINT-Plus software was used for data extraction.[6] The absorption corrections were performed with the help of SADABS program.[7] The structures were solved by direct methods and refined on F^2 by full-matrix

least-squares procedures. In all the structures, the non-hydrogen atoms were refined using anisotropic thermal parameters. The hydrogen atoms were included in the structure factor calculations at idealized positions by using a riding model. The SHELX-97 programs[8] available in the WinGX package[9] were used for structure solution and refinement. The ORTEX6a[10] and Platon[11] packages were used for molecular graphics. Selected crystal and refinement data are listed in Table 7.1.

Table 7.1. Crystallographic Data for **27**·2H_2O, **29**, and **32**

Complex	**27**·2H_2O	**29**	**32**
formula	$V_2C_{10}H_{18}N_6O_8$	$V_2C_{14}H_{22}N_6O_6$	$V_4C_{34}H_{50}N_6O_{16}$
fw, g/mol	452.18	472.26	1002.56
cryst syst	triclinic	monoclinic	triclinic
space group	$P\bar{1}$	$P2_1/c$	$P\bar{1}$
a, Å	7.3716(9)	7.196(3)	7.5769(15)
b, Å	7.4285(9)	18.252(8)	10.388(2)
c, Å	9.0578(11)	8.082(4)	15.675(3)
α, deg	106.516(2)	90	76.922(4)
β, deg	96.129(2)	112.156(7)	76.429(4)
γ, deg	107.765(2)	90	72.404(4)
V, Å^3	442.58(9)	983.1(8)	1127.1(4)
Z	1	2	1
μ, mm^{-1}	1.108	0.994	0.875
reflns collected	4645	9294	12878
unique reflns	1744	2303	5130
reflns [$I \geq 2\sigma(I)$]	1537	1508	3235
parameters	125	130	278
$R1^a$, $wR2^b$ [$I \geq 2\sigma(I)$]	0.0358, 0.0929	0.0498, 0.1036	0.0724, 0.1689
$R1^a$, $wR2^b$ [all data]	0.0417, 0.0964	0.0875, 0.1146	0.1176, 0.1868
GOF^c on F^2	1.062	0.946	1.038
max/min $\Delta\rho$ (e Å^{-3})	0.379/–0.202	0.530/–0.326	0.670, –0.329

[a] $R1 = \Sigma(||F_o|| - ||F_c||)/\Sigma|F_o|$. [b] $wR2 = [\Sigma(w(|F_o|^2 - |F_c|^2)^2)/\Sigma(w|F_o|^2)]^{1/2}$. [c] GOF = $[\Sigma w(|F_o|^2 - |F_c|^2)^2]/(n-p)^{1/2}$, where n is the number of reflections, and p is the number of refined parameters.

7.4. Results and discussion:

7.4.1. Synthesis and some properties

The divanadium(V) complexes, $[(hc)O_2V(\mu\text{-diah})VO_2(hc)]$ (**27**–**29**), were synthesized in acetonitrile-water mixture under aerobic condition using H_2diah, $[VO(acac)_2]$, and the corresponding heterocycle (hc) in 1:2:2 mol ratio in moderate yields. Here the oxygen in air acts as the oxidant for the oxidation of the metal center from +4 to +5 state. These yellow complexes are insoluble in common organic solvents except for dimethylsulfoxide. The linear tetravanadium(IV,V,V,IV) complexes, $[(acac)_2OV(\mu\text{-O})VO(hc)(\mu\text{-diah})(hc)OV(\mu\text{-O})VO(acac)_2]$ (**30**–**32**), were synthesized by the same general procedure used for **27**–**29** using H_2diah, $[VO(acac)_2]$, and the corresponding heterocycle (hc) in 1:4:2 mol ratio. Thus the two-fold increase of the metal ion starting material, $[VO(acac)_2]$, results into the attachment of the excess amount at the two ends of **27**–**29** and hence the formation of two coordinatively unsymmetrical $\{OV(\mu\text{-O})VO\}^{3+}$ motifs in **30**–**32**. These complexes are green in color and like **27**–**29** they are also soluble only in dimethylsulfoxide. Electronic spectroscopic measurements indicate the formation of the tetravanadium species (**30**–**32**) in solution by addition of two equivalents of $[VO(acac)_2]$ to yellow dimethylsulfoxide solutions of the divanadium(V) complexes (**27**–**29**). The microanalysis data (Table 7.2) are consistent with the molecular formula of the complexes. In dimethylsulfoxide, all the complexes are electrically non-conducting. The divanadium(V) complexes are diamagnetic, while the tetravanadium complexes are paramagnetic. The effective magnetic moments ($\mu_{eff.}$) of **30**–**32** at 298 K are within 2.31–2.37 μ_B (Table 7.6). These values are consistent with the two unpaired electrons present at the two terminal vanadium(IV) centers of these complexes.

Table 7.2. Elemental analysis data

Complex	Found (Calc.)		
	C	**H**	**N**
27	26.36 (26.56)	4.18 (4.18)	18.42 (18.59)
28	28.54 (28.86)	3.17 (3.39)	19.83 (20.19)
29	35.49 **(**35.61**)**	4.78 (4.70)	17.64 (17.80)
30	37.94 (38.07)	4.49 (4.47)	8.69 (8.88)
31	37.81 (38.07)	4.24 (4.47)	8.52 (8.88)
32	40.49 (40.73)	5.15 (5.03)	8.16 (8.38)

7.4.2. Molecular structures

The molecular structures of **27**, **29**, and **32** are shown in Figs. 7.1 and 7.2 and the bond parameters associated with the metal centers are listed in Tables 7.2 and 7.3. In each of the three structures, the two halves of the molecule are related by a crystallographically imposed inversion center situated at the middle of the N–N bond of the dinucleating ligand $diah^{2-}$. The metal centers in **27** and **29** are in O_3N_2 coordination sphere constituted by the imine-N and the amide-O of $diah^{2-}$, the imine-N of the heterocycle, and the two terminal oxo groups (Fig. 7.1). In both complexes, the sum of the three O–V–O angles (359.9°) indicates that the metal atom is essentially at the center of the O_3 triangular plane. However, these O–V–O angles are in the ranges 108.74(11)–130.78(9)° and 109.45(13)–132.29(11)° in **27** and **29**, respectively. The N(1)–V–N(2) angle in **27** is 155.75(9)° and that in **29** is 154.09(9)°.

Thus in both cases the geometry of the O_3N_2 coordination sphere can be best described as trigonal bipyramidal, where the three O-atoms form the trigonal plane and the two N-atoms occupy the axial positions. The V–N(imine) and the V–O(amide) bond lengths are similar to the corresponding bond lengths observed in vanadium(V) complexes having the same coordinated atoms.[1] The V–N(heterocycle) bond lengths in **27** and **29** are significantly shorter than the corresponding bond lengths reported for vanadium(IV) complexes.[12] The V=O bond lengths are unexceptional when compared with the same in pentavalent vanadium complexes.[1–3] The V(1)···V(1)′ distances are 4.9292(8) and 4.953(2) Å in **27** and **29**, respectively. The V(1)···V(1)′ distance (4.946(2) Å) in **30** is very similar to that of **29**. Except for the V(1)–O(2) bond length, the remaining bond parameters in this

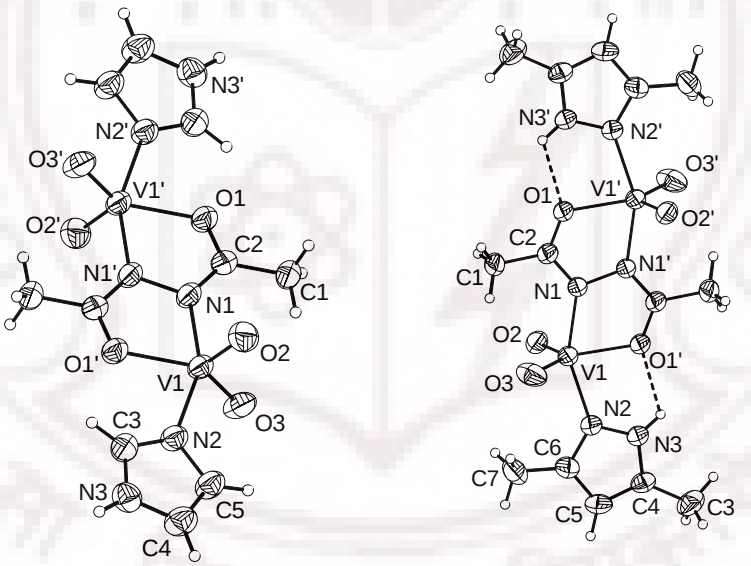

Fig. 7.1. Molecular structures of (a) [(Himdz)O_2V(μ-diah)VO_2(Himdz)] (**27**) and (b) [(Hdmpyz)O_2V(μ-diah)VO_2(Hdmpyz)] (**29**) with the atom numbering scheme. All non-hydrogen atoms are represented by their 50% probability thermal ellipsoids

central dinuclear fragment of **30** (Fig. 7.2) are also similar to the corresponding bond parameters found in complex **29**. The lengthening of V(1)–O(2) in **32** is due to its coordination to the metal center of the terminal $[VO(acac)_2]$ unit at the *trans* position with respect to its oxo atom O(8). The V(2)–O(2) bond length is 2.418(4) Å. As a consequence of this coordination, the V–O(acetylacetonate) bond lengths (1.977(4)–1.986(4) Å) of the terminal distorted octahedral vanadium(IV) centers of **32** are marginally longer than that (1.967(1)–1.970(1) Å) observed in the structure of $[VO(acac)_2]$ where the metal center is in square-pyramidal geometry.[13] For the same reason the displacement of the vanadium(IV) center from the O_4 square-plane formed by the two acetylacetonate ligands towards the terminal oxo group is significantly less (0.365(2) Å) in **32** than the displacement (0.5447(4) Å) observed in the structure of $[VO(acac)_2]$.[13] However, the V(2)=O(8) bond length (1.585(4) Å) is very similar to that (1.584(2) Å) of isolated $[VO(acac)_2]$.[13] The V(1)···V(2) distance and the V(1)–O(2)–V(2) bridge angle in the $\{OV(\mu\text{-}O)VO\}^{3+}$ cores of **32** are 3.951(1) Å and 154.0(2)°, respectively.

The configuration of the mixed-valent $\{OV(\mu\text{-}O)VO\}^{3+}$ core has been found to be very important with respect to its electronic structure.[2g,l] So far three configurations namely *anti*-linear, *anti*-bent and *syn*-bent have been detected in structurally characterized complexes of this core.[1,2,3] For ideal *anti* and *syn* configurations the O=V···V=O torsion angles are 180 and 0°, respectively. There is a single example for a configuration which is in between *syn*- and *anti*-bent. Here the O=V···V=O torsion angle is 83.7°.[2h] Such a configuration is also called as 'twist-angular'.[30] In all these species, the two (bridging)O–V=O angles are similar and less than 180°. The same is true for the two V···V=O angles. Interestingly, the bent $\{OV(\mu\text{-}O)VO\}^{3+}$ cores in **32** are very different with respect to these angles. The O(2)–V(1)–O(3) angleis 109.18(19)°, but the O(2)–V(2)–O(8) angle is 178.41(17)°. The V(2)···V(1)–O(3) and V(1)···V(2)–O(8) angles are 124.6(1)

Table 7.3. Selected bond lengths (Å) and angles (°) for **27**.2H_2O and **29**

V(1)–N(1)	2.0751(19)	2.082(2)
V(1)–N(2)	2.070(2)	2.089(3)
V(1)–O(2)	1.6172(19)	1.622(2)
V(1)–O(3)	1.6152(18)	1.607(2)
V(1)–O(1)′	1.9921(17)	2.0165(19)
N(1)–V(1)–N(2)	155.75(9)	154.09(9)
N(1)–V(1)–O(2)	98.12(9)	99.16(10)
N(1)–V(1)–O(3)	97.18(9)	95.78(11)
N(1)–V(1)–O(1)′	74.70(7)	74.17(8)
N(2)–V(1)–O(2)	98.14(9)	99.16(10)
N(2)–V(1)–O(3)	94.47(9)	95.22(11)
N(2)–V(1)–O(1)′	81.58(7)	81.08(8)
O(2)–V(1)–O(3)	108.74(11)	109.45(13)
O(2)–V(1)–O(1)′	120.42(9)	118.12(11)
O(3)–V(1)–O(1)′	130.78(9)	132.29(11)

Symmetry transformations used to generate equivalent atoms:
[a] –x+1, –y, –z. [b] –x, –y+1, –z+1.

Table 7.4. Selected Bond Lengths (Å) and Angles (°) for **32**[a]

V(1)–N(1)	2.088(4)	V(1)–N(2)	2.090(4)
V(1)–O(2)	1.632(4)	V(1)–O(3)	1.589(4)
V(1)–O(1)′	1.990(3)		
V(2)–O(2)	2.418(4)	V(2)–O(4)	1.986(4)
V(2)–O(5)	1.977(4)	V(2)–O(6)	1.979(4)
V(2)–O(7)	1.983(3)	V(2)–O(8)	1.585(4)
N(1)–V(1)–N(2)	156.30(16)	N(1)–V(1)–O(2)	97.34(16)
N(1)–V(1)–O(3)	98.73(17)	N(1)–V(1)–O(1)′	74.35(14)
N(2)–V(1)–O(2)	94.05(16)	N(2)–V(1)–O(3)	97.02(18)
N(2)–V(1)–O(1)′	82.66(15)	O(2)–V(1)–O(3)	109.18(19)
O(2)–V(1)–O(1)′	132.91(18)	O(3)–V(1)–O(1)′	117.86(17)
O(2)–V(2)–O(4)	77.97(14)	O(2)–V(2)–O(5)	80.08(14)
O(2)–V(2)–O(6)	81.39(15)	O(2)–V(2)–O(7)	78.11(13)
O(2)–V(2)–O(8)	178.41(17)	O(4)–V(2)–O(5)	90.00(15)
O(4)–V(2)–O(6)	159.34(16)	O(4)–V(2)–O(7)	85.47(15)
O(4)–V(2)–O(8)	100.51(18)	O(5)–V(2)–O(6)	87.40(16)
O(5)–V(2)–O(7)	158.19(15)	O(5)–V(2)–O(8)	100.46(18)
O(6)–V(2)–O(7)	89.36(15)	O(6)–V(2)–O(8)	100.12(18)
O(7)–V(2)–O(8)	101.34(17)		

[a] Symmetry transformation used to generate equivalent atoms: –x, –y+1, –z+1.

and 168.4(2)°, respectively. These variations in two halves of the {OV(μ-O)VO}$^{3+}$ core are primarily due to the trigonal-bipyramidal and distorted octahedral coordination geometry around the V(1) and V(2), respectively and the *trans* relationship between the bridging and the terminal oxo groups at the V(2). However, in relation to only the O(3)–V(1)···V(2)–O(8) torsion angle (–166.2(7)°), the {OV(μ-O)VO}$^{3+}$ cores in **32** fall in the *trans*-bent category. So far the largest V···V distance reported is 3.7921(7) Å for a divanadium(V) species containing an unsymmetrical 'twist angular' {OV(μ-O)VO} core.[14] Possibly the unusually large V(1)···V(2) distance (3.951(1) Å) in **32** is due to the atypical configuration of the {OV(μ-O)VO}$^{3+}$ core. Interestingly the V···V distance (3.3084(6) Å) in an unsymmetrical complex of {OV(μ-O)VO}$^{4+}$ unit where one metal center is square-pyramidal and the other one is distorted octahedral with a configuration very close to that observed in **32** is significantly smaller.[14]

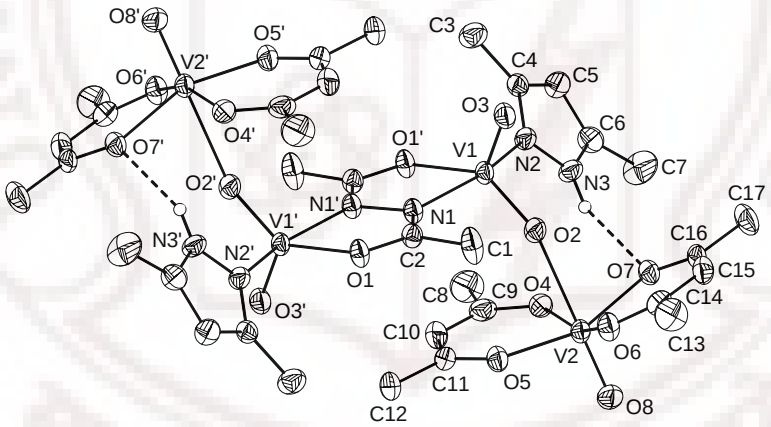

Fig. 7.2. Molecular structure of [(acac)$_2$OV(μ-O)VO(Hdmpyz)(μ-diah)(Hdmpyz)OV(μ-O)VO(acac)$_2$] (**30**) with the atom numbering scheme. All non-hydrogen atoms are represented by their 30% probability thermal ellipsoids. All hydrogen atoms except for the NH hydrogen atom are omitted for clarity.

7.4.3. Hydrogen Bonding and Self-assembly

We have scrutinized all the three structures for possible N–H···O type hydrogen bonding inetraction as these complex molecules contain the heterocycle N–H group and fairly basic vanadium(IV/V) bound oxo groups as well as metal coordinated O-atoms. Two water molecules are also present in the unit cell of **27**, which can participate in hydrogen bonding interactions as donor as well as acceptor.

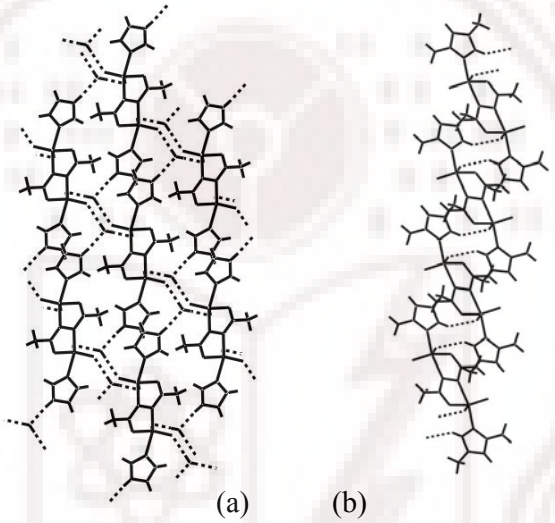

Fig. 7.3. (a) Two-dimensional network of **27**·2H_2O and (b) one-dimensional chain structure of **29**.

In the case of **27**·2H_2O, the Himdz N–H group participates in an intermolecular N–H···O hydrogen bond involving the O-atom O(4) of the lattice water as acceptor. The N(3)···O(4) distance and the N(3)–H···O(4) angle are 2.786(3) Å and 170^o, respectively. The lattice water itself acts as donor in two intermolecular O–H···O hydrogen bonds involving the two metal coordinated oxo groups O(2) and O(3) as acceptors. The O(4)···O(2) and the O(4)···O(3) distances are 2.846(3) and 2.871(3) Å, respectively. The O(4)–H···O(2) and the O(4)–H···O(3) angles are 173(5) and 174(4)^o,

respectively. Due to these three intermolecular hydrogen bonding interactions, **27**·2H_2O units assemble into a two-dimensional sheet structure (Fig. 7.3(a)). There is no other siginificant interaction between these parallel layers in the crystal lattice.

The Hdmpyz N–H group of **29** is involved in an intermolecular hydrogen bonding interaction with one of the metal bound oxo group O(2). Here, the N(3)···O(2) distance and the N(3)–H···O(2) angle are 2.979(4) Å and 140°, respectively. Due to this N–H···O interactions the molecules of **29** form a one-dimensional chain like structure in the crystal lattice (Fig. 7.3(b)). The N–H group is also close to the metal coordinated amide O-atom O(1′). The N(3)···O(1′) distance and the N(3)–H···O(1′) angle are 2.701(3) Å and 112°, respectively (Fig. 7.1). These parameters perhaps indicates the involvement of the N–H group in bifurcated hydrogen bonds of inter- and intramolecular type.

In the case of **32**, there is no intermolecular hydrogen bonding and hence the molecules exist as discrete units in the crystal lattice. However, the Hdmpyz N–H group participates in an intramolecular N–H···O hydrogen bond involving one of the metal coordinated acetylacetonate O-atoms (Fig. 7.2). The N(3)···O(7) distance and the N(3)–H···O(7) angle are 3.114(6) Å and 153°, respectively. Interestingly this hydrogen bond indicates that there is a difference in the orientation of the Hdmpyz ring in the central dinuclear unit of **32** when compared with the isolated dinuclear species **29** where the N–H group is near the amide O-atom O(1) (Fig.7.1). An approximately 180° rotation of the Hdmpyz ring along the V(1)–N(2) will take away the N–H group from the amide O-atom O(1) and bring it near the acetylacetonate O-atom O(7) coordinated to terminal metal center V(2) (Fig. 7.2).

7.4.4. Spectroscopic properties

The infrared spectra of **27**–**29** display a strong band in the range 1564–1545 cm^{-1}. This band is assigned to the C=N stretch of the dinucleating

ligand diah^{2-}. A strong and a moderately strong band are observed in the ranges 959–932 and 898–850 cm^{-1} in the spectra of complexes **27**–**29**. These are attributed to the γ_{as} and γ_s stretches of the VO_2^+ unit.[3c–f] Complexes **30**–**32** display a pair of strong bands in the 995–959 and 936–900 cm^{-1} regions due to the V^V=O and V^{IV}=O stretches, respectively.

Electronic spectral profiles of **27**–**29** in dimethylsulfoxide are very similar. A representative specrum is shown in Fig. 7.4. The spectra display two strong absorptions at ~308 and ~275 nm due to ligand-to-metal and ligand centered transitions. Complexes **30**–**32** display similar two strong absorptions at ~313 and ~274 nm. In addition to these two absorptions, they also display two weak absorptions in the ranges 575–550 and 415–423 nm. Considering the trapped valence character of **30**–**32** in solution at room temperature (*vide infra*), it is very unlikely that any of these weak absorptions is due to inter

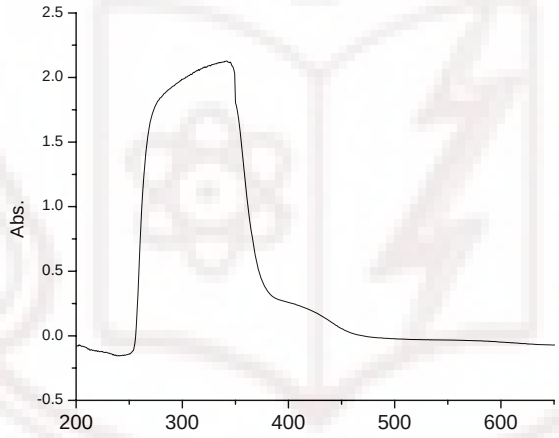

Fig.7.4. Electronic spectrum of [(acac)$_2$OV(μ-O)VO(Himdz)(μ-diah)(Himdz)OV(μ-O)VO(acac)$_2$] (**30**) in dimethylsulphoxide solution.

valence transition. The electronic spectrum of [VO(acac)$_2$] in dimethylsulfoxide shows three absorptions at 650 (ε = 330 M^{-1} cm^{-1}), 453 (ε = 73 M^{-1} cm^{-1}), and 280 nm (ε = 875 M^{-1} cm^{-1}). Thus the weak absorptions

observed in the visible region for **30**–**32** are assigned to the d-d transitions associated with the terminal vanadium(IV) centers.

The ^{1}H NMR spectra of **27**–**29** have been recorded in $(CD_3)_2SO$. All the spectra display a singlet corresponding to three protons at 2.50–2.52 ppm. This resonance is assigned to the methyl group of the dinucleating ligand diah^{2-}. The heterocycle NH proton appears as a broad singlet in the range 12.03–13.15 ppm. In the case of **27**, the three imidazole CH protons are observed as singlets at 6.25, 7.60, and 8.18 ppm. Three singlets observed at 6.26, 7.59, and 9.68 ppm for **28** are assigned to the three CH protons of the pyrazole ring. The 3- and 5-methyl protons of the Hdmpyz of **29** are observed as two singlets at 2.27 and 2.11 ppm, respectively. The lone CH proton of the Hdmpyz resonates as a singlet at 5.73 ppm. The ^{51}V NMR spectra of all the three complexes display a singlet in the region −516 to −542 ppm (Table 7.6). These chemical shifts are comparable with the chemical shifts observed for similar dioxovanadium(V) complexes.[1,15]

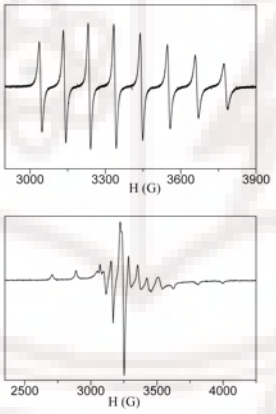

Fig. 7.5. X-band EPR spectra of $[(acac)_2OV(\mu\text{-}O)VO(Hdmpyz)(\mu\text{-}diah)(Hdmpyz)OV(\mu\text{-}O)VO(acac)_2]$ (**32**) in dimethylsulpfoxide at (a) 298 K and (b) 120 K.

As expected the dinuclear complexes **27**–**29** are EPR inactive. The tetranuclear complexes **30**–**32** in dimethylsulfoxide at room temperature (298 K) display a clear eight line ^{51}V (I = 7/2) hyperfine structure due to the terminal vanadium(IV) centers. The g_{iso} and A_{iso} values are within 1.97–1.98 and 94–97 x 10^{-4} cm^{-1}, respectively. In frozen (120 K) solution, all three complexes display typical well resolved axial spectra ($g_{\|}$ = 1.95–1.96, $A_{\|}$ = 166–173 x 10^{-4} cm^{-1} and $g_{\perp}$ = 1.97–1.98, $A_{\perp}$ = 57–63 x 10^{-4} cm^{-1}). Representative room temperature and frozen solution spectra are depicted in Fig. 7.2. Observation of the room temperature eight-line solution spectra instead of the fifteen line spectra indicates the very rare localized electronic structure of the $\{OV(\mu\text{-}O)VO\}^{3+}$ cores in **30**–**32**.[1,2g,i,l] Thus in fluid condition the valence delocalization commonly observed for mixed-valence $\{OV(\mu\text{-}O)VO\}^{3+}$ species is not favored in **30**–**32** due to the very different coordination environment around the vanadium(IV) and vanadium(V) centers.

Table 7.6. Magnetic susceptibility[a], EPR[b] spectroscopic and ^{51}V NMR[c] data

Complex	μ_{eff} (μ_B)	g_{η} ($A\eta$ ($cm^{-1}\times 10^4$))	$g_{\perp}$($A_{\perp}$ ($cm^{-1}\times 10^4$))	δ(ppm)
(**27**)	–	–	–	–542
(**28**)	–	–	–	–536
(**29**)	–	–	–	–516
(**30**)	2.37	1.96 (173)	1.98 (63)	–
(**31**)	2.31	1.95 (166)	1.95 (166)	–
(32)	2.36	1.95 (169)	1.98 (58)	–

[a] In 298 K
[b] In frozen (123 K) dimethylsulfoxide solution
[c] In dmso-d_6

7.4.5. Electrochemical Properties.

Electron transfer properties of **27**–**32** in dimethylsulfoxide have been investigated with the help of cyclic voltammetry. The potential data have

been listed in Table 7.7 and representative cyclic voltammograms are shown in Fig. 7.6. The divanadium(V) complexes (**27**–**29**) display a reduction in the potential range –0.78 to –0.94 V (vs. Ag/AgCl). On the other hand, the tetravanadium(IV,V,V,IV) complexes (**30**–**32**) display a reduction as well as an oxidation in the potential ranges –0.82 to –0.90 V and 0.96 to 1.12 V (vs. Ag/AgCl), respectively. All these responses are irreversible because of unequal anodic and cathodic peak currents and large ΔE_p or complete absence of the E_{pa} or E_{pc} (Table 7.7, Fig. 7.6). As the deprotonated bridging ligand ($diah^{2-}$) and the heterocycles do not show any such redox response in the above potential range. Thus the reduction response observed for all the

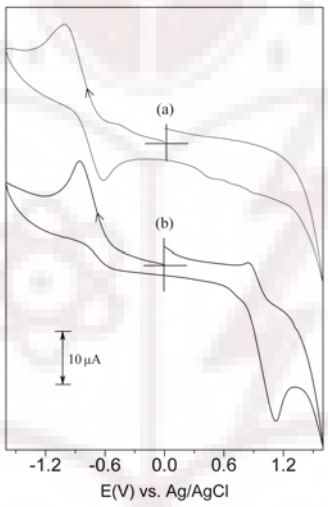

Fig. 7.6. Cyclic voltammograms (scan rate100 mVs^{-1}) of (a) [(Hpyz)O_2V(μ-diah)VO_2(Hpyz)] (**28**) and (b) [$(acac)_2$OV(μ-O)VO(Hpyz)(μ-diah)(Hpyz)OV(μ-O)VO$(acac)_2$] (**31**) in dimethylsulfoxide(0.1 M TBAP) at 298 K.

complexes is assigned to the vanadium(V) → vanadium(IV) process, while the oxidation response observed for only the tetravanadium species (**30**–**32**) is

attributed to the terminal vanadium(IV) → vanadium(V) process. The one electron nature of these responses has been validated by comparing the peak currents with known one electron transfer processes under identical conditions.[2,17] It may be noted that the reduction potentials of **30**–**32** are higher than the reduction potentials of **27**–**29**. This anodic shift of the vanadium(V) → vanadium(IV) reduction is the result of the weakening of V^{V}=O bond in the dinuclear unit (**27**–**29**) due to the coordination of the oxo group to the terminal vanadium(IV) center in **30**–**32**.

Table 7.7. Cyclic voltammetric[a] data

Complex	**Reduction**	**Oxidation**
	$E_{1/2}$[b] **(V) (** ΔE_p[c] **(mV)**	$E_{1/2}$[b] **(V) (**ΔE_p[c] **(mV)**
(**27**)	–0.94[d]	–
(**28**)	–0.81 (380)	–
(**29**)	–0.78 (260)	–
(**30**)	–0.90[d]	0.96 (260)
(**31**)	–0.86[d]	0.99 (290)
(32)	–0.82[d]	1.12[e]

[a] In dimethylsulfoxide (298 K) at a scan rate of 100 mVs^{-1}. [b] $E_{1/2} = (E_{pa} + E_{pc})/2$, where E_{pa} and E_{pc} are anodic and cathodic peak potentials, respectively. [c] $\Delta E_p = E_{pa} - E_{pc}$. [d] E_{pc}. [e] E_{pa}.

7.5. Conclusion

Dinuclear dioxovanadium(V) complexes $[(hc)O_2V(\mu\text{-diah})VO_2(hc)]$ (**27**–**29**) with O,N,N,O-donor N,N′-diacetyl hydrazine (H_2diah) and neutral N-donor heteroycles (hc) have been synthesized using $[VO(acac)_2]$ as the metal ion source. In these complexes, the metal centers are in trigonal bipyramidal N_2O_3 coordination sphere. Use of double the amount of $[VO(acac)_2]$ required for the synthesis of **27**–**29** provides linear tetravanadium(IV,V,V,IV) species $[(acac)_2OV(\mu\text{-O})VO(hc)(\mu\text{-diah})(hc)OV(\mu\text{-O})VO(acac)_2]$ (**30**–**32**) containing two unsymmetrical $\{OV(\mu\text{-O})VO\}^{3+}$ cores. X-ray structure of one of the tetravanadium species reveals that the mixed-valence core is in a trapped valence situation and it has a very unusual configuration with the largest V···V separation for this type of core.[14] Electronic spectra of **27**–**29** exhibit only ligand-to-metal-chrage transfer and ligand based transitions in the UV region, while that of **30**–**32** show additional ligand field transitions in the visible region. The EPR results exhibit very rare valence localized electronic structure for **30**–**32** in the fluid matrix. All complexes are redox active. The divanadium(V) species display a vanadium(V) to vanadium(IV) reduction, while the tetravanadium(IV,V,V,IV) species display an additional vanadium(IV) to vanadium(V) oxidation with the metal centered reduction.

7.6. References

1. A. Sarkar, S. Pal, *Eur. J. Inorg. Chem.*, 2009, 622.
2. (a) M. Nishizawa, K. Hirotsu, S. Ooi, K. Saito, *J. Chem. Soc., Chem. Commun.,* 1979, 707. (b) P. Blanc, C. Madic, J. –P. Launay, *Inorg. Chem.,* 1982, **21,** 2923. (c) F. Babonneau, C Sanchez, J. Livage, J. –P. Launay, M. Daoudi, Y. Jeannin, *Nouv. J. Chem.,* 1982, **6**, 353. (d) A. Kojima, K. Okajaki, S. Ooi, K Saito, *Inorg. Chem.,* 1983, **22**, 1168. (e) J. –P. Launay, Y. Jeannin, M. Daoudi, *Inorg. Chem.,* 1985, **24**, 1052. (f) J.C. Pessoa, J.A.L. Silva, A.L. Vieira, L. Vilas-Boas, P. O'Brien, P. Thornton,*J. Chem. Soc. Dalton Trans.,*

1992, 1745. (g) D. Schultz, T. Weyhermüller, K. Weighardt, B. Nuber, *Inorg. Chim. Acta,* 1995, **40**, 217. (h) S. Mondal, P. Ghosh, A. Chakravorty, *Inorg. Chem.,* 1997, **36**, 59. (i) M. Mahroof-Tahir, A.D Keramidas, R.B. Goldfarb, O.P. Anderson, M.M Miller; D.C. Crans, *Inorg. Chem.,* 1997, **36**, 1657. (j) S.K. Dutta, S.B. Kumar, S. Bhattacharyya, E.R.T. Tiekink, M. Chaudhury, *Inorg. Chem.,* 1997, **36**, 4954. (k) R.A. Holwerda, B.R. Whittlesey, M.J. Nilges, *Inorg. Chem.,* 1998, **37**, 64. (l) S.K. Dutta, S. Samanta, S.B. Kumar, O.H. Han, P. Burckel, A.A. Pinkerton, M. Chaudhury, *Inorg. Chem.,* 1999, **38**, 1982.

3. (a) Kumagai, H.; Kawata, S.; Kitagawa, S.; Kanamori, K.; Okamoto, K. *Chem. Lett.,* 1997, **26**, 249. (b) A. Neves, L.M. Rossi, A.J. Bortoluzzi, A.S. Mangrich, W. Haase, O.R. Nascimento, *Inorg. Chem. Commun.,* 2002, **5**, 418. (c) C. Drouza, A.D. Keramidas, *Inorg. Chem.,* 2008, **47**, 7211.
4. R.A. Rowe, M.M. Jones, *Inorg. Synth*., 1957, **5**, 113.
5. *SMART version 5.630* and *SAINT-plus version 6.45*, Bruker-Nonius Analytical X-ray Systems Inc., Madison, WI, USA, 2003.
6. G.M. Sheldrick, *SADABS*, Program for Area Detector Absorption Correction, University of Göttingen, Göttingen, Germany, 1997.
7. G.M. Sheldrick, *SHELX-97*, Structure Determination Software, University of Göttingen, Göttingen, Germany, 1997.
8. L.J. Farrugia, *J. Appl. Crystallogr*., 1999, **32**, 837.
9. P. McArdle, *J. Appl. Crystallogr*., 1995, **28**, 65.
10. A.L. Spek, *PLATON,* A Multipurpose Crystallographic Tool, Utrecht University, Utrecht, The Netherlands, 2002.
11. W.E. Hatfield, in *Theory and Applications of Molecular Paramagnetism*; Boudreaux, E. A.; Mulay, L. N., Eds.; Wiley: New York, 1976; p. 491.
12. (a) H. Yue, D. Zhang, Y. Chen, Z. Shi, S. Feng, *Inorg. Chem. Commun.,* 2006, **9**, 959. (b) E. Kine-Hunt, K. Spartalian, M. DeRusha, C.M. Num, C.J. Carrano, *Inorg. Chem.,* 1989, **28**, 4392.
13. E. Shuter, S. Rettig, C. Orvig, *Acta Crystallogr. Sect. C*, 1995, **51**, 12.

14. P.B. Chatterjee, S. Bhattacharya, A. Audhya, K.-Y. Choi, A. Endo, M. Chaudhury, *Inorg. Chem.,* 2008, **47**, 4891.

15. (a) X. Li, M.S. Lah, V.L. Pecoraro, *Inorg. Chem.,* 1988, **27**, 4657. (b) C.A. Root, J.D. Hoeschele, C.R. Cornman, J.W. Kampf, V.L. Pecoraro, *Inorg. Chem.,* 1993, **32,** 3855. (c) A.G.J. Ligtenbarg, A.L. Spek, R. Hage, B.L. Feringa, *J. Chem. Soc.*, *Dalton Trans.* 1999, 659. (d) M.R. Maurya, S. Khurana, C. Schulzke, D. Rehder, *Eur. J. Inorg. Chem.,* 2001, 779.

16. (a) S.G. Sreerama, S. Pal, *Inorg. Chem.,* 2005, **44**, 6299. (b) R. Raveendran, S. Pal, *Eur. J. Inorg. Chem.,* 2008, 5540.

List of Publications

Thesis work:

1. Some ternary complexes of oxovanadium(IV) with acetylacetone and N-(2-pyridyl)-N′-(salicylidene)hydrazine and its derivatives.
   A. Sarkar and S. Pal,
   Polyhedron, 2006, **25**, 1685.

2. Dioxovanadium(V) complexes with N,N,O-donor monoanionic ligands: Synthesis, structure and properties.
   A. Sarkar and S. Pal,
   Polyhedron, 2007, **26**, 1205.

3. Complexes of oxomethoxovanadium(V) with tridentate thiobenzhydrazide based Schiff bases.
   A. Sarkar and S. Pal,
   Inorg. Chimica. Acta., 2008, **361**, 2296.

4. An Unsymmetric Chiral Mixed-valent Divanadium(IV/V) Complex.
   A. Sarkar and S.Pal,
   Eur.J.Inorg Chem , 2009, **5**, 622.

5 Divanadium(V) complexes with 4-*R*-benzoic acid (1-methyl-3-oxo-butylidene)-hydrazides: Syntheses, structures and properties.
   A. Sarkar and S. Pal,
   Inorg. Chimica. Acta., (Under revision)

6 Divanadium(V) and Trapped Valence Linear Tetravanadium(IV,V,V,IV) Complexes: Syntheses, Structures and Physical Properties.
   A. Sarkar and S. Pal, (to be communicated)

Other publication:

1 Decavanadates with $[Et^3NH]^+$ and $[Me_2HN(CH_2)_2NHMe_2]^{2+}$: Variation in protonation state and self-assembly.
   Anindita Sarkar and S Pal,
   Polyhedron., 2008**, 27**, 3472.